HARVARD UNIVERSITY

THE GRADUATE SCHOOL OF ARTS AND SCIENCES

THESIS ACCEPTANCE CERTIFICATE

(To be placed in Original Copy)

The undersigned, appointed by the

Division

Department of Astronomy

Committee

have examined a thesis entitled

RADIO RECOMBINATION LINE OBSERVATIONS
OF THE IONIZED GAS
IN THE GALACTIC CENTER

presented by Luis F. Rodriguez

candidate for the degree of Doctor of Philosophy and hereby certify that it is worthy of acceptance.

Signature Eric Chaisson

Typed name Eric Chaisson

Signature A. Dalgarno

Typed name Alexander Dalgarno

Signature Giovanni Fazio

Typed name Giovanni Fazio

Signature Jonathan Grindlay

Typed name Jonathan Grindlay

Signature James Moran

Typed name James Moran

Signature Edward Purcell

Typed name Edward Purcell

Date December 19, 1978

RADIO RECOMBINATION LINE OBSERVATIONS OF THE IONIZED GAS IN THE GALACTIC CENTER

A thesis presented

by

Luis Felipe Rodriguez

to

The Department of Astronomy

in partial fulfillment of the requirements

for the degree of

Doctor of Philosophy

in the subject of

Astronomy

Harvard University

Cambridge, Massachusetts

December, 1978

To my wife.

ABSTRACT

We present radio recombination line observations of the various components of ionized gas at the Galactic Center.

We find Sgr B2 to have a He II zone with radius about 80% of that of the H II zone. This explains the beam-dependent He^+/H^+ variations. The smaller He II zone could be due to preferential absorption of helium-ionizing photons by dust having a smoothly increasing absorptivity shortward of 912 Å.

The ionized gas in the extended thermal component, the second object studied in this thesis, is characterized by a low degree of excitation, as indicated by the observed upper limits to the once- and twice-ionized helium abundances. We favor as the ionizing agent a large number ($\sim 10^4$) of early B-type stars remaining from a huge burst of star formation that could have occurred at the Galactic Center about 10^7 years ago.

Finally, we also studied Sgr A West, the H II region coincident with the kinematic nucleus of our Galaxy. We find that a core-halo model satisfactorily accounts for the infrared and radio results. The unusually low electron temperature (5000 K) determined for this nebula is found to be related to the heavy element enrichment deduced from our reinterpretation of the middle-infrared neon line observations. The dynamics of the region are consistent with Keplerian rotation caused by the normal stellar population plus a 5×10^6 $M_\odot$ non-stellar source at the center.

TABLE OF CONTENTS

ACKNOWLEDGEMENTS

I am most indebted to my advisor, Professor E. J. Chaisson, for his guidance and collaboration in the accomplishment of the research presented in this thesis. He offered me both incisive counsel and cordial friendship.

Several members of the Faculty and the Radio Astronomy Division gave me valuable advice on matters of research; Drs. J. M. Moran, G. G. Fazio, C. J. Lada, C. A. Gottlieb, G. B. Rybicki, and R. Giacconi.

I am also grateful to Drs. A. Dalgarno, J. E. Grindlay, and E. M. Purcell for having accepted being members of my examining committee.

Discussions with several graduate and undergraduate students were beneficial for me. I am particularly thankful to S. M. Lichten, D. Jaffe, L. DaCosta, I. Cruz-Gonzalez, J. A. Garcia-Barreto, J. M. Vrtilek, and G. Garay.

I will also take advantage of this opportunity to acknowledge the inspiration received from two teachers of my undergraduate years; Eng. J. Joubert-Villa and Dr. S. Torres-Peimbert.

Many of the observations presented in this thesis were made at the Haystack Observatory. All the personnel were extremely helpful; in particular I thank Director P. B. Sebring, B. G. Leslie, Dr. M. L. Meeks, J. C. Carter, H. L. Sellers, S. Sanders, S. Murray, D. Maciorowski, J. Donahue, N. Donald, and G. Catuna.

During my graduate studies I received scholarships from the Consejo Nacional de Ciencia y Tecnologia (Mexico) and from the Department of Astronomy of Harvard University.

Invaluable administrative and clerical assistance was given to me by R. Mandalian, D. Carey, D. Beaudoin, A. Najarian, and J. Andersen.

I am also thankful to my parents and family for the continuous flow of moral and financial support that I required throughout these four and a half years.

Finally, the patience, cooperation, and support of my wife were basic to achieve this goal, particularly in the difficult first and last years.

INTRODUCTION

The importance of studying the ionized gas at the center of our Galaxy derives mainly from three facts: 1) Galactic centers (of our Galaxy as well as of any other galaxy) possess very different physical conditions than the well-studied solar vicinity. These conditions could result in illuminating new phenomena. 2) The center of our Galaxy is the closest galactic center and we can study it with very small angular resolution as well as to detect intrinsically weak line and continuum emissions at many frequencies. 3) Ionized gas is the dominant gaseous form in the inner 200 pc of galactocentric distance.

Unfortunately, heavy obscuration impedes the use of the powerful and well-established methods of the optical astronomy and most knowledge has been obtained at radio and infrared wavelengths. Radio recombination lines at various frequencies constitute most of the observational data presented in this thesis. The basic physics of radio recombination lines has been discussed by many authors (Palmer 1968, Chaisson 1976, Seaton 1972). We use these line observations to draw inferences about the density, temperature, kinematics, and chemical composition of the ionized gas at the Center of our Galaxy. Our results are also related to the gas-to-dust ratio, to the nature of the ionizing agents, and to the possible existence of a massive non-stellar component at the kinematic nucleus.

REFERENCES

Chaisson, E. J. 1976, in Frontiers of Astrophysics, ed. E. H. Avrett (Harvard University Press) p. 259.

Palmer, P. 1968, unpublished Ph. D. Dissertation, Harvard University.

Seaton, M. J. 1972, in Atoms and Molecules in Astrophysics, ed. Carson Roberts (Academic Press Inc.: London), p. 121.

CHAPTER I

A GENERAL DESCRIPTION OF THE GALACTIC CENTER

We will define the Galactic Center region to be the volume interior to a Galactic Radius of R_G = 200 pc. The main justification for this definition is that at this radius we find the "expanding and rotating molecular disk", one of the more characteristic structures of our Galaxy. The mass content of the Galactic Center is amply dominated by late-type stars, mainly K and M dwarfs. This result comes fundamentally from the 2.2 μ observations of Becklin and Neugebauer (1968) who found the stellar content and distribution of our nucleus to be very similar to that of M31. Nevertheless, as we will see later, recent studies of the ionized gas at the few inner pc suggest the presence of a massive ($\sim 5 \times 10^5 M_\odot$), non-stellar component at the kinematic center.

Oort (1977) gives the mass density due to stars as a function of R_G. His tabulation can be parametrized to a function of the form

$$\rho = 4.3 \times 10^5 R_G^{-1.8}$$

where ρ is the mass density in $M_\odot$ pc^{-3} and R_G is the galactic radius in pc. The mass interior to R_G is then given by (assuming spherical symmetry):

$$M = \int_0^{R_G} \rho \; 4\pi r^2 \, dr$$

which gives

$$M = 4.5 \times 10^6 \; R_G^{1.2}$$

The circular velocity for pure Keplerian rotation is given by

$$V_c = \left(\frac{G M}{R_G} \right)^{1/2}$$

and this gives

$$v_c = 1.4 \times 10^2 \, R_G^{0.1}$$

where v_c is in km s^{-1}.

Thus, the bulk parameters of the stellar content are reasonably parameterized in terms of R_G. By contrast, the gaseous content occurs in a variety of forms (atomic, molecular, and ionized) and its description is more complicated.

From about 500 to 100 pc there is a nuclear disk of atomic neutral hydrogen (H I). This disk has been studied in detail by Sanders and Wrixon (1973) who find it to increase in density from ~ 0.2 cm^{-3} at the outer edge to ~ 5 cm^{-3} at the inner edge. A total mass of 2×10^6 $M_\odot$ is estimated for this disk. The gas density is found to increase with decreasing galactic radius in a form similar to the stellar density (that is, as $R_G^{-1.8}$). From the above discussion one can find that in the nuclear disk the ratio of gas mass density to stellar mass density is $\sim 10^{-3}$. This H I nuclear disk rotates in orbits that are close to circular with a radial dependence in the velocity in agreement with (1). It is very interesting that the nuclear disk shows little non-radial motions, since both exterior and interior to it there are expanding gaseous structures; at $R_G \gtrsim 3$ kpc there is the well-known "3-kpc expanding arm" while at about 200 pc there is the "expanding and rotating molecular ring".

As the density of H I in the nuclear disk increases to several particles per cm^3 we start finding a new structure, the "expanding and rotating molecular ring". This ring has been studied in OH, H_2CO, NH_3, and CO (Robinson and McGee; 1970, Scoville et al.- 1972, Kaifu et al.; 1975, Solomon et al.; 1972). It consists of several molecular clouds that can

be crudely approximated by a ring with both radial and circular motions. Bania (1977) has fitted the observations to a ring of radius 190 pc, expanding at an average velocity of 150 km s^{-1} and rotating with a circular velocity of 65 km s^{-1}. The nuclear disk and the expanding and rotating molecular ring are not totally separate spatially, actually the molecular clouds are surrounded by the atomic gas of the inner edge of the nuclear disk. The molecular clouds that constitute the ring have diameters $\sim$30 pc and masses in the range 10^4 - 10^6 $M_\odot$. The total mass present in this molecular ring is estimated to be 10^7 - 10^8 $M_\odot$. Finally, in the volume interior to the molecular ring ($R_G \lesssim 150$ pc) we arrive at the region where the ionized gas becomes dominant. Again, as in the transition from the nuclear disk to the molecular ring, the boundary between the molecular ring and the ionized gas is not sharply defined.

The ionized gas distribution is complicated on its own and it is convenient to divide it into three distinct components: 1) The well-defined H II regions, of which Sgr B2 is the brightest and best studied, 2) the extended thermal component, and 3) Sgr A West, an H II region coincident with the kinematic nucleus of the Galaxy. Both the molecular ring, the H II regions, and the extended thermal component are rather asymmetric with respect to the dynamic center of the Galaxy. The molecular clouds and H II regions are more abundant at positive longitudes ($l^{II} > 0$), and the extended thermal component is centered at $l^{II} \simeq 0.^\circ 2$ (Mezger 1974).

REFERENCES

Bania, T. M. 1977, Ap. J., 216, 381.

Becklin, E. E. and Neugebauer, G. 1968, Ap. J., 151, 145.

Kaifu, N., Morris, M., Palmer, P., and Zuckerman, B. 1975, Ap. J., 201 98.

Mezger, P. G. 1974, Proc. ESO/SRC/CERN Conference on Research Programmes for Large Telescopes, p. 79.

Oort, J. H. Ann. Rev. Astron. Ap., 15, 295.

Robinson, B. J. and McGee, R. X. 1970, Australian J. Phys., 23, 405.

Sanders, R. H. and Wrixon, G. T. 1974, Astr. and Ap., 33, 9.

Scoville, N. Z., Solomon, P. M., and Thaddeus, P. 1972, Ap. J., 172, 335.

Solomon, P. M., Scoville, N. Z., Jefferts, K. B., Penzias, A. A., and Wilson, R. W. 1972, Ap. J., 178, 125.

CHAPTER II

INTRODUCTION TO SGR B2

Sgr B2 is the most bright and studied of the H II regions in the Galactic Center. This H II region is associated with the Sgr B2 molecular cloud, considered the most massive molecular cloud in the Galaxy. In considerable part the study of the Sgr B2 H II region has been motivated by the fact that the Sgr B2 molecular cloud is the richest in molecular species. Many of the more exotic molecules have been found only in this molecular cloud. During the early seventies the Sgr B2 molecular cloud was the favorite hunting ground for new molecular species. In the last few years this distinction has been disputed by other very interesting clouds, particularly Cloud 2 and the Orion Molecular Cloud 1.

The Sgr B2 H II region is very luminous and the large amount of ionized gas present there requires $\sim 3 \times 10^{50}$ ionizing photons s^{-1} to maintain the ionization. It was thus assumed that, as in other giant H II regions in the galactic disk, the ionization was being provided by a cluster or clusters of recently formed O stars. According to Salpeter's initial mass function it was expected that clusters luminous enough to provide the large amount of ionizing photons needed would have among their members several early type O stars, of the O5 type and possibly earlier. Theoretical models of ionization structures of H II Regions using the integrated stellar spectra of an early type O cluster predict He^+ and H^+

ionized volumes approximately coincident. This is indeed what is observed in the giant H II regions of the Galactic Disk. Occasionally, small H II regions are found where the He^+ sphere is substantially smaller than the H^+ sphere (for example, this is the case in Orion B). Nevertheless, in these cases the explanation is that the modest amount of ionizing photons can be provided by a late O-type or early B-type star. These type of stars have much smaller fractions of helium-ionizing photons than the early O-type stars that dominate the ionizing flux of recently formed massive ($\sim$2000 $M_\odot$) OB clusters. Sgr B2 is a very luminous H II region and several OB clusters are needed to explain its ionization. Approximately coincident He^+ and H^+ spheres were then expected.

It came as a major surprise when Churchwell and Mezger (1973) reported their measurements of the antenna-averaged He^+ to H^+ number ratio, y^+. Instead of the expected $y^+ \simeq 0.08 - 0.10$, a very stringent upper limit of $y^+ \lesssim 0.02$ was set. Various fascinating possibilities were suggested, among them that the Galactic Center did not have any He. This could have been a major objection to the cosmological theory of the Big-Bang, where in the first few minutes of the Universe all matter becomes contaminated with a total He to H ratio, y, of $\approx 0.06 - 0.08$. Another possibility was to propose that the Sgr B2 H II region was being ionized by stars of late spectral type (B0 or later). A major problem with this suggestion was that a very large number of such stars is required ($\sim$700 B0V stars).

To help clarify the situation we did a thorough multifrequency study of y^+ in Sgr B2 that is presented in the next chapter. Our main results were:

1) The upper limit of Churchwell and Mezger (1973) was underestimated and this aggravated the reality of the situation. They set $y^+ \lesssim 0.02$. With the same antenna (the NRAO 140-foot) at almost the same frequency but using a cooler receiver we actually detected $y^+ = 0.031$.

2) The results are consistent with a normal y ratio of 8 to 10 percent if dust with a smoothly increasing absorptivity shortward of 912 Å is present inside the H II region and effectively competes with the gas for the high-frequency ($h\nu \gtrsim 24.6$eV) helium-ionizing photons. This creates a He^+ sphere smaller than the H^+ sphere and accounts for the observations.

3) A non-LTE model involving stimulated emission in cold gas outside the H II region (Brown and Gomez-Gonzalez 1974, 1975) was shown to be untenable.

REFERENCES

Brown, R. L. and Gomez-Gonzalez, J. 1974, Ap. J., 188, 475.

_____ 1975, Ap. J., 200, 598.

Churchwell, E. and Mezger, P. G. 1973, Nature, 242, 319.

THE ASTROPHYSICAL JOURNAL, 221:810–815, 1978 May 1

CHAPTER III

THE HELIUM PROBLEM IN SAGITTARIUS B2

ERIC J. CHAISSON,* STEPHEN M. LICHTEN, AND LUIS F. RODRIGUEZ†
Harvard-Smithsonian Center for Astrophysics
Received 1977 June 20; accepted 1977 November 7

ABSTRACT

New observations of hydrogen and helium radio recombination lines emitted from the Sgr B2 nebula near the galactic center have yielded values for an ionized abundance ratio, $N(He^+)/N(H^+)$, considerably less than 10% by number. These measurements are consistent, however, with a normal total helium-to-hydrogen ratio of 8%–10%, provided the nebular dust preferentially absorbs helium-ionizing photons, giving rise to a region of He II with a radius about 80% that of H II. As the radio telescope beamwidth decreases, the He II zone is better resolved and the measured $N(He^+)/N(H^+)$ ratio increases correspondingly. Our model is consistent with a dust absorptivity which is a smoothly increasing function of frequency shortward of 912 Å; an absorptivity that increases dramatically near 500 Å, as has been previously suggested, is not required by our observations. Our results also suggest that an external maser model in which the observed ratio $N(He^+)/N(H^+)$ is determined primarily by non-local thermodynamic equilibrium processes occurring in a cold, partially ionized gas surrounding the H II region, does not apply to Sgr B2.

Subject headings: galaxies: nuclei — nebulae: abundances — nebulae: individual — radio sources: lines

I. INTRODUCTION

Perhaps the most intriguing gaseous nebula in our Milky Way, the Sagittarius B2 (G0.7–0.0; W24) H II region is located near the galactic center, about 10 kpc from Earth. Optically obscured by galactic dust, it has been studied by numerous radio and infrared researchers—for example, Harper and Low (1971), Martin and Downes (1972), Chaisson (1973*a*), Balick and Sanders (1974), and Churchwell, Mezger, and Huchtmeier (1974). The region is remarkable not only because it is one of the most massive and most excited galactic nebulae known but also because its associated, giant molecular cloud is the source of more observed interstellar molecular features than any other region discovered to date.

Although most observed characteristics of the Sgr B2 nebula appear to mimic those of other galactic H II regions, the entire Sgr B2 region is sometimes considered peculiar because of its apparent lack of certain substances abundant in similar regions elsewhere. For example, certain interstellar molecules present in the spectra of the Orion molecular cloud or the Taurus dark cloud appear to be underabundant or missing altogether in the Sgr B2 molecular cloud. In addition, until recently, evidence for neither helium nor carbon radio recombination lines, regular features of all other H II region spectra, could be found.

In this paper, we examine the helium problem in the ionized gas of Sgr B2. Particularly vexing until recently, early attempts to measure the number density abundance ratio $y^+ \equiv N(He^+)/N(H^+)$ by observing radio recombination lines led only to upper limits of about a few percent (Churchwell and Mezger 1973; Chaisson 1973*a*). But restrictions placed on the total (neutral plus ionized) helium abundance by the big-bang theory, where about 8% helium is thought to be produced in the first few minutes of the universe (thereby contaminating all matter), as well as a lack of viable mechanisms that could destroy helium once formed, led researchers to postulate special conditions that could give rise to anomalously low y^+ ratios.

For some years, Mezger and colleagues (Churchwell, Mezger, and Huchtmeier 1974; Smith and Mezger 1976) have argued that dust, mixed with the ionized gas, can compete with the gas for helium-ionizing photons produced by the central exciting stars. Although there is presently no evidence whatsoever for a dramatic rise in the dust absorptivity near 500 Å, these authors have shown that dust of this nature could compete effectively with the greater than 25 eV photons necessary to ionize helium once. The resulting ionized helium Strömgren sphere, considerably smaller than that of ionized hydrogen, would in this case produce an observed helium signal increasingly weakened (or diluted) relative to that of hydrogen as the radio telescope beam is made larger. Furthermore, Mezger and Smith (1976) have recently reported the detection of weak He109α and He91α recombination lines, consistent with y^+ of 3%–4%, and argue that their observations support the model of selective absorption of helium-ionizing photons by the nebular dust. The major difficulty with their interpretation is the complete lack of evidence for a markedly increased

* Alfred P. Sloan Foundation Research Fellow.

† Becario del Consejo Nacional de Ciencia y Tecnologia, Mexico.

dust absorptivity at or near 500 Å, a condition necessary to justify a total number density ratio

$$y \equiv \frac{N(\mathrm{He}^0) + N(\mathrm{He}^+) + N(\mathrm{He}^{++})}{N(\mathrm{H}^0) + N(\mathrm{H}^+)}$$

of 8%–10%.

On the other hand, Brown and Lockman (1975) have observed a relatively strong He76α recombination line, consistent with an observed y^+ of about 8.5%. They claim that this supports the theory of Brown and Gomez-Gonzalez (1975), who argue that non-LTE processes in a cold, partially ionized region exterior to the Sgr B2 nebula cause y^+ to vary with frequency. Their model essentially predicts that the observed hydrogen signal is amplified more than the observed helium signal upon radiative transfer through cold, nonnebular gas, producing an observed y^+ considerably smaller at low radio frequencies than the total y of 8%–10%.

In the course of our analysis of this problem, we have noticed that Mezger and colleagues, proponents of strong dust absorption, report relatively weak helium signals, while Brown and colleagues, proponents of strong non-LTE processes, report relatively strong helium signals. Consequently, we have undertaken an independent observational study of helium recombination lines emitted from Sgr B2. Our objective here is to distinguish between the two models noted above by measuring He65α, He92α, and He110α lines and hence to estimate y^+ at frequencies ranging from 23.4 to 4.9 GHz and with telescope beamwidths spanning 1'.3–6'.5.

II. OBSERVATIONS AND DATA REDUCTION

All observations were accomplished at the continuum peak of Sgr B2 as determined from the map of Kapitzky and Dent (1974), viz., $\alpha(1950) = 17^h44^m07^s$, $\delta(1950) = -28°21'24''$.

a) The 65α Set

The 65α set at 23.4 GHz was measured during 1975 January and September with the 36.5 m (120 foot) antenna of the Haystack Observatory.[1] The half-power beamwidth measures 1'.3 at this frequency. The receiver consisted of a traveling-wave ruby maser amplifier, cryogenically cooled to provide an overall system temperature of about 150 K on cold sky. A 20 MHz frequency regime centered midway between the H65α and He65α lines was sampled by a 100-channel autocorrelator. To provide gain stability over such a wide frequency interval, it was necessary

[1] The Haystack Observatory of the Northeast Radio Observatory Corporation is supported in part under grant GP-25865 from the National Science Foundation.

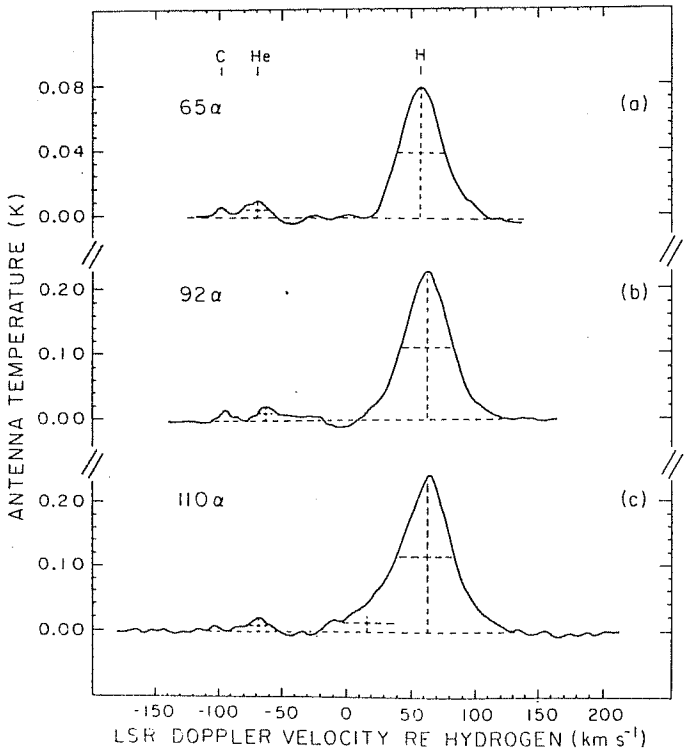

FIG. 1.—Spectra for each of three radio recombination-line α sets. The dashed lines indicate the least-squares-fitted Gaussian functions. (*a*) The 65α set observed at 23.4 GHz. (*b*) The 92α set observed at 8.3 GHz. (*c*) The 110α set observed at 4.9 GHz.

TABLE 1

NEW OBSERVATIONS OF SAGITTARIUS B2*

Transition	T_L (K)	Δv_L (km s^{-1})†	V_{LSR} (km s^{-1})	T_c (K)	T_e (K)	y^+
H65α.....	0.079 ± 0.001	39.0 ± 0.4	62.0 ± 0.2	0.46 ± 0.04	8400 ± 700	0.074 ± 0.02
He65α.....	0.011 ± 0.002	20.9 ± 3.5	56.8 ± 1.4	...	...	...
C65α.....	0.006 ± 0.001	30.7 ± 13	56.1 ± 6	...	...	...
H92α.....	0.218 ± 0.001	41.6 ± 0.3	64.7 ± 0.2	4.6 ± 0.4	8900 ± 700	0.040 ± 0.01
He92α.....	0.020 ± 0.002	18.3 ± 4	63.8 ± 2.1	...	...	...
C92α.....	0.012 ± 0.002	13.2 ± 3	60.1 ± 2	...	...	...
H110α.....	0.229 ± 0.013	44.7 ± 1.6	63.1 ± 1.4	9.8 ± 0.9	8600 ± 1100	0.031 ± 0.01
	0.034 ± 0.009	41.0 ± 13	18.0 ± 10	...	...	...
He110α.....	0.018 ± 0.004	17.0 ± 4	53.9 ± 1.6	...	...	...

* Errors are 1 standard deviation.

† Uncorrected for instrumental broadening.

to switch the radiometer input at a 5 Hz rate against a sky horn while OFF and ON the source.

Figure 1*a* shows the spectrum smoothed to an effective spectral resolution of 24 km s^{-1} after the removal of a parabolic baseline. Table 1 lists the line parameters obtained from a simultaneous least-squares fit of three Gaussian functions. T_L denotes the peak line intensity, Δv_L the full width at half-intensity in velocity space, and V_{LSR} the velocity of each line referenced to the local standard of rest. The fit to the C65α line is only meant to be suggestive, though its velocity mimics that of the nebula; even if real, its width is artificially broadened by the instrument.

b) The 92α Set

The 92α set at 8.3 GHz was measured in 1977 January and May, also with the Haystack antenna. At this frequency, the beamwidth measures 4′. A cryogenically cooled parametric amplifier provided an overall system temperature of 80 K when observing cold sky in the total-power mode. A new 1024-channel autocorrelator sampled the data with a 13.3 MHz bandwidth.

Figure 1*b* shows the data from which a polynomial baseline was removed. The spectrum has been smoothed to an effective resolution of 14 km s^{-1}. Table 1 lists the parameters derived from the least-squares fit of three Gaussian functions, including a weak C92α line.

c) The 110α Set

The 110α set at 4.9 GHz was measured in 1977 April with the 42.7 m (140 foot) antenna of the NRAO.[2] The beamwidth measures 6′.5 at this frequency. A dual-channel receiver enabled us to sample horizontal and vertical polarizations in two separate autocorrelation spectrometers, each of which distributed 192 channels across 10 MHz. These were then added together to form the final spectrum centered midway between the H110α and He110α lines. The overall system temperature averaged 70 K during total-power operation on cold sky.

Figure 1*c* shows the 110α spectrum after smoothing to an effective resolution of 6 km s^{-1} and after removal of a polynomial baseline. Table 1 lists the line parameters describing the H110α and He110α signals.

The nearby H138β line was also observed with sensitivity comparable to the 110α set. Figure 2 shows the spectrum of this higher-order recombination line, and the caption lists its least-squares–fitted line parameters.

[2] The National Radio Astronomy Observatory is operated by Associated Universities, Inc., under contract with the National Science Foundation.

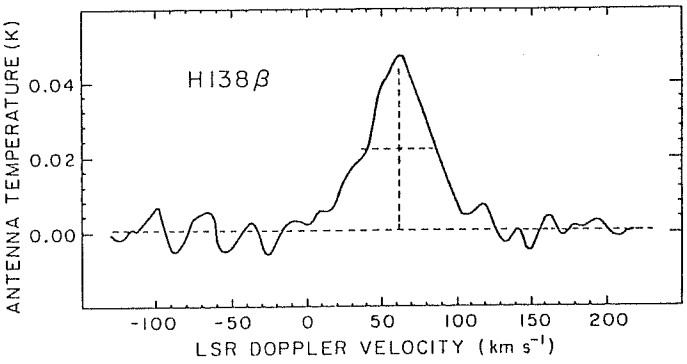

FIG. 2.—The H138β line whose parameters measure, at 4.9 GHz, $T_L = 0.044 \pm 0.001$ K, $\Delta v_L = 50.4 \pm 2$ km s^{-1}, and $V_{LSR} = 61.8 \pm 0.6$ km s^{-1}.

Also given in Table 1 are the continuum antenna temperature T_c of Sgr B2 measured simultaneously with the line at each frequency, the electron temperature T_e derived from an analysis of the line-to-continuum ratio with the assumption of LTE and optical thinness, and the observed ratio $y^+ = N(\mathrm{He}^+)/N(\mathrm{H}^+) = T_L(\mathrm{He})\Delta v_L(\mathrm{He})/T_L(\mathrm{H})\Delta v_L(\mathrm{H})$. For the 110$\alpha$ set, y^+ is calculated by using only the H110α line having the same velocity as the He110α line.

III. THE HELIUM ABUNDANCE

In this section, we attempt to distinguish between the stimulated emission model and the dust absorption model. To ensure consistency in observational techniques as well as data reduction, we use only our new results presented in the previous section. In § IV, we draw some comparisons between our data and those of other researchers.

The principal objective is to determine whether the observed values of y^+ can be made consistent with a normal helium-to-hydrogen abundance ratio of 8%–10% by number. We consider first the non–LTE model.

a) Observational Consequences of Stimulated Emission

Brown and Gomez-Gonzalez (1975) have noted that radiative transfer of nebular radio recombination lines through a cold (less than $\sim$100 K), partially ionized [$N(\mathrm{H}^+)/N(\mathrm{H}) \leqslant 10^{-4}$] gas can enhance hydrogen lines to a greater extent than helium lines, since, in the cold gas, the $N(\mathrm{He}^+)/N(\mathrm{H}^+)$ ratio can be low (less than $\sim$0.01) under the excitation conditions discussed by Brown and Gomez-Gonzalez (1974). Depending upon the precise conditions of temperature and density, and upon the degree of ionization in this cold molecular cloud–H II interface region, y^+ can appear to be anomalously low at those (generally low) frequencies where stimulated emission dominates. But since the observed line parameters T_L and Δv_L can vary by several orders of magnitude when the density and temperature of the cold gas are altered only slightly, it is difficult to test the non–LTE model directly.

Observations of a higher-order recombination line, however, can also provide a test. The Brown and Gomez-Gonzalez model specifically predicts that, since a cold, partially ionized gas dominates the Sgr B2 emission, ratios of higher-order to principal (alpha) lines should exceed those expected for conditions of LTE. This is particularly true for those low frequencies where y^+ is thought to be substantially altered by the effect of stimulated emission. But an analysis of our H138β line shows it to have an integrated intensity 22% ± 4% that of the H110α line, a moderate departure from the value of 28% expected for an LTE model of hot nebular gas. Our observed β/α ratio appears to be in direct contradiction to the much greater than 28% value predicted by the Brown and Gomez-Gonzalez model, as has already been noted by Smith and Mezger (1976) who measured the H137β line to be 19% ± 2% of the H109α line.

Further evidence against the Brown and Gomez-Gonzalez model is the observational fact that the quantity $\Phi \equiv \Delta\nu_L T_L T_c^{-1} \nu_L^{-2.1}$ is approximately frequency invariant for our hydrogen-line observations (and for all hydrogen-line observations to date, except the 91α data of Smith and Mezger 1976). For $\Delta\nu_L$ in kHz and ν_L (the line frequency) in GHz, Φ remains well behaved between 0.5 and 0.7, in apparent disagreement with the Brown and Gomez-Gonzalez prediction that Φ should vary irregularly over a wide range in frequency (cf., e.g., their Fig. 9). The near constancy of Φ is tantamount to the statement that the values of T_e (8500–9000 K), derived from the α lines under LTE conditions, are nearly independent of frequency, a statement that we should not be able to make if Φ depends on the parameters of the cold, largely molecular gas.

In summary, we can find no observational evidence that amplification of nebular recombination lines by a cold, partially ionized foreground gas affects, to any measurable extent, the observed hydrogen and helium line profiles.

b) Observational Consequences of Dust Absorption

Nebulae having He II zones that are substantially smaller than their H II zones will give rise to an observed y^+ that varies with telescope beam. This is the case, for example, for the low-excitation nebula NGC 2024, where the exciting star is of sufficiently low luminosity to produce a small He II zone and hence an apparently low value of y^+ at some frequencies (Chaisson 1973*b*; MacLeod, Doherty, and Higgs 1975). But the Lyman continuum luminosity of the (unseen) excitation sources in Sgr B2 is so large that the assumption of an initial mass function implies complete ionization of helium throughout a dust-free H II region.

Sgr B2, of course, contains dust as well as gas. Hence we seek here, as have Smith and Mezger (1976) and others, a model where nebular dust can preferentially absorb helium-ionizing photons and thus lead to a variation of y^+ with beamwidth.

When hydrogen and helium emission occurs over different path lengths s, the observed y^+ becomes

$$y^+ = \frac{(T_L\Delta\nu_L)_{\mathrm{He}}}{(T_L\Delta\nu_L)_{\mathrm{H}}} = \frac{\int_{S(\mathrm{He}^+)} N(\mathrm{He}^+) N_e ds}{\int_{S(\mathrm{H}^+)} N(\mathrm{H}^+) N_e ds} \frac{\delta(\Theta_A/\Theta_{\mathrm{He}})}{\delta(\Theta_A/\Theta_{\mathrm{H}})} .$$

Here, $\delta(\Theta_A/\Theta_s)$ is a dilution factor relating the antenna half-power beamwidth Θ_A and the source diameter Θ_s. It is essentially a measure of the amount of helium signal dilution and can, for a spherical source, be evaluated for both hydrogen and helium, where $x = (2\Theta/\Theta_s)^2$, by the relation

$$\delta(\Theta_A/\Theta_s) = \ln 2\,(\Theta_s/\Theta_A)^2 \times \int_0^1 \exp\left(-\ln 2\Theta_s^2 x/\Theta_A^2\right)(1-x)^{1/2} dx .$$

For the condition that the quantity $N_e N(H^+)$ is constant throughout the nebula, these relationships reduce to a simpler form relating observed abundance y^+, the total abundance y, the dilution factor δ, and the angular source sizes Θ_s:

$$y^+ = \frac{\delta(\Theta_A/\Theta_{He})}{\delta(\Theta_A/\Theta_H)} \frac{\Theta_{He}}{\Theta_H} y .$$

This expression is valid, provided there are no large density gradients in the Sgr B2 nebula. Note that, in the small beamwidth limit $\Theta_A \to 0$, $y^+ = (\Theta_{He}/\Theta_H)y$, the maximum possible observed y^+. In the other limit—$\Theta_A \gg \Theta_H$, Θ_{He}—then $y^+ = (\Theta_{He}/\Theta_H)^3 y$, which is just a ratio of ionized hydrogen and helium zone volumes.

For a source width at half-intensity of 3'.8—a mean size found by many observers—we find, for the spherical model, $\Theta_H = 3'.8 \times 1.47 = 5'.6$. The solution to the dust absorption model then requires a determination of Θ_{He} and y.

Figure 3 shows several curves for varying Θ_{He}, but with a fixed $y = 0.09$. As can be seen, when this y is assumed (and we assumed it, of course, to alleviate any abundance anomaly at the galactic center), our three sets of new observations of y^+ are consistent with a He II zone about 75% the size of the H II zone. Consequently, we can state that our presently reported observations of y^+ at 23.4, 8.3, and 4.9 GHz are consistent with a size ratio $(\Theta_{He}/\Theta_H) = 0.70$–$0.80$, or a volume ratio $(\Theta_{He}/\Theta_H)^3 = 0.3$–$0.5$, provided the total $y = 0.08$–0.10.

Our solution is essentially the same *type* of solution as that proposed by Mezger, Smith, and Churchwell (1974) and Smith and Mezger (1976), though, in order to explain their modeled volume ratio $(\Theta_{He}/\Theta_H)^3 < 0.2$, they were compelled to conclude that the dust absorptivity increases dramatically at or near 500 Å. Their model requires the absorptivity at 500 Å to exceed that at 900 Å by about a factor of 10. Few researchers regard such extreme cross section behavior as reasonable, especially in view of the extinction and scattering efficiencies measured for interstellar dust shortward of 1500 Å (cf., e.g., Bless and Savage 1972; Witt and Lillie 1973).

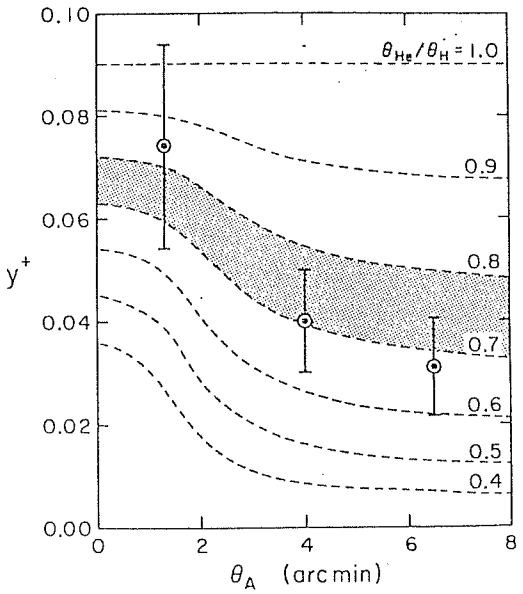

FIG. 3.—The variation of y^+ with Θ_A. The family of curves corresponds to varying Θ_{He}/Θ_H ratios noted to the right of each curve. All the curves utilize $y = 0.09$ and $\Theta_H = 5'.6$.

However, the dust absorptivity need not behave like a step function near 500 Å, if our solution, $(\Theta_{He}/\Theta_H)^3 = 0.3$–$0.5$, is correct. For example, calculations by Sarazin (1977) show that, if the ionizing stars have the spectral distribution of the Salpeter initial mass function, a dust absorptivity of the type $\kappa_\nu = \kappa_1(\nu/\nu_1)^2$ can give rise to an H II region with $(\Theta_{He}/\Theta_H)^3 = 0.44$. Here, ν_1 is the hydrogen ionization threshold corresponding to 912 Å and κ_1 is the cross section at ν_1. Therefore, our observations of y^+ appear to be consistent with a dust absorptivity that increases smoothly with frequency shortward of 912 Å. The absorptivity need be only about a factor of 3 larger at 500 Å than at 900 Å.

IV. COMPARISONS WITH OTHER OBSERVATIONS

We hesitate to enter into a detailed discussion of previous recombination-line observations of Sgr B2. Almost all the published line data can be criticized and reanalyzed from the point of view of hindsight. If all of it—that is, the data of Mezger and colleagues as well as Brown and colleagues, in addition to the values reported in this paper—were to be plotted in Figure 3 or in a y^+ versus ν graph, a scatter diagram would result and little sense could be made of it.

Such a plot would show the Brown and Lockman (1975) y^+ value at 76α to be higher than allowed by the reasonable range of solutions of Figure 3. However, we believe that their He76α line, considerably wider ($\sim$38 km s^{-1}) and more blueshifted than those found by other researchers, is moderately contaminated by unrecognized C76α emission; indeed, a small ($\sim$20%) decrease in their He76α line width would bring their He^+/H^+ value into agreement with the model presented by us here. On the other hand, the Mezger and colleagues values of y^+ appear to be consistently low; indeed, the Bonn technique of fitting different linear baseline segments for different parts of an obviously curved spectrum clearly leads to a minimum possible helium line strength (cf., e.g., Fig. 2 of Mezger and Smith 1976). Similarly, we believe that previous upper limits of $y^+ \leqslant 0.02$ for the He109α line with a 6' beam (Churchwell and Mezger 1973) and for the He92α line with a 4' beam (Chaisson 1973*a*) are underestimated; the former limit appears to be inconsistent with the true peak-to-peak noise variations in the 109α spectrum, while the latter limit ignores some baseline curvature that probably masked a stronger He92α signal. Furthermore, unrecognized weak carbon line signals could make ambiguous the measured y^+ values.

V. CONCLUSIONS

New observations of several hydrogen and helium radio recombination lines toward Sgr B2 are consistent with a normal helium-to-hydrogen number abundance ratio of 8%–10%. Our measurements of helium lines at three different frequencies appear consistent with emission from zones of ionized gas slightly smaller for helium than for hydrogen. Our solution mimics that suggested by Mezger and colleagues, but differs from their model in the important sense that our observations imply a He II zone having nearly 80% the radius of the H II zone, a nebular condition consistent with a *smoothly* increasing dust absorptivity shortward of 912 Å. Our model requires neither a dramatic increase in the dust absorptivity at or near 500 Å nor substantial amounts of stimulated emission either inside or outside of the nebula. In particular, we can find no observational evidence that non–LTE stimulated emission in cold, nonnebular gas plays any appreciable role in the determination of the relative intensities of hydrogen and helium recombination lines.

We acknowledge the excellent assistance provided by the engineering staffs of the Haystack Observatory and of the NRAO.

REFERENCES

Balick, B., and Sanders, R. H. 1974, *Ap. J.*, **192**, 325.
Bless, R. C., and Savage, B. D. 1972, *Ap. J.*, **171**, 293.
Brown, R. L., and Gomez-Gonzalez, J. 1974, *Ap. J.*, **188**, 475.
———. 1975, *Ap. J.*, **200**, 598.
Brown, R. L., and Lockman, F. J. 1975, *Ap. J. (Letters)*, **200**, L155.
Chaisson, E. J. 1973*a*, *Ap. J.*, **186**, 555.
———. 1973*b*, *Ap. J.*, **182**, 767.
Churchwell, E., and Mezger, P. G. 1973, *Nature*, **242**, 319.
Churchwell, E., Mezger, P. G., and Huchtmeier, W. 1974, *Astr. Ap.*, **32**, 283.
Harper, D. A., and Low, F. J. 1971, *Ap. J. (Letters)*, **165**, L9.
Kapitzky, J. E., and Dent, W. A. 1974, *Ap. J.*, **188**, 27.
MacLeod, J. M., Doherty, L. H., and Higgs, L. A. 1975, *Astr. Ap.*, **42**, 195.
Martin, A. H. M., and Downes, D. 1972, *Ap. Letters*, **11**, 219.
Mezger, P. G., and Smith, L. F. 1976, *Astr. Ap.*, **47**, 143.
Mezger, P. G., Smith, L. F., and Churchwell, E. 1974, *Astr. Ap.*, **32**, 269.
Sarazin, C. L. 1977, *Ap. J.*, **211**, 772.
Smith, L. F., and Mezger, P. G. 1976, *Astr. Ap.*, **53**, 165.
Witt, A. N., and Lillie, C. F. 1973, *Astr. Ap.*, **25**, 397.

ERIC J. CHAISSON, STEPHEN M. LICHTEN, and LUIS F. RODRIGUEZ: Harvard-Smithsonian Center for Astrophysics, 60 Garden Street, Cambridge, MA 02138

CHAPTER IV

THE EXTENDED THERMAL COMPONENT AT THE GALACTIC CENTER: ALTERNATIVES AND IMPLICATIONS OF THE STAR-FORMATION BURST MODEL.

From a study of continuum maps at various radiofrequencies, Mezger (1974) proposed the existence of an extended ($\sim$ 30' or 100 pc) thermal component at the Galactic Center. As in some peculiar conditions non-thermal emission can mimic the flat spectra characteristic of thermal emission ($S_\nu \propto \nu^{-0.1}$), the reality of this component remained uncertain. In an important paper, Kesteven and Pedlar (1977) detected broad ($\Delta v \simeq 100$ km s^{-1}) emission coming from an extended region around the Galactic Center. We confirmed this broad emission and found that it appeared to be close to LTE, at least in the 1-10 GHz range, by detecting the H94α (7.8 GHz) radio recombination line. These results are discussed in Chapter V.

Further research was made by us at 3 GHz trying to address the nature of the ionizing agent of this extended gas. We present these results in Chapter VI.

The main conclusions of these two papers are: 1) the ionized gas forming the extended thermal component is very close to LTE, and 2) this gas has a low degree of excitation, as indicated by the observationally-determined upper limits to the ratios of once- and twice-ionized helium to ionized hydrogen, $y^+ \lesssim 0.03$, and $y^{++} \lesssim 0.01$.

In Chapter VI we favor as the ionizing agent (4×10^{51} phot s^{-1} are needed) of the extended thermal component a large number ($\sim 10^4$) of early B-type stars remaining from a huge burst of star formation that may have occurred at the Galactic Center about 10^7 years ago.

To a suggestion of Dr. G. G. Fazio we explore in this chapter an alternate possibility; that of having a synchrotron (non-thermal) source

as the ionizing agent. This possibility is attractive because we know that the gas observed in quasars and nuclei of radio galaxies is most probably being ionized by a luminous synchrotron source.

A one-component synchrotron source is characterized by three frequency regimes (see Figure 1):

1) The optically thick or self-absorbed regime. It occurs at frequencies below the turnover frequency, ν_{TURN}, and has a flux dependent on frequency as $S_\nu \propto \nu^{2.5}$. The turnover frequency is given approximately by (Kellermann and Pauling-Toth 1969):

$$\left(\frac{\nu_{TURN}}{GHz}\right) \simeq 34\left(\frac{B}{gauss}\right)^{1/5}\left(\frac{S_{max}}{Jy}\right)^{2/5}\left(\frac{\theta}{arc\ sec}\right)^{-4/5} ,$$

where B is the magnetic field, S_{max} is the flux at maximum (which occurs at $\sim \nu_{TURN}$), and θ is the angular diameter of the source.

2)The optically thin regime. It occurs at frequencies $\nu_{TURN} \lesssim \nu \lesssim \nu_{CUT}$, where ν_{CUT} is the cutoff frequency given approximately by

$$\left(\frac{\nu_{CUT}}{GHz}\right) \simeq \left(\frac{B}{gauss}\right)^{-3}\left(\frac{t}{years}\right)^{-2} ,$$

where t is the time since the last injection of relativistic particles. In the optically thin regime the flux has a frequency dependence $S_\nu \propto \nu^{-\alpha}$, where α is the spectral index, related to the slope in the cosmic ray flux, p, by

$$\alpha = \frac{p-1}{2} .$$

Typically, $p \simeq 2.4$, and thus $\alpha \simeq 0.7$.

3) The turned-off regime. It occurs at $\nu \gtrsim \nu_{CUT}$ and no significant emission is expected.

To evaluate the excitation (the relative amounts of He , He^+, and He^{++}) of an H II region ionized by a synchrotron source, we will start by considering the simplest case, that is, a spectrum with a single spectral index extending from the radio frequencies to the gamma-ray frequencies. This is the typical ionizing source assumed in QSO models such as those of Chan and Burbidge (1975).

The ratio of He-ionizing photons to H-ionizing photons is given by:

$$R^+ = \frac{\int_{\nu_{He}}^{\nu_{CUT}} \nu^{-(\alpha+1)}\, d\nu}{\int_{\nu_H}^{\nu_{CUT}} \nu^{-(\alpha+1)}\, d\nu}$$

where $h\nu_H$ = 13.6 eV and $h\nu_{HE}$ = 24.6 eV.

The ratio of He^+-ionizing photons to H-ionizing photons is given by:

$$R^{++} = \frac{\int_{\nu_{He^+}}^{\nu_{CUT}} \nu^{-(\alpha+1)}\, d\nu}{\int_{\nu_H}^{\nu_{CUT}} \nu^{-(\alpha+1)}\, d\nu}$$

where $h\nu_{HE^+}$ = 54.4 eV. As $\nu_{CUT} \gg \nu_{He^+}$, we integrate to obtain

$$R^+ = (0.55)^{\alpha}$$

$$R^{++} = (0.25)^{\alpha}.$$

For the typical $\alpha = 0.7$ we get $R^+ = 0.66$ and $R^{++} = 0.38$. These large fractions of He- and He^+-ionizing photons would produce $y^{++} \simeq 0.05 - 0.10$, in disagreement with the observed $y^{++} \lesssim 0.01$.

Two variations of the model can be proposed to account for the low

degree of excitation of the extended thermal continuum: 1) a larger value of α, or 2) a $\nu_{CUT} \simeq 24$ eV. In what follows we discuss these two variations in detail.

1) A larger value of α.

A more steep slope will have a smaller fraction of energetic photons and could produce a lower excitation. To be consistent with the observed $y^{++} \lesssim 0.01$, we need $R^{++} \lesssim 0.04$. From the formula above we find that $\alpha \simeq 2.3$ is required. As far as we know there are no slopes this steep ever reported in radio galaxies or QSOs. Curiously, the nonthermal spectrum of pulsars is usually very steep, $\alpha \simeq$ 2-3, and could account for the low excitation. Unfortunately, pulsars have very little emission at high frequencies. To discuss this quantitatively we first note that the number of H-ionizing photons, N_i, produced by a synchrotron source is given by

$$\left(\frac{N_i}{\text{photons s}^{-1}}\right) = 1.8 \times 10^{47} \left(\frac{D}{\text{kpc}}\right) \frac{1}{\alpha} \left(\frac{S_\nu}{\text{Jy}}\right) \left(\frac{\nu}{3.3\text{X}10^6 \text{ GHz}}\right)^{\alpha}$$

where D is the distance to the source, α the spectral index, and S_ν the flux measured at a frequency ν.

As an example, we will calculate the number of ionizing photons produced by PSR1133 + 16, a pulsar at D $\simeq$ 0.2 kpc, and with $S_\nu \simeq$ 1 Jy at 1 GHz. Its spectral index is $\alpha \simeq 2.5$. We find $N_i \simeq 1.5 \times 10^{29}$ phot s^{-1}. About 2×10^{22} pulsars would be needed to ionize the extended thermal component. As the inner 200 pc of our Galaxy has a mass of about 3×10^9 $M_\odot$, we can totally rule out this possibility, since each pulsar is believed to have a mass of about 1 $M_\odot$.

An exception to the typical low luminosity of pulsars at high energies

is the Crab Pulsar, which has strong optical, UV, X-ray and gamma-ray emission. The Crab Pulsar has D = 2 kpc, and at $\nu \simeq 10^6$ GHz, $S_\nu \simeq 0.01$ Jy, $\alpha \simeq 1$. This gives $N_i \simeq 2 \times 10^{45}$. About 2×10^6 "Crab Pulsars" would be needed to explain the ionization. This is not inconsistent with the mass known to exist within 200 pc of galactocentric radius. Anyway, two serious difficulties appear: i) the spectral index, $\alpha \simeq 1$, would produce a high degree of excitation, and ii) each one of these 2×10^6 pulsars would be expected to be associated with a young supernova remnant, such as the Crab Nebula. At ν = 10 GHz the Crab Nebula has $S_\nu \simeq 400$ Jy. At the Galactic Center they would add to give $S_\nu = 3 \times 10^7$ Jy, about four orders of magnitude larger than the observed $S_\nu \simeq 1000$ Jy, of which a fraction is actually thermal.

Similar arguments rule out supernova remnants as the ionizing agent of the extended thermal component. The Crab Nebula has D = 2 kpc, and at $\nu \simeq 10^5$ GHz, $S_\nu \simeq 10$ Jy, and $\alpha = 1$. We obtain $N_i \simeq 2 \times 10^{47}$ phot s^{-1}. About 2×10^4 are needed and at the Galactic Center they would produce (at ν = 10 GHz), $S_\nu \simeq 3 \times 10^5$, about two orders of magnitude larger than observed.

2) A frequency cutoff at about 24 eV.

This second variation will ionize H, but not He, and could be obtained by proposing that the last particle injection took place 500 years ago (for $B \simeq 10^{-4}$ gauss).

Finally, we would like to discuss what turns out to be the major difficulty for a synchrotron model: the impossibility of keeping $\nu_{TURN} \gtrsim 100$ GHz for a considerable amount of time. We need a self-absorbed synchrotron source because, as we mentioned, there is no strong radio source at the Galactic Center (this is, of course, relative to radio active galaxies).

To provide the 4×10^{51} photons s^{-1} required to mantain the observed ionization we would need (for a source with $\nu_{TURN} \simeq 100$ GHz, $B \simeq 10^{-4}$ gauss, and $\alpha \simeq 0.7$); $S_{max} \simeq S_{100\ GHz} \simeq 2 \times 10^5$ Jy. Due to the self-absorption, we would also have $S_{10\ GHz} \simeq 10^3$ Jy, consistent with the measured values. We can determine the angular diameter of the required source by inverting the expression for the turnover frequency. We obtain:

$$\left(\frac{\theta}{\text{arc sec}}\right) \simeq 82 \left(\frac{\nu_{TURN}}{\text{GHz}}\right)^{-5/4} \left(\frac{B}{\text{gauss}}\right)^{1/4} \left(\frac{S_{max}}{\text{Jy}}\right)^{1/2} .$$

From the given parameters we obtain $\theta \simeq 12''$. At the Galactic Center this is equivalent to 0.6 pc.

As the energy content of these sources is large, they expand at $\sim$ c. We then find that it was created only about 2 years ago. From the van der Laan (1966) model we find that ν_{TURN} will displace to lower frequencies with time as

$$\nu_{TURN} \propto t^{-2.5},$$

while S_{max} changes as

$$S_{max} \propto t^{-3.1}.$$

In just about 10 years we will have $\nu_{TURN} \simeq 10$ GHz and $S_{max} \simeq 10^4$ Jy.

This would be very notorious since the 10 GHz flux would be an order of magnitude larger than what is observed. Furthermore, all the flux would appear concentrated in a dominant, intense source. This is not observed, and to assume that we are only within two years of the formation of the source implies that we are now living in an extremely privileged moment.

In summary, we find that although there is no physical impossibility in creating a synchrotron source capable of ionizing considerable amounts of hydrogen without strong emission in the radio, the situation is unstable in time and lasts only about 10 years.

In what remains of this chapter we will discuss some astrophysical consequences of the star-formation burst model proposed in Chapter VI. In brief, the model consists in assuming that there was a huge burst of star formation at the Galactic Center about 10^7 years ago. This is not unreasonable, since van der Kruit (1971) has proposed the same epoch for the ejection of matter that may have created the 3-kpc arm. We propose that a large amount of gas ($\sim 4 \times 10^6$ $M_\odot$) was transformed into stars in this burst. Although considerable, this mass is only $\sim 10\%$ of the mass now present in molecular clouds at the Galactic Center (Oort 1977). As we really do not know the details of the star formation process at the Galactic Center, we assumed that, as it happens in the Galactic Disk, OB clusters of ~ 2000 $M_\odot$ are formed, with a mass distribution following the initial mass function of Salpeter (1955). These clusters are assumed to have a continuous distribution od stars in the range of spectral types from O5 to K5. We do not consider later spectral types because OB clusters are known to be deficient in low-mass stars (von Hoerner 1968). It is educative to consider how the

2000 $M_\odot$ are distributed in each cluster. About 1300 stars are formed from the 2000 $M_\odot$. From the tabulations of Mezger, Smith, and Churchwell (1974) we find that the stars are distributed approximately as follows: 7 O-type, 90 B-type, 160 A-type, 190 F-type, 270 G-type, and 570 K-type.

After a few million years the earliest O-type stars arrive at the end of their main sequence life (most probably becoming a supernova), and we consider them to cease contributing to the cluster's ionizing radiation. After $\sim$12 million years all early O-type stars are gone and the cluster's luminosity is dominated by the late O-type and early B-type stars. This is the stage where we believe to be now. We need to allow the clusters to evolve because the early O-type stars present at the beginning would ionize helium to produce $y^+ \simeq 0.1$, in disagreement with the observed $y^+ \lesssim 0.03$.

An important aspect of this problem is that a large number of supernova (SN) are expected to be produced by the 2000 evolving clusters. We have to dispose of $\sim 10^4$ O-type stars is a lapse of $\sim 10^7$ years. This gives a production rate of $\sim$1 SN every 10^3 years. For a comparison, the Galaxy as a whole produces $\sim$ 20 SN every 10^3 years (Montmerle 1978).

We will consider two aspects of this problem: 1) the non-thermal radio emission expected from the supernova remnants (SNR), and 2) the gamma-ray emission expected from the interaction of the cosmic rays produced by the SNR with the dense molecular clouds also present at the Galactic Center.

1) The Non-Thermal Radio Emission.

A young (~300 years) supernova remnant like Cas A would produce $S_{10\ GHz} \simeq 50$ Jy, if located at the Galactic Center. The flux density for this SNR decreases with time as (Shklovsky 1960, Scott et al. 1969):

$$S_\nu \propto t^{-1.3}.$$

Its flux in time can be then described as

$$S_{10\ GHz} \simeq 10 \left(\frac{t}{1000\ \text{years}} \right)^{-1.3} .$$

We can integrate the total flux expected from all past SNR:

$$S_{10\ GHz}(\text{TOTAL}) = \sum_{t=0}^{10^4} 10(t + t_{\text{LAST SN}})^{-1.3} .$$

In this equation, t is the time in units of 10^3 years and $t_{\text{LAST SN}}$ is the time in units of 10^3 years since the last SN. In Table 1 we give (from a numerical summation) the non-thermal flux expected from the Galactic Center as a function of $t_{\text{LAST SN}}$. Note that the total flux is largely dominated by the contribution from the last SN.

We can certainly rule out $t_{\text{LAST SN}} \leq 100$ years because we do not see a dominant strong source. For $100 \leq t_{\text{LAST SN}} \leq 1000$ years we find that even the highest values for the flux are consistent with

the estimated upper limit of less than a few 10^2 Jy of non-thermal emission at 10 GHz. Sgr A East, the dominant non-thermal source at the Galactic Center would be, in this hypothetical scenario, the last SN. Its size ($\theta \simeq 2'$) suggests an age of $\sim$ 300 years (if we assume an expansion velocity of 10^4 km s^{-1}). Its expected flux at 10 GHz would be 50 Jy and this is consistent within a factor of 2 with the observed 100 Jy.

We conclude that the predicted non-thermal flux from the SNRs is consistent with the observed values.

2) The Gamma-Ray Emission.

This aspect of the problem was noted to us by Dr. J. E. Grindlay. There is recent evidence that the spatial coincidence of young SNR with OB associations appears to be conducive to gamma-ray emission (Montmerle 1978). These spatial coincidences, named SNOBs by Montmerle, are assumed by him to generate the γ-ray emission in a three-step sequence. Young stars undergoing an eruptive or flaring stage inject low-energy (MeV range) cosmic rays to the surrounding medium. These low-energy cosmic rays are then accelerated to higher energies (GeV range) by SNR shock fronts (by means of the first-order Fermi mechanism). Finally, These high-energy cosmic rays interact with the nuclei of the gas in the dense molecular clouds to which the OB associations are related. Pions are produced in these cosmic ray interactions within the cloud and the decay of π^0 mesons yields $\sim$100 MeV γ-rays.

Montmerle estimates that every SNOB emits $\sim 2 \times 10^{39}$ photons s^{-1} above 100 MeV.

About 20 SNR are formed in our Galaxy every 10^3 years (Montmerle 1978). As only young ($<10^4$ years) SNOBs are expected to be γ-ray emitters, a total of 200 SNOBs is expected to exist in the Galaxy, located mainly in the 5-kpc ring. By the same token, as we have estimated an SN rate of $\sim$1 every 10^3 years, we expect $\sim$10 SNOBs capable of γ-ray emission within a radius of 200 pc from the center.

How much γ-ray emission is then expected from the Galactic Center? The expected flux is

$$P(\text{phot}\gtrsim 100 \text{ MeV cm}^{-2} \text{ s}^{-1}) \simeq \frac{10 \times 2 \times 10^{39}}{4\pi \ (10 \text{ kpc})^2} \simeq 1.7 \times 10^{-6} \text{ phot cm}^{-2} \text{ s}^{-1}.$$

Hermsen et al. (1977) give the flux of the sources detected by the γ-ray satellite COS B in units relative to the intensity of the Crab (CG 185-5), $P(\text{Crab}) = 3.5 \times 10^{-6}$ phot cm^{-2} s^{-1}. We then have $P(\text{Galactic Center}) \simeq 0.5\ P(\text{Crab})$.

Recent results from COS B (Bennett et al. 1978) give $P(\text{Galactic Center}) \lesssim 1.2\ P(\text{Crab})$, so we conclude that their upper limit is consistent with our estimate, and that our star-formation burst model does not predict γ-ray fluxes exceeding the observed upper limits.

REFERENCES

Bennett, K., Bignami, G. F., Buchcheri, R., Hermsen, W., Kanbach, G., Lebrun, F., Mayer-Hasselwander, H. A., Paul, J. A., Piccinotti, G., Scarsi, L., Soroka, F., Swanenburg, B. N., and Wills, R. D. 1978, Recent Advances in Gamma-Ray Astronomy. ESA Symposium, P. 83.

Blaauw, A. 1964, Ann. Rev. Astr. Ap., 2, 213.

Chan, Y. T., and Burbidge, E. M. 1975, Ap. J., 198, 45.

Hermsen, W., Swanenburg, B. N., Bignami, G., Boella, G., Buccheri, R., Scarsi, L., Kanbach, G., Mayer-Hasselwander, H. A., Masnou, J. L., Paul, J. A., Bennett, K., Higdon, J. C., Lichti, G. G., Taylor, B. G., and Wills, R. D. 1977, Nature, 269, 494.

Kellermann, K. I., and Pauliny-Toth, I. I. K. 1969, Ap. J., 155, L71.

Kesteven, M. J., and Pedlar, A. 1977, M.N.R.A.S., 180, 731.

Mezger, P. G. 1974, Proc. ESO/SRC/CERN Conference on Research Programmes for Large Telescopes, p. 79.

Mezger, P. G., Smith, L. F., and Churchwell, E. 1974, Astr. Ap., 32, 269.

Montmerle, T. 1978, submitted to Ap. J.

Oort, J. H. 1977, Ann. Rev. Astron. Ap., 15, 295.

Salpeter, E. E. 1955, Ap. J., 121, 161.

Scott, P. F., Shakeshaft, J. R., and Smith, M. A. 1969, Nature, 223, 1139.

Shklovsky, I. S. 1960, Soviet Astronomy, 4, 243.

van der Kruit, P. C. 1971, Astr. Ap., 13, 405.

van der Laan, H. 1966, Nature, 211, 1131.

von Hoerner, S. 1968, in Interstellar Ionized Hydrogen, New York: W. A. Benjamin Inc., p. 101.

TABLE 1.

NON-THERMAL RADIATION EXPECTED FROM ALL PAST SUPERNOVAE AT THE GALACTIC CENTER

$t_{LAST\ SN}$ (10^3 yrs)	$S_{10\ GHz}$(TOTAL) (Jy)	FRACTION CONTRIBUTED BY THE LAST SN
0.1	235	0.85
0.2	115	0.70
0.3	81	0.59
0.4	65	0.51
0.5	55	0.45
0.6	49	0.40
0.7	45	0.35
0.8	42	0.32
0.9	39	0.29
1.0	37	0.27

FIGURE CAPTION.

Figure 1. The three frequency regimes of a one-component synchrotron source.

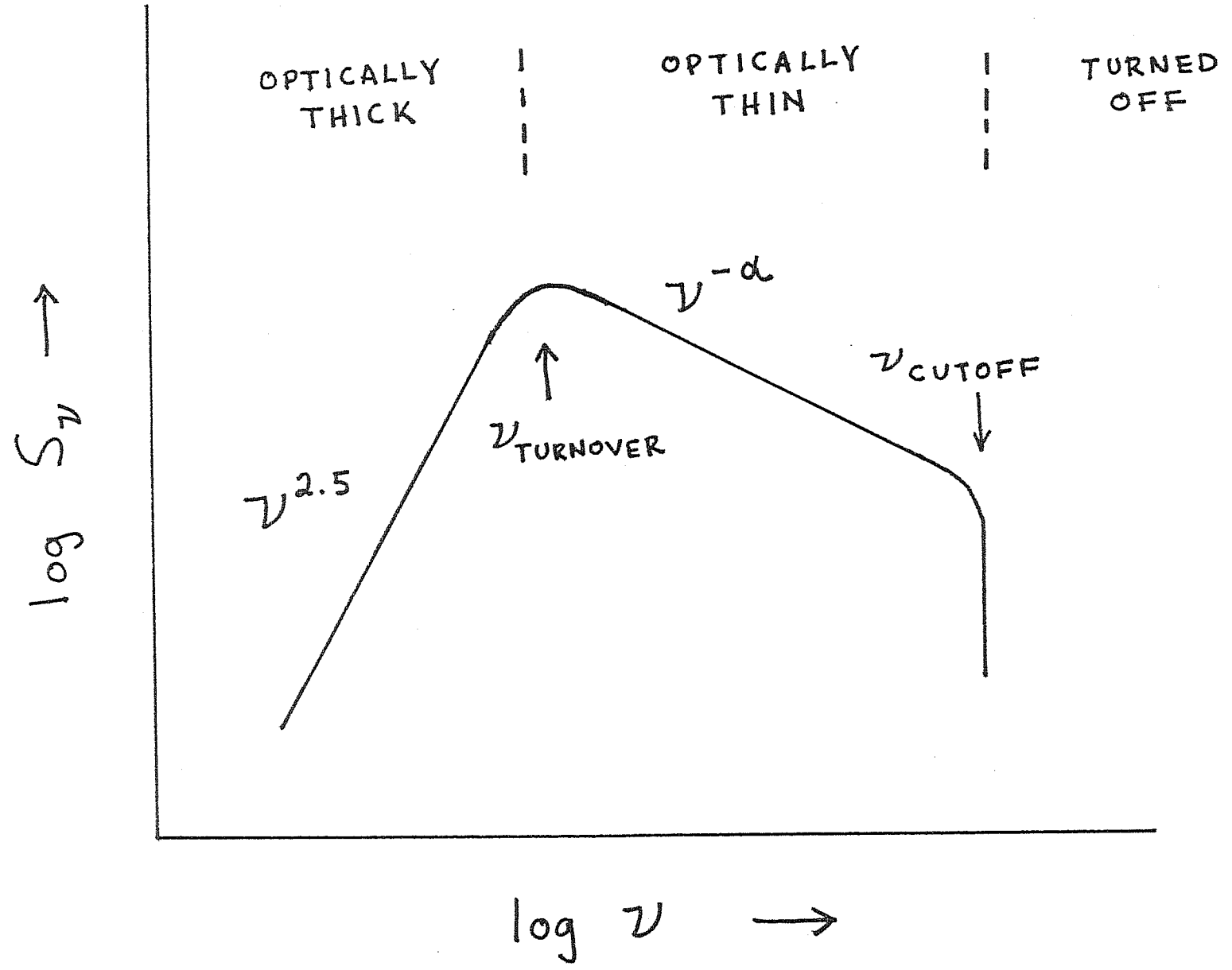
OPTICALLY THICK
OPTICALLY THIN
TURNED OFF
$\nu^{-\alpha}$
ν_{CUTOFF}
$\nu_{TURNOVER}$
$\nu^{2.5}$
log S_ν →
log ν →

FIGURE 1

Mon. Not. R. astr. Soc. (1978) 184, 145–148

CHAPTER V

Broad-line H94α emission from the extended thermal component in the Galactic Centre

Luis F. Rodriguez* and Eric J. Chaisson† *Harvard–Smithsonian Center for Astrophysics, 60 Garden Street, Cambridge, Massachusetts 02138, USA*

Received 1977 December 7

Summary. Observations of broad-line H94α (7.8 GHz) radio recombination emission from the extended thermal component in the Galactic Centre agree well with the expected high-frequency counterpart of the H166α (1.4 GHz) observations by Kesteven & Pedlar. The kinematics and possible ionizing agents of this extended gas are discussed.

Introduction

Based on comparisons of radio-continuum maps of the Galactic Centre, Mezger (1974) proposed the existence of an extended (~30 arcmin or 100 pc) thermal component of moderate emission measure (EM ~ 10^5 cm^{-6} pc). The reality of this component remained controversial since, although radio-recombination lines are observed in several compact sources at the Galactic Centre, there was no clear indication of extended line-emission.

Recently, a 1.4-GHz map by Kesteven & Pedlar (1977) produced strong evidence favouring Mezger's hypothesis; they observed broad-line (~100 km/s) H166α emission coming from an extended region in the vicinity of the Galactic Centre. To obtain further information on the nature of this extended ionized gas we observed its broad-line emission at substantially higher frequency and spatial resolution.

Observations

At 7.8 GHz, the 36.6-m radiotelescope of the Haystack Observatory has a beam size at half power of 4 arcmin and a sensitivity of 6 Jy/K for a point source. A cooled parametric amplifier fed the signal into a 100-channel autocorrelation spectrometer sampling a 25-MHz bandwidth. The main-beam output was switched at 5 Hz against that from a sky horn. Five-minute comparison observations taken about 5 minutes to the west of the source were subtracted from signal observations of equal duration on the source. To achieve even greater baseline stability, we (i) added equal numbers of observing runs with the Cassegrain subreflector in its normal position and with it defocused λ/4 toward the main reflector, and

* Becario del Consejo Nacional de Ciencia y Tecnologia, Mexico.
† Alfred P. Sloan Foundation Research Fellow.

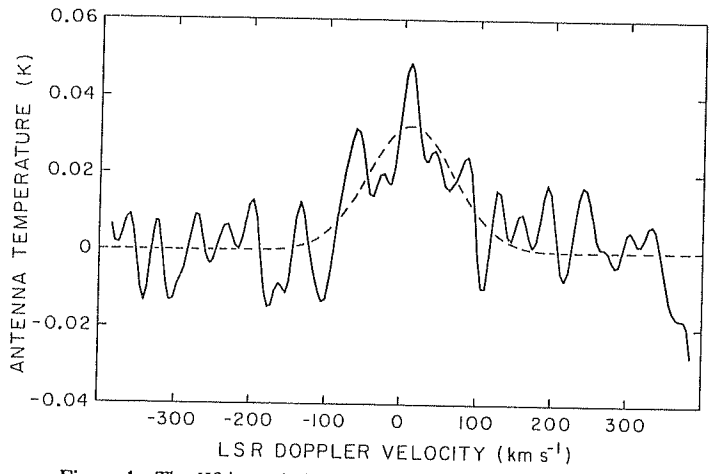

Figure 1. The H94α emission after removal of a linear baseline.

(ii) restricted our observations to ±1hr from transit. The system temperature averaged 130 K, of which approximately 30 K were contributed by the microwave switch. The observations were taken at $\alpha = 17^{h}43^{m}25^{s}$, $\delta = -28^{\circ}51'19''$, epoch 1950.0, in the direction of the source G0.16 − 0.15. Previous radiospectroscopic observations of this source (Pauls *et al.* 1976) did not detect recombination lines, possibly because of the relatively narrow bandwidth used. We observed the source during three consecutive nights. The data were Hanning-weighted, resulting in a velocity resolution of 19 km/s. Fig. 1 shows the resulting spectrum after removal of a linear baseline.

To measure the bulk parameters of the line emission we fitted by least-squares a Gaussian curve to the data. The resulting values are: antenna line-temperature, $T_L = 0.032 \pm 0.004$ K; full width at half power, $\Delta v = 134 \pm 26$ km/s; and velocity with respect to the local standard of rest, $v_{LSR} = 11 \pm 10$ km/s. We also measured simultaneously a continuum temperature $T_c = 3.86 \pm 0.14$ K.

Interpretation

The broad-line H94α emission observed by us agrees with the expected high-frequency counterpart of the H166α extended emission detected by Kesteven & Pedlar (1977). As these researchers did not directly observe the position $l = 0^{\circ}.16$, $b = -0^{\circ}.15$, we have interpolated the parameters of their observations at $l = 0^{\circ}.2$, $b = 0^{\circ}.0$ and at $l = 0^{\circ}.0$, $b = -0^{\circ}.2$ to compare with our data. This procedure is reasonable since the line emission appears to vary smoothly with position. Correcting our data for a beam efficiency of 0.53 we find

$$\frac{\left[\int T_L^B \, dv\right] 1.4 \text{ GHz}}{\left[\int T_L^B \, dv\right] 7.8 \text{ GHz}} = 5.4 \pm 1.5,$$

where T_L^B is the brightness line-temperature. This value agrees well with the ratio of 5.6 expected under conditions of local thermodynamic equilibrium (LTE) and the agreement, obtained for lines at considerably different frequencies, suggests that in both cases we are observing ionized gas close to LTE.

Another interesting parameter to determine is the electron temperature, T_e. From the mean values by Kesteven & Pedlar previously discussed and the ratio of line to continuum,

we obtain

$T_e \leqslant 9000 \pm 2000$ K,

on the assumption that the gas is optically thin and in LTE. The inequality is due to the possibility that part of the continuum emission could be of non-thermal origin. Similarly, the line to continuum ratio of our data yields:

$T_e \leqslant 15\,000 \pm 3000$ K.

Again, the inequality is due to a possible non-thermal contribution in the continuum measurement. We estimate that approximately one-third of our 7.8-GHz continuum value arises as non-thermal emission from the source G0.16 − 0.15 itself; should this be the case, the corrected value of T_e becomes approximately 10 000 K. The data of Kesteven & Pedlar were taken with a larger beam, and any possible compact non-thermal emission becomes diluted with respect to the extended thermal emission.

Our observations and those of Kesteven & Pedlar can be used to eliminate three possible mechanisms for the unusual broadening of this line emission. Thermal broadening alone is discounted on the basis of the above upper limits for the electron temperature. Pressure broadening alone is also unlikely since observations at very different frequencies show approximately the same linewidths. Finally, broadening due to projected galactic rotation appears unfeasible because our observation and several of the positions of Kesteven & Pedlar's map were at small galactic longitude where the projected components of the rotation velocity of this extended ionized gas are small. Furthermore, it is unlikely that these three broadening mechanisms could combine to produce a line width of the order of 100 km/s as observed.

The two more plausible mechanisms of line broadening appear to be systematic expansion or contraction, as proposed by Kesteven & Pedlar, and supersonic turbulence. Both mechanisms have difficulties of their own. Our H94α observation was made with considerable spatial resolution at one edge of the extended thermal component; consequently a substantial narrowing of the line is expected for a spherically symmetric expansion or contraction. Our H94α line, however, is not appreciably narrower than their H166α line. On the other hand, supersonic turbulence requires a strong source of mechanical energy to be maintained against dissipation.

Possible ionizing agents

From the results of Mezger (1974), Kesteven & Pedlar (1977) and this paper, we find that the following parameters approximately describe the extended thermal component in the Galactic Centre (assuming spherical symmetry and $T_e = 10^4$ K):

Emission measure, EM $\simeq 10^5$ cm^{-6} pc
Linear dimension, $L \simeq 100$ pc
Rms electron density, $\langle n_e^2 \rangle^{1/2} \simeq 30$ cm^{-3}
Ionized mass, $M_{\mathrm{H\,II}} \simeq 4 \times 10^5 M_\odot$
Flux density at 7.8 GHz, $S \simeq 400$ Jy
Lyman continuum photon rate required to maintain the observed ionization, $N_i \simeq 4 \times 10^{51}$ photon/s.

In what follows we discuss three possible ionizing agents for the extended thermal component. Fortunately, each one of them produces different ratios of once- and twice-ionized helium to ionized hydrogen, He^+/H^+ and He^{++}/H^+, and future experiments should be able to distinguish which agent, if any, is dominating the ionization.

(1) Late O and early B stars outside dense H II regions, such as those possibly responsible for the ionization of the low-density interstellar medium (Torres-Peimbert, Lazcano-Araujo & Peimbert 1974). From the tabulations by Panagia (1973) we find that about a thousand O8 main-sequence stars would be required. In this case one expects $0.00 \leqslant He^{+}/H^{+} \leqslant 0.05$ and $He^{++}/H^{+} = 0.00$.

(2) UV photons escaping from the OB associations in the nuclear disk. The ionizing flux of about a hundred O5 main-sequence stars can provide the observed ionization but, since a substantial fraction of the photons produced by OB associations are used in ionizing their own parent nebula, a larger number of stars would have to be involved. Observations should yield $0.05 \leqslant He^{+}/H^{+} \leqslant 0.10$ and $He^{++}/H^{+} = 0.00$.

(3) Nuclei of planetary nebulae. This agent is particularly interesting, although estimates of the expected ionizing rate appear to indicate that it is insufficient. Oort (1977) gives $5 \times 10^{8} M_{\odot}$ for the mass within 50 pc of the Galactic Centre. Assuming that 1.3×10^{48} photon/s is the ionization rate per planetary nebula (Terzian 1974), we find that the number of planetary nebulae per unit mass required to explain the ionization of the extended thermal component is $\kappa = 6 \times 10^{-6}/M_{\odot}$. This value is only a factor of 2 higher than the estimates of κ from Cahn & Kaler (1971). Unfortunately, recent estimates by Alloin, Cruz-Gonzalez & Peimbert (1976) indicate that κ could be substantially smaller. If this were the dominant mechanism, we would expect to measure $0.00 \leqslant He^{+}/H^{+} \leqslant 0.05$ and $0.05 \leqslant He^{++}/H^{+} \leqslant 0.10$.

Conclusions

We have observed broad-line H94α emission arising from the extended thermal component in the Galactic Centre. The parameters of this line agree with the expected high-frequency counterpart of the extended H166α emission observed by Kesteven & Pedlar (1977), indicating that both line emissions come from ionized gas close to LTE. Plausible mechanisms capable of explaining the large width of this emission are systematic expansion or contraction, or supersonic turbulence. Observations of helium radio recombination-lines may clarify the nature of the ionizing agent of this extended gas.

Acknowledgments

We are grateful to M. L. Meeks and H. L. Sellers for their collaboration concerning subreflector defocusing techniques. The Haystack Observatory of the Northeast Radio Observatory Corporation is supported in part under grant GP 25865 from the National Science Foundation.

References

Alloin, D., Cruz-Gonzalez, C. & Peimbert, M., 1976. *Astrophys. J.*, 205, 74.
Cahn, J. H. & Kaler, J. B., 1971. *Astrophys. J. Suppl.*, 22, 319.
Kesteven, M. J. & Pedlar, A., 1977. *Mon. Not. R. astr. Soc.*, 180, 731.
Mezger, P. G., 1974. *Proc. ESO/SRC/CERN Conference on Research Programmes for Large Telescopes*, p. 79.
Oort, J. H., 1977. *A. Rev. Astr. Astrophys.*, 15, 295.
Panagia, N., 1973. *Astr. J.*, 78, 929.
Pauls, T., Downes, D., Mezger, P. G. & Churchwell, E., 1976. *Astr. Astrophys.*, 46, 407.
Terzian, Y., 1974. *Astrophys. J.*, 193, 93.
Torres-Peimbert, S., Lazcano-Araujo, A. & Peimbert, M., 1974. *Astrophys. J.*, 191, 401.

CHAPTER VI.

ON THE IONIZING AGENT OF THE EXTENDED THERMAL COMPONENT IN THE GALACTIC CENTER

Luis F. Rodriguez and

Eric J. Chaisson*

Harvard-Smithsonian Center for Astrophysics

*Alfred P. Sloan Foundation Research Fellow

ABSTRACT

Observations of radio recombination lines at 3.3 GHz are used to confirm that the ionized gas in the extended thermal component of the Galactic Center is close to local thermodynamic equilibrium at microwave frequencies and to discuss the nature of its ionizing agent. The low degree of excitation implied by our observations suggests that the most probable source of ionization is a large number ($\sim 10^4$) of B-type stars remaining from a huge burst of star formation that may have occurred $\sim 10^7$ years ago at the Galactic Center.

I. INTRODUCTION

The extended thermal component in the Galactic Center is a large ($\sim$100 pc or 30') region of moderate emission measure ($\sim 10^5$ cm^{-6} pc) that was first recognized by Mezger (1974) from a comparison of radio continuum maps made at different frequencies. Radio recombination line emission from this ionized gas has been observed at 1.4 GHz (H166α) by Kesteven and Pedlar (1977) and at 7.8 GHz (H94α) by Rodriguez and Chaisson (1978). This line emission is broad (with a full width at half power of about 100 km s^{-1}), and Rodriguez and Chaisson (1978) suggest that it arises in gas close to local thermodynamic equilibrium (LTE). The data obtained by both groups of researchers imply that the electron temperature is similar to those of normal Galactic Disc HII regions ($T_e \sim 10^4$ K), although an accurate determination of T_e is difficult, since non-thermal radiation contaminates the continuum measurements.

Although the basic physical parameters (such as size, temperature, rms electron density, required flux of ionizing photons, etc.) of the extended thermal component are known, many basic questions about the nature of this interesting region remain unanswered. In particular, not well understood are the origin and destiny of this gas, as well as the nature of its ionizing agent or agents.

In this paper we present a search for the H125α, He125α, H158β, and He$^+$199α radio recombination lines. Such observations allow us to narrow the number of possible sources of ionization. The H125α and H158β lines are also used to confirm that this gas is close to LTE, at least in the 1 to 10 GHz range.

II. OBSERVATIONS

All observations were made with the 140-foot antenna of the National Radio Astronomy Observatory[1]. At the observing frequency of 3.3 GHz, we determined a half-power beam width of 10', an aperture efficienty of 0.44, and a beam efficiency of 0.60. A dual channel receiver was used to observe different lines simultaneously in two separate digital autocorrelation spectrometers. Each spectrometer had 192 channels distributed across a 10-MHz bandwidth, yielding a velocity resolution of 9.5 km s^{-1} after Hanning weighting. Receiver A was used to observe the 125α set during all four days of observation, while receiver B was used to observe the H158β line the first two days and the He^+ 199α line the remaining two days. During total-power operation on cold sky the system temperatures averaged 50 and 40 K for receivers A and B respectively. The observations were taken at the position, $\alpha = 17^h\ 42^m\ 55^s$, $\delta = -28°\ 44'\ 48''$, epoch = 1950.0 ($l^{II} = 0.°2$, $b^{II} = 0.°0$), which is the estimated centroid of the extended thermal component (Mezger 1974, Schmidt 1978).

Figure 1 shows the resulting spectra for the 125α and 158β sets as well as a search for the He^+199α line. A cubic polynomial of small curvature has been removed from these spectra. To measure the parameters of the H125α and H158β line emission, we least-squares fitted them with Gaussian functions simultaneously with the

[1]The National Radio Astronomy Observatory is operated by Associated Universities, Inc., under contract with the National Science Foundation.

baseline. The He125α and He^{+}199α lines were not detected, and significant upper limits were set in both cases. Table 1 lists the fitted line parameters as well as the upper limits. In all observations the antenna continuum temperature was measured simultaneously to be 26 ± 1 K.

III DISCUSSION

It is important to confirm our previously suggested close-to-LTE nature of this gas, since otherwise the upper limits on the once ionized and twice ionized helium that we discuss later would be meaningless. For α and β lines at approximately the same frequency arising from gas in LTE we expect a β/α ratio of 0.28. From Table 1 we find

$$\frac{[T_L\ \Delta V]_{H158\beta}}{[T_L\ \Delta v]_{H125\alpha}} = 0.29 \pm 0.02.$$

Another way of checking if the gas is close to LTE is to analyze the frequency dependence of the intensity of several α lines. For this purpose, we used the H166α (1.4 GHz) line of Kesteven and Pedlar (1977), the H94α (7.8 GHz) line of Rodriguez and Chaisson (1978), and the H125α (3.3 GHz) line reported in this paper. In each case, we determined the apparent brightness temperature of the line (the true brightness temperature convolved with the antenna beam pattern) by assuming $T_b = T_L/\eta_B$, where T_b is the apparent brightness temperature of the line, T_L is the antenna line temperature, and η_B is the beam efficiency of the antenna. The H94α line was observed at a different position than the other two lines and its intensity has been corrected assuming that its spatial variation in intensity is similar to that of the H166α line. For a source more extended than the observing beams (as it is in our case), LTE theory predicts a dependence of the form $[T_L \Delta V] \propto \nu^{-1}$ Figure 2 shows that, within the observational errors, this dependence is confirmed.

Confident that the ionized gas in the extended thermal component is close to LTE, we then proceed to a discussion of the once and twice ionized helium upper limits. For Hnα and He nα radio recombination lines of the same set, the antenna-convolved He^+ to H^+ ratio is given by $y+ = [T_L\ \Delta v]_{He n\alpha} / [T_L\ \Delta v]_{Hn\alpha}$. We then obtain, from the measurements given in Table 1, $y^+ \lesssim 0.03$. Similarly, for Hnα and He^+ n'α radio recombination lines at approximately the same frequency ($n' \simeq 4^{1/3} n$), the antenna-convolved He^{++} to H^+ ratio is given by $y^{++} = [T_L \Delta v]_{He^+ n'\alpha} / 4 [T_L \Delta v]_{Hn\alpha}$ (Chaisson and Malkan 1976). Again, from the results presented in Table 1 we find $y^{++} \lesssim 0.01$. Rodriguez and Chaisson (1978) gave a simplified description of how determinations or upper limits to y^+ and y^{++} values could be used as indicators of the degree of excitation of the gas and thus of the nature of the ionizing agent. In this respect, the low degree of excitation implied by our upper limits can be used to rule out two possible agents, at least as important or dominant contributors: nuclei of planetary nebaulae and O-type stars outside dense H II regions. Nuclei of planetary nebulae are unlikely to be an ionizing agent of significance because we would expect to measure $y^{++} \simeq 0.05$, several times larger than the observed upper limit of $y^{++} \lesssim 0.01$. This upper limit is consistent with recent results (Alloin, Cruz-Gonzalez, and Peimbert 1976) suggesting that the number of planetary nebulae per unit mass in our Galaxy is smaller than previously thought. In addition, the upper limit of $y^+ \lesssim 0.03$ makes it unlikely that O-type stars not embedded in dense H II regions could be the ionizing mechanism, for y^+ would then be expected to be in the range

of 0.05 to 0.10, in disagreement with the observed upper limit.

We make a distinction between O-type stars inside and outside dense H II regions, because there is an important difference in the way the dust absorption affects the ionization of dense and tenuous H II regions. For a given ionizing stellar cluster and nebular gas-to-dust ratio, the fraction of ionizing photons absorbed by the nebular dust becomes larger with increasing density of the surrounding H II region. This occurs because the optical depth for dust absorption for a given length increases in proportion to the hydrogen density, n_H (or equivalently, as the electron density, n_e, since the gas is practically fully ionized within the H II region), while the radius of the H II region has a dependence proportional to $n_e^{-2/3}$. To first order, then, the optical depth of dust within the H II region increases as $n_e^{1/3}$. The importance of dust absorption of ionizing photons is thus more important with increasing nebular densities. In particular, the selective dust absorption (Mezger, Smith, and Churchwell 1974; Chaisson, Lichten, and Rodriguez 1978; Thum et al. 1978) that preferentially absorbs helium-ionizing photons to produce low y^+ values is also expected to be important only at high densities. To evaluate quantitatively this effect as a function of n_e, we have considered an OB cluster with 2000 $M_\odot$ and an ionizing flux of 4.4×10^{49} photons s^{-1} (Mezger, Smith, and Churchwell 1974), creating an H II region with an electron temperature of 10^4 K. Using the approximate expressions given by Panagia and Smith (1978), we evaluated the expected y^+ values as a function of n_e. We adopted a dust absorption cross

section for H-ionizing photons of 8×10^{-22} cm^2/H-atom, a value of 4 for the ratio of the dust absorption cross sections for He-ionizing to H-ionizing photons, and a value of 0.1 for the total helium-to-hydrogen number ratio. Figure 3 summarizes these results. As can be seen, low y^+ values ($y^+ < 0.03$) can be produced only in H II regions of high density ($n_e \geq 3000$ cm^{-3}). By contrast, in a low density medium (as is the case of an unclumped extended thermal component having $n_e \simeq 10^2$ cm^{-3}), selective absorption does not affect y^+ significantly. From this we conclude that if O-type stars physically located in the extended thermal component were ionizing it, we would expect to see $y^+ \simeq 0.10$, in disagreement with our observations.

O-type stars embedded within dense H II regions (such as Sgr B2 and G0.5-0.0) constitute another possible ionizing agent. Some of their radiation could be leaking out of the nebula after suffering selective dust absorption of helium-ionizing photons. A major problem plagues this possibility, however, for an exceedingly large number of ionizing photons (4×10^{51} photons s^{-1}) is needed to keep the extended thermal component ionized. The selective dust absorption in the dense H II region will have then to account not only for the low excitation observed in them (already difficult to explain) but also for the low excitation of the extended thermal component. An even greater selectiveness in the dust absorption would be required, and this is believed to be unlikely (Panagia and Smith 1978).

One last possible ionizing agent is the presence of a large number of early B-type stars. From the tabulations of Panagia (1973),

we find that about 10^4 B0 V stars are needed to provide the observed ionization. Such a number of B- type stars could satisfactorily explain the low degree of excitation of the gas. If so, though, another problem appears. Should OB star formation in the Galactic Center take place in clusters having masses $\sim 2000\ M_\odot$, as is the case in the Galactic Disc, then we are compelled to conclude that, since no O-type stars are present in the clusters, they must have evolved for at least 10^7 years.

To discuss this situation in more detail, we have computed a simple evolutionary model of the parameters of a 2000 $M_\odot$ OB cluster. We have used the stellar parameters of Mezger, Smith, and Churchwell (1974), the initial mass function of Salpeter (1955), and assumed that a star ceased to contribute to the integrated radiation of the cluster at the end of its main sequence life. Figure 4 shows the time dependence of the cluster's luminosity, number of ionizing photons, and fraction of helium-ionizing photons for the period $0 \lesssim t \lesssim 1.5 \times 10^7$ years. Although changes in the model occur in discrete steps, we have smoothed the results to allow easier interpolation.

To account for the low degree of ionization observed for the extended thermal component, this model suggests that the many clusters responsible for the ionization have an age $t \gtrsim 10^7$ years. Compared to their zero-age values, the luminosity of the clusters has decreased by a factor of ~ 4 in this time interval, while the number of ionizing photons has decreased by a factor of ~ 20. This also implies that the mass involved in the formation of the clusters responsible for the

ionization of the extended thermal component is large, $\sim 4.0 \times 10^6$ $M_\odot$. This is a substantial fraction (10%) of the mass of gas available for star formation in the form of molecular clouds in the vicinity of the Galactic Center (Oort 1977). These approximately 2000 OB star clusters could have been produced in a burst of star formation about 10^7 years ago. This is the same epoch proposed by van der Kruit (1971) for a massive ejection of Galactic Center material that may have caused the outward motion of the 3-kpc arm. This same event may have also triggered star formation on a large scale by causing the collapse of an appreciable fraction of the gas in the molecular clouds present at the Galactic Center.

IV. CONCLUSIONS

We present 3.3 GHz observations of several radio recombination lines from the extended thermal component in the Galactic Center. Analysis of these lines confirms that this gas is close to LTE. Upper limits to the once- and twice-ionized helium abundances are used to suggest that the most probable ionizing agent is a large number of B-type stars remaining from a burst of star formation that may have occurred at the Galactic Center about 10^7 years ago.

REFERENCES

Alloin, D., Cruz-Gonzalez, C., and Peimbert, M. 1976, Ap. J., 205, 74.

Blaauw, A. 1964, Ann. Rev. Astron. Ap., 2, 213.

Chaisson, E. J. and Malkan, M. A. 1976, Ap. J., 210, 108.

Chaisson, E. J., Lichten, S. M., and Rodriguez, L. F. 1978, Ap. J. 221, 810.

Kesteven, M. J. and Pedlar, A. 1977, Mon. Not. R. Astr. Soc., 180, 731.

Mezger, P. G. 1974. Proc. ESO/SRC/CERN Conference on Research Programmes for Large Telescopes, p. 79.

Mezger, P. G., Smith, L. F., and Churchwell, E. 1974, Astr. Ap., 32, 269.

Oort, J. H. 1977, Ann. Rev. Astron. Ap., 15, 295.

Panagia, N. 1973, Astron. J., 78, 929.

Panagia, N. and Smith, L. F. 1978, Astr. Ap., 62, 277.

Rodriguez, L. F. and Chaisson, E. J. 1978, Mon. Not. R. Astr. Soc., 184, 145.

Salpeter, E. E. 1955, Ap. J., 121, 161.

Schmidt, J. 1978, Ph. D. Thesis, University of Bonn.

Thum, C., Mezger, P. G., Pankonin, V., and Schraml, J. 1978, Astr. Ap., 62, 277.

van der Kruit, P. C. 1971, Astr. Ap., 13, 405.

TABLE 1

LINE PARAMETERS

Line	Antenna line temperature, T_L. (K)	Full width at half-power, Δv. ($km\ s^{-1}$)	Velocity with respect to the local standard of rest, v_{LSR}. ($km\ s^{-1}$)
H125α	0.234 ± 0.003	82 ± 1	-1.0 ± 0.4
He125α	≤ 0.008[1]	---	---
H158β	0.066 ± 0.002	85 ± 4	-1.0 ± 1.0
He^+199α	≤ 0.009[1]	---	---

[1]Three-sigma upper limit after smoothing to an effective velocity resolution of 80 $km\ s^{-1}$).

FIGURE CAPTIONS

Figure 1. Spectra of the 125α set, the 158β set, and the frequency at which the He^{+}199α line should appear. Velocity resolution is 9.5 km s^{-1}.

Figure 2. Frequency dependence of the integrated line intensity. The dashed line is the LTE model given by $[T_b \Delta v] = 85\ \nu^{-1}$, where T_b is in K, Δv in km s^{-1}, and ν is in GHz. Error bars are estimated to be twice the standard deviation.

Figure 3. The observed ionized helium to hydrogen ratio plotted as a function of the electron density of the H II region for a 2000 $M_\odot$ zero-age OB cluster.

Figure 4. Early time evolution of the luminosity, number of ionizing photons, and fraction of helium-ionizing photons for a 2000 $M_\odot$ OB cluster.

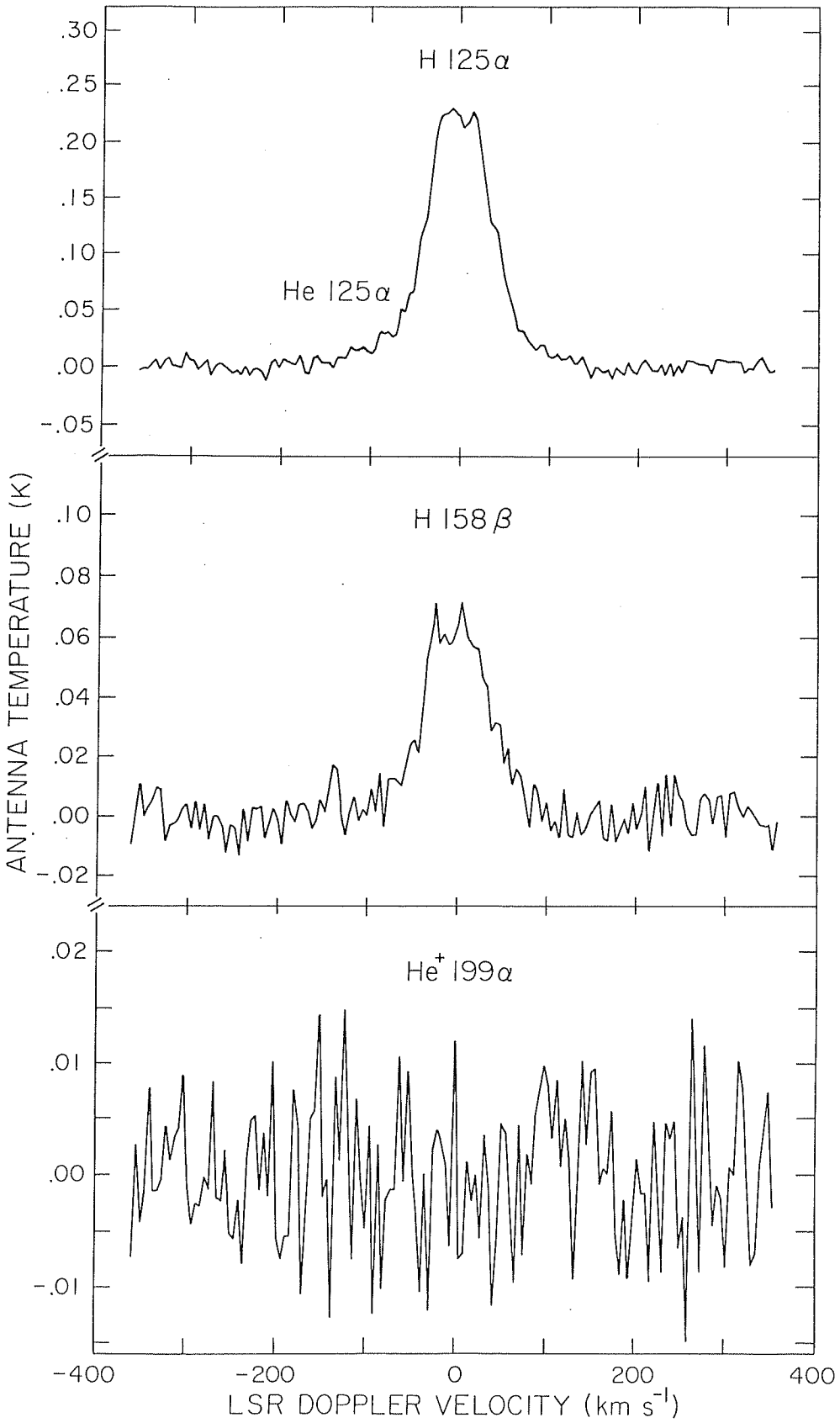
H 125α
He 125α
H 158β
He+ 199α
ANTENNA TEMPERATURE (K)
.30
.25
.20
.15
.10
.05
.00
-.05
.10
.08
.06
.04
.02
.00
-.02
.02
.01
.00
-.01
-400
-200
0
200
400
LSR DOPPLER VELOCITY (km s-1)

Figure 1

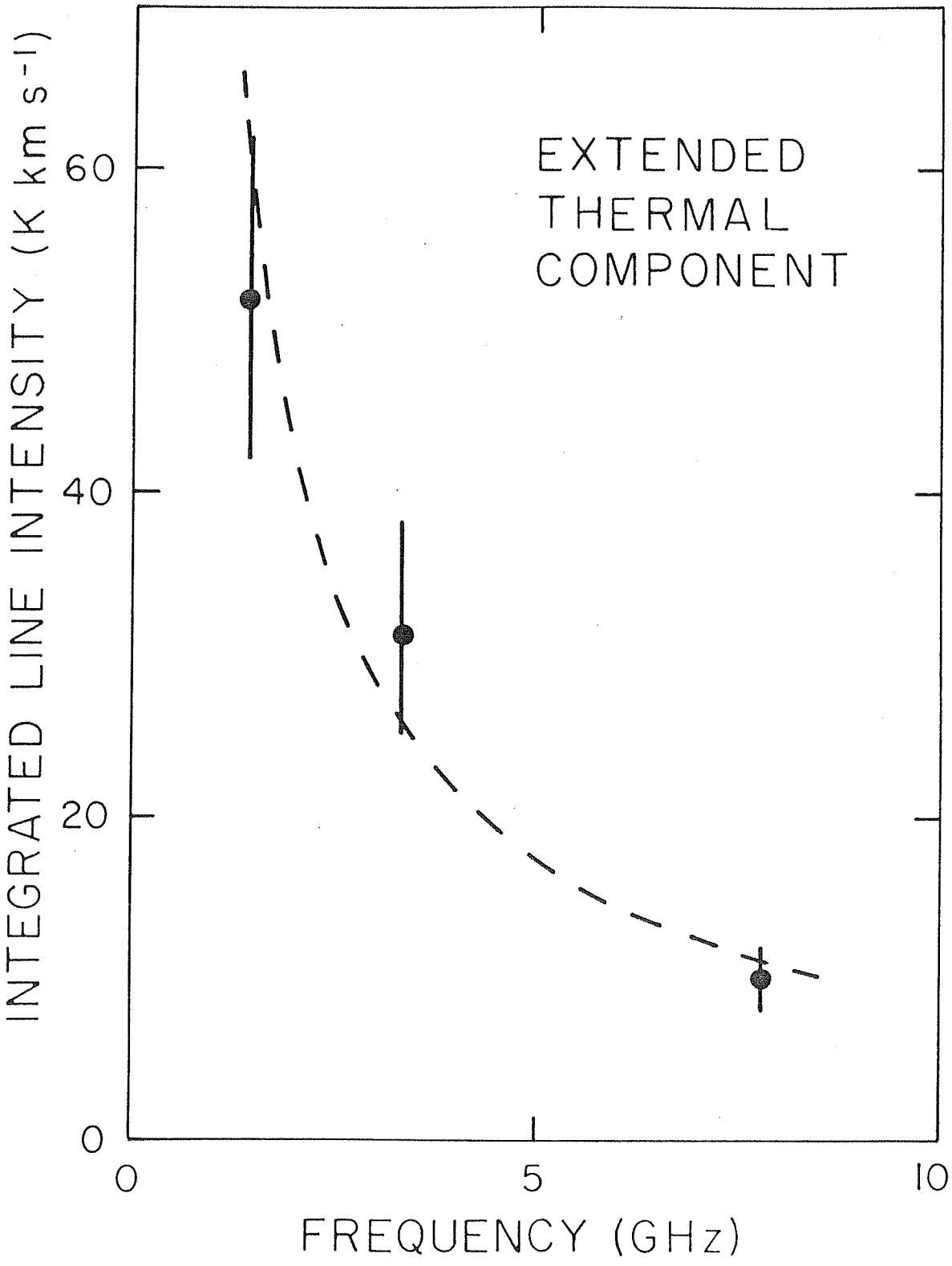
EXTENDED
THERMAL
COMPONENT
INTEGRATED LINE INTENSITY (K km s-1)
0
20
40
60
0
5
10
FREQUENCY (GHz)

Figure 2

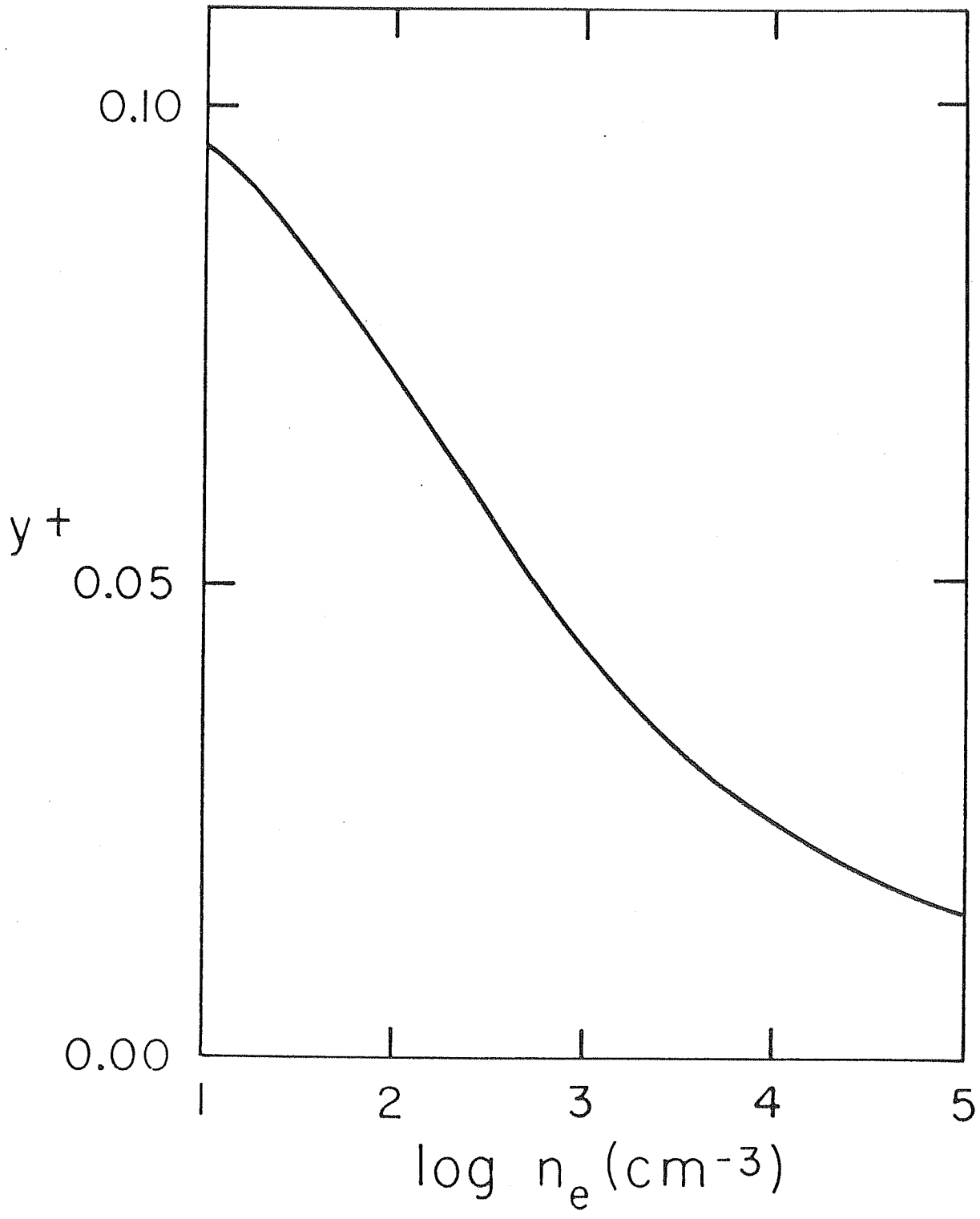

Figure 3

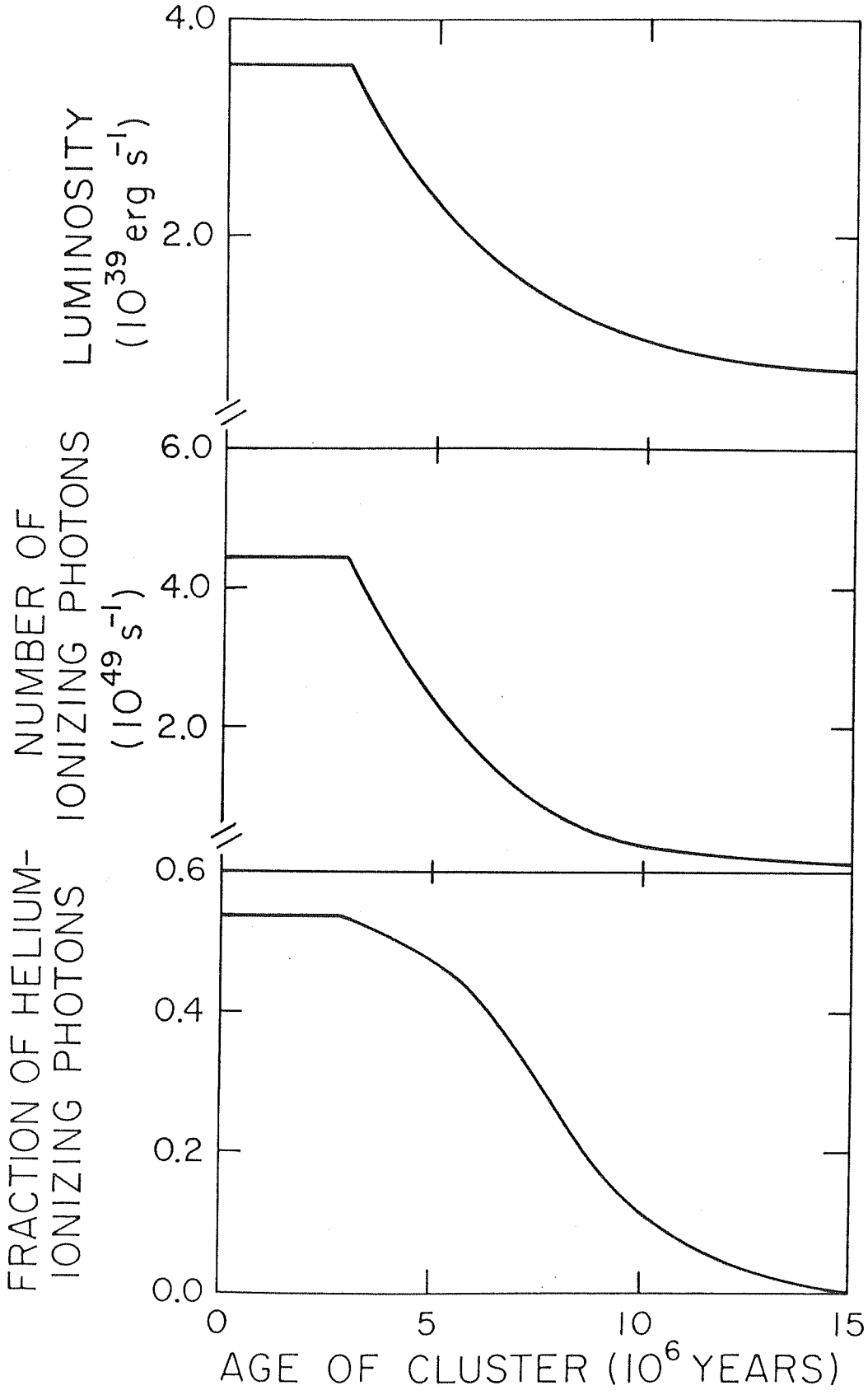
LUMINOSITY
(10^{39} erg s^{-1})
4.0
2.0
NUMBER OF
IONIZING PHOTONS
(10^{49} s^{-1})
6.0
4.0
2.0
FRACTION OF HELIUM-
IONIZING PHOTONS
0.6
0.4
0.2
0.0
0
5
10
15
AGE OF CLUSTER (10^6 YEARS)

Figure 4

CHAPTER VII

INTRODUCTION TO SGR A WEST

Sgr A West is an H II region with a very special characteristic; it coincides with the kinematic nucleus of our Galaxy. The study of its characteristics, in particular its dynamics, is very important. Due to the richness of objects observed in the direction of the Galactic Nucleus it took several years to start disentangling them. Sgr A West was detected by Downes and Martin (1971) on the basis of its flat (thermal) radio continuum spectrum.

There is a considerable number of radio recombination lines observed towards the Galactic Nucleus. Their interpretation is complex and it is convenient to separate them into two groups: low-frequency ($\nu \lesssim 1$ GHz) and high-frequency ($\nu \gtrsim 1$ GHz).

i) Low-frequency lines.

Observations made in the range 240 MHz to 1.6 GHz have been discussed by Pedlar et al. (1978). The main observational characteristics of line emission at these frequencies are the following:

1) The line emission is dominated by a feature with Δv = 20-30 km s^{-1} and $v_{LSR} \simeq 0$ km s^{-1}.

2) The peak line temperature, T_L, increases with wavelength faster than linearly. Since $T_L \propto \lambda$ is the expected LTE dependence, this indicates that non-LTE conditions are present for the low-frequency lines.

3) The ratio of peak line to continuum temperature remains approximately constant over the observed frequency range (as opposed to the LTE dependence, $T_L/T_c \propto \nu$).

Pedlar et al. adequately interpret this emission as being stimulated emission coming from a low-density ($n_e \simeq 10$ cm^{-3}), low emission measure (EM $\simeq 1500$ cm^{-6} pc) H II region located along the line of sight to the Galactic Center. These authors estimate the temperature of the ionized gas to be $T_e \simeq 5000$ K. This H II region is extended ($\sim 1^\circ$) and the lines are stimulated by the strong non-thermal background continuum from the Galactic Center. At its largest, the amplification factor,

$$T_L \text{ (observed)}/T_L\text{(LTE)},$$

is about 4. This occurs at $\nu = 240$ MHz.

All low frequency observations have been made with $\theta_A \gtrsim 10'$ and are dominated by this line-of-sight H II region. Correspondingly they give no information on the ionized gas in the vicinity of the Galactic Nucleus which extends only over about 1'. Severe beam dilution makes this small structure ionized gas essentially unobservable for the low-frequency, large-beam observations. Furthermore, even if better resolution were available (using a very large dish or array), then pressure broadening and optical thickness effects would conspire to make the observations very difficult.

By contrast, the high-frequency, small-beam observations can properly measure the small, high-EM structure, but cannot observe the extended, low-EM line-of-sight H II region responsible for the low-frequency lines. For example, at 10 GHz the line-of-sight H II region will produce $T_L \simeq$ 0.002 K, well below the sensitivity of the best radiotelescopes.

ii) High-frequency lines.

It is at the higher frequencies (and for a given antenna, smaller beamwidths) that we start observing the wide lines ($\Delta v \simeq 200$ km s^{-1})

that characterize the ionized gas in the immediate neighborhood of the Galactic Nucleus. The detection of this wide line emission was made by Pauls, Mezger, and Churchwell (1974). In the following two chapters we present two papers closely related to the problem of the ionized gas at the Galactic Nucleus. The first (Chapter VIII) clearly establishes the existence of a thermal gradient in disk H II regions; the closer the H II region is to the Galactic Center, the cooler it is. This effect is most probably due to an enrichment in the heavy element content with decreasing galactocentric distance. We speculate on the possibility of this gradient extending to the Galactic Nucleus. The second paper (Chapter IX) presents a multifrequency study of the ionized gas in Sgr A West. Several important conclusions are reached in this study and they are discussed in detail in Chapter IX.

REFERENCES

Downes, D. and Martin, A. H. M. 1971, Nature, 233, 112.

Pauls, T., Mezger, P. G., and Churchwell, E. 1974, A. A., 34, 327.

Pedlar, A., Davies, R. D., Hart, L., and Shaver, P. A. 1978, M.N.R.A.S., 182, 473.

CHAPTER VIII

A HYDROGEN AND HELIUM RADIO RECOMBINATION LINE SURVEY OF GALACTIC H II REGIONS AT 10 GHZ

Stephen M. Lichten, Luis F. Rodriguez*, and Eric J. Chaisson†

Harvard-Smithsonian Center for Astrophysics

To appear in the April 15, 1979 issue
of The Astrophysical Journal.

*Becario del Consejo Nacional de Ciencia y Tecnologia, Mexico

†Alfred P. Sloan Foundation Research Fellow

ABSTRACT

The results of a radio recombination line survey of twenty galactic H II regions are used here as a diagnostic probe of the Galaxy. At a frequency of 10.2 GHz, we do not find appreciable departures from local thermodynamic equilibrium; each H II region can be satisfactorily characterized by an average electron density and temperature. The nebular electron temperature is found to decrease monotonically by about 3000 K between 13 and 5 kpc from the Galactic Center. This Galaxy temperature gradient most probably results from an increase in the heavy element abundance by a factor of about five from 13 to 5 kpc from the Galactic Center. The observed temperature and suggested chemical gradients may extend to the Galactic Center, but observations from that region are difficult to interpret unambiguously. The ionized helium abundance also varies among different nebulae. However, since radio observations do not provide a reliable means of estimating the amount of neutral helium within H II regions, it is not feasible to determine Galaxy gradients in the total He/H ratio.

Subject headings: Galaxies: Milky Way - Nebulae: General - Nebulae: Abundances
Radio Sources: Lines.

I. INTRODUCTION

Radio recombination line observations of galactic H II regions made at frequencies less than a few GHz can sometimes be affected by departures from local thermodynamic equilibrium (LTE). Even when these departures are moderate ($\sim$ 50 %), they limit the utility of low-frequency radio recombination lines as accurate probes of the physical conditions of the ionized gas. At higher frequencies, the departures become considerably less pronounced, but other difficulties appear: The lines are weak and the atmospheric attenuation becomes substantial.

We chose 10.2 GHz for this recombination-line survey in order to minimize any non-LTE effects while simultaneously escaping serious atmospheric attenuation. The H86α, He86α, and H108β lines and their underlying continuum were measured for twenty H II regions whose positions lie between 0 and 13 kpc from the Galactic Center. The results were used to study the magnitude of the temperature gradient across the Galaxy.

II. OBSERVATIONS AND DATA REDUCTION

All observations reported here were made with the 36.6-m, radome-enclosed antenna of the Haystack Observatory[1] during November 1977 and March 1978.

---

[1]The Haystack Observatory of the Northeast Radio Observatory Corporation is supported in part under grant GP25865 from the National Science Foundation.

At 10.2 GHz, we measured a half-power beamwidth of 3!5 and an aperture efficiency of 0.34. The radiometer was a cryogenically cooled parametric amplifier, and the spectrometer a 1024-channel digital autocorrelator. An effective bandwidth of 13.3 MHz was used and each observation was Fourier transformed into a power spectrum with a Hanning weighted resolution of

1.92 km s^{-1}. The system temperature on cold sky averaged 90 K.

Spectral-line observations were made in the total-power mode. Five-minute off-source integrations were subtracted from on-source integrations of equal duration. Line and continuum temperatures were measured simultaneously. One half of the accumulated spectrum for each source was taken with the subreflector moved a quarter-wavelength inside its normal focus position. This defocusing technique was employed to minimize the baseline sinusoidal ripple resulting from reflections between the feed and the subreflector. A considerably improved spectral baseline resulted which in many cases could be fitted linearly, although sometimes a polynomial of small curvature was used.

Figure 1 shows the spectra of the observed sources. Each spectrum was least-squares fitted with Gaussian functions simultaneously with the baseline. In columns 1 thru 6, respectively, of Table 1, we list the name of the source, the 1950.0 right ascension, the 1950.0 declination, the integration time on the source, the spectral velocity resolution, and the continuum temperature T_C. Column 8 gives the line antenna temperature T_L for each of the transitions measured toward each source. These lines were usually H86α, He86α, and H108β; in some H II regions, we also measured the C86α line or a second component of the H86α line. The H86α line intensities were diminished by a small amount because of the blending of a weak He108β line. The approximate correction factor equals the product of the measured He^+/H^+ ratio and the theoretically expected β/α ratio of 0.276. We made this correction in Table 2, amounting to a change of less than 2.5 %; the results of our study are largely insensitive to it. Columns 9 and 10 tabulate for each line the full width at half intensity Δv, and the velocity with respect to the local standard of rest v_{LSR}.

The line and continuum measurements presented in Table 1 were used to determine several physical and chemical properties of the observed H II regions. Table 2 summarizes these derived quantities, which should be considered bulk, average values characteristic of each nebula as a whole: Column 1 gives the name of the source, while columns 2 and 3 list the distance of each H II region from the sun, D_S, and from the Galactic Center, D_G; these distances are in kpc and unless otherwise noted are taken from Churchwell et al. (1978). Columns 4 and 5 tabulate $T_e^*(H86\alpha)$ and $T_e^*(H108\beta)$, the electron temperatures calculated from the H86α and H108β lines using the optically thin, LTE formulation and neglecting pressure broadening. Column 6 gives y^+, the observed He^+/H^+ ratio for the 86α set, while column 7 lists the ratio, $\beta/\alpha = (T_L \Delta v)_{H108\beta} / (T_L \Delta v)_{H86\alpha}$, which equals 0.276 for gas in LTE.

III. THE RELIABILITY OF ELECTRON TEMPERATURES DETERMINED FROM HIGH-FREQUENCY RADIO RECOMBINATION LINES

The electron temperatures of Table 2 were calculated assuming that, (1) the observed lines are unaffected by pressure broadening, (2) the nebulae are optically thin at the observing frequency, (3) the line intensities are close to those expected for LTE, and (4) the derived T_e^* is an average value of the bulk electron temperature of the nebular region sampled by the antenna beam.

These are generally time-honored assumptions made by many researchers throughout the past decade. One or more of them appeared to be violated, as nebular values derived optically often differed from those found via radio techniques. Recently, however, Chaisson and Dopita (1977) suggested that the past radio-optical inconsistencies are untrue; when examined with similar spatial resolution and with modern observing techniques, gaseous nebulae appear

to be characterized by the same bulk parameters regardless of whether they are examined in the optical or radio portion of the electromagnetic spectrum.

Lockman and Brown (1978) have nonetheless claimed that several of these assumptions are not satisfied. However, as noted by Shaver (1978), the parameters of the nebulae modeled by Lockman and Brown are unrealistic, and exaggerate departures from LTE. We generally concur with Shaver's analysis. In particular, we can show both theoretically and observationally, that our assumptions are well justified at 10 GHz for nebulae having densities and emission measures in the ranges, $10^2 \lesssim N_e \lesssim 10^4$ cm^{-3} and $10^{5.0} \lesssim EM \lesssim 10^{6.5}$ cm^{-6}pc.

A) Pressure broadening.

The ratio r of total (pressure plus Doppler) to Doppler widths for hydrogen recombination lines having a Doppler full width at half-power of 25 km s^{-1} and arising from ionized gas having $T_e = 10^4$ K is (after Brocklehurst and Seaton 1972);

$$r = \frac{\Delta v_{\text{total}}}{\Delta v_{\text{Doppler}}} = \{1 + [0.12\ (\frac{n}{100})^{7.4}\ (\frac{N_e}{10^4})]^2\}^{1/2} .$$

For $N_e \lesssim 10^4$ cm^{-3}, we find $1 \lesssim r(H86\alpha) \lesssim 1.001$, and $1 \lesssim r(H108\beta) \lesssim 1.022$. Hence, pressure broadening should be negligible for both lines. Observationally, we confirm this by plotting, in Figure 2, $\Delta v(H108\beta)$ against $\Delta v(H86\alpha)$. There is no evidence that the H108β line is systematically wider than the H86α line, as expected if pressure broadening were significant.

B) Optical thinness.

For H II regions with $EM \lesssim 10^{6.5}$ cm^{-6}pc, we find an optical depth in the continuum, $\tau_{10\ \text{GHz}} \lesssim 0.008$. Thus, our assumption of optical thinness is substantiated. (Of course, the actual τ could be larger than the apparent τ derived here if the nebulae are heavily clumped, a physical condition that is nonetheless unsupported by current observations.)

C) Departure from LTE.

In Figure 3(a), we show the expected ratio of the real electron temperature to the LTE-derived electron temperature, T_e/T_e^*. This calculation is valid for H86α line measurements along the line of sight of a homogeneous and isothermal gas characterized by the range of electron densities and emission measures noted above. These calculations are shown only for $T_e = 10^4$ K since the results are relatively insensitive to this parameter. At lower frequencies, non-LTE corrections may become necessary. For example, as shown in Figure 3(b), departures from LTE are expected to become appreciable at about 5 GHz where previous surveys have been conducted (cf., e.g., Churchwell et al. 1978). But at 10 GHz, the expected departure from LTE is not significant. This theoretically expected, close-to-LTE situation at 10 GHz is confirmed by the average value ($=0.28 \pm 0.05$) of the β/α ratios observed for all the sources of our survey. This ratio may be compared to the 0.276 value expected for strict LTE.

We do not venture to say that all nebulae are close to LTE at all radio frequencies. Nor do we claim that any nebula is actually in LTE at any frequency. However, for observations of typical nebulae at 10 GHz, the assumption of LTE seems statistically justified given the experimental error inherent in any spectral measurement.

D) T_e^* as an average nebular electron temperature.

Attributing to the nebular gas a single electron density and temperature does not necessarily mean that H II regions are homogeneous and isothermal. Nor does it favor any particular nebular geometry. Indeed, radio interferometry has revealed high emission measure clumps in some nebulae. But these clumps are small and few in number, and their contribution to the total radio flux is insignificant in most cases. Furthermore, gross fluctuations in T_e have not

been observed in H II regions. Instead, the single-dish antenna beam averages over a large nebular volume and, for optically thin gas unaffected by pressure broadening and close to LTE, any nebula can be characterized by an average density, temperature, and length.

Our initial assumptions verified, we henceforth let $T_e^* = T_e$.

III. CORRELATION OF ELECTRON TEMPERATURE WITH GALACTOCENTRIC DISTANCE.

Linear regression analyses were performed to evaluate any correlation between T_e and D_G. For the H86α observations, we find a temperature gradient from D_G = 5 - 13 kpc of 390 $\pm$ 70 K/kpc. Mathematically, the relation can be expressed as, $T_e(K) = 4700 + 390\ D_G\ (kpc)$, provided $5 \lesssim D_G(kpc) \lesssim 13$. Figure 4 shows the data used and the fit derived. The correlation coefficient is r = 0.815, indicating a better than 99.9 % confidence level. Similarly, the H108β observations yield a gradient of 250 $\pm$ 150 K/kpc, with r = 0.375 (89 % confidence level). Table 3 gives the parameters for each fit. It should be emphasized that this gradient applies only to nebulae within the range D_G = 5 - 13 kpc; the gradient possibly breaks down near the Galactic Center, so Sgr B2 will be discussed separately in a later section.

Such a temperature gradient has been previously suggested for our Galaxy. Churchwell and Walmsley (1975) examined early H109α data and claimed a marginal positive correlation between T_e and D_G. A more recent H109α survey by Churchwell et al. (1978) has yielded more reliable results. They found a gradient of 310 K/kpc. Evidence for an electron temperature gradient has also been found from optical studies of a few H II regions (Peimbert, Torres-Peimbert, and Rayo 1978). Their value, 1100 K/kpc, is substantially larger than

the radio determinations of Churchwell et al.(1978) and of this paper. The reasons for this discrepancy are unclear, but increasing the number of nebulae in the optical determination would be highly desireable.

Lockman and Brown (1978) have argued that a Galaxy temperature gradient straightforwardly deduced from radio observations cannot be real. According to them, H II regions at great distances, D_s, from the sun should have lower radio-determined T_e values; since nebulae farther from the sun need to be stronger sources in order to be observed, they should have generally higher emission measures, producing stimulated line emission and thus an apparent depression in T_e^*. Low-frequency radio observations aside, we do not agree with their interpretation. Our analysis in § III indicates that this effect is not expected to be significant, at least around 10 GHz. Our statements are observationally confirmed since a regression analysis between T_e and D_s shows no systematic trend. We derive a correlation coefficient $r = -0.03$, suggesting that T_e and D_s are uncorrelated. Thus, we conclude, as have Churchwell et al. before us, that the Galaxy temperature gradient is real.

There are three effects that could account for the temperature change of about 3000 K observed in the 5 to 13 kpc range:

A) Dust in the H II regions.

If the dust possesses an absorption cross section that increases with frequency throughout the ultraviolet regime (Mezger et al. 1974), then it could effectively compete with the gas for the most energetic ionizing photons. This should produce a "softening" of the radiation field and a lower value of T_e. An increase in the dust content of H II regions towards the Galactic Center could then produce a Galaxy temperature gradient. Sarazin (1977) has computed model H II regions having a wide range of parameters, including those thought

to characterize all H II regions in the 5 to 13 kpc region. For nebulae ionized by an initial-mass-function distribution of stars, he finds the temperature change to be approximately 1500 K, provided the optical depth approaches unity for the inner regions. This value falls considerably short of the observed value of 3000 K found from our survey. At any rate, our observation of normal y^+ for nebulae with $D_G \simeq 5$ kpc seems to contradict this hypothesis.

B) Effective temperature of the exciting stars.

If the average effective temperature of the nebular exciting stars decreases toward the inner regions of the Galaxy, then a decrease in T_e with D_G would also be expected. From the calculations of Balick and Snedon (1976), we estimate that a decrease in the stellar effective temperature from 50,000 to 35,000 K would produce a T_e decrease of only about 1500 K. Lower stellar effective temperatures necessary to account for the 3000 K variation in T_e would produce $y^+ \simeq 0$ for $D_G \simeq 5$ kpc, in disagreement with the observations.

C) Heavy-element abundance.

Heavy elements (primarily oxygen, nitrogen, and sulfur) are the dominant cooling agents in H II regions. From the calculations of Balick and Snedon (1976), we estimate that an increase in the heavy element abundance from about half the solar value at $D_G \simeq 13$ kpc to about twice the solar value at $D_G \simeq 5$ kpc would produce a decrease in T_e by about 3000 K. Such a trend of heavy element enrichment toward the Galactic Center is consistent with abundance gradients found in the solar neighborhood from stellar studies by Mayor (1976) and for nebular studies by Peimbert et al. (1978). It is also consistent with heavy element enrichment previously observed toward other spiral galaxies (Searle 1971; Rubin et al. 1972; Shields 1974; Smith 1975; Shields and Searle 1978), and which is taken as evidence for an increased rate of nuclear processing toward the inner Galaxy regions.

Of the three possible interpretations suggested, the heavy element enrichment is probably the most viable. Nonetheless, since the uncertainties of each interpretation are considerable, it seems unsafe at this point to favor conclusively any of them. In fact, it is not unreasonable that all three mechanisms may contribute significantly to the observed Galaxy temperature gradient.

V. THE GALACTIC CENTER

Although the gradients measured at radio frequencies extrapolate to predict $T_e \simeq 5000$ K for nebulae near the Galactic Center, Sgr B2 has been consistently measured to have $T_e \simeq 10{,}000$ K over a wide range of frequencies (Smith and Mezger 1976; Chaisson, Lichten, and Rodriguez 1978). Sgr B2, however, is a peculiar H II region, It has very low y^+ values, its β/α ratio is the lowest in our survey, and its lines are wider than those from other nebulae. Thum et al. (1978) propose that there is an optically thick component in Sgr B2 which could conceivably explain the high value of T_e. Also, should Sgr B2 be characterized by anomalously large N_e ($\sim 10^4$ cm^{-3}), as suspected, then collisional de-excitation becomes enhanced, cooling impaired, and T_e increased. For example, an increase of about 3000 K could result for $Ne \simeq 10^4$ cm^{-3} (Osterbrock 1974).

There is another reason why Sgr B2 may be peculiar. Observations of several radio recombination lines from another H II region near or at the Galactic Center, Sgr A West, imply $T_e \simeq 5000$ K (Rodriguez and Chaisson 1978). If this is representative of the Galactic Center regions, then the Galaxy temperature gradient could extend all the way to $D_G = 0$ kpc.

VI. THE IONIZED HELIUM TO HYDROGEN RATIOS

The dependence of the total helium to hydrogen ratio, y = He/H, on galactocentric distance is especially relevant to cosmological studies and to our knowledge of the chemical evolution of our Galaxy. However, the quantity

directly measured by radiofrequency spectroscopy is $y^+ = He^+/H^+$, the ionized helium to hydrogen ratio as determined by the convolution of the nebula and the antenna beam. When He^+ and H^+ occupy the same volume, then $y^+ = y$. Unfortunately, these two ionized species are often not distributed coincidentally. Either cooler stellar effective temperatures or dust that preferentially absorbs helium-ionizing photons could enable substantial amounts of helium to remain neutral within the HII zone (Batchelor 1974). In this case, $y^+ < y$. Although an estimate of the correction factor can be made by observing the nebula with different beamwidths (cf. e.g., Chaisson et al. 1978), this correction is usually inadequate to provide the accurate y values needed to test the small Galaxy helium gradient expected theoretically.

We find no correlation between y^+ and D_G. The correlation coefficient ($r = 0.03$) derived from our data is insignificant. Eight of the twenty observed nebulae have an underabundance of ionized helium ($y^+ < .06$). We feel that the signal-to-noise ratio of the helium lines, as well as the presence of neutral helium, conspire against a straightforward analysis of a helium gradient in the Galaxy.

VII. SUMMARY

From a radio recombination line survey of 20 galactic H II regions at 10.2 GHz, we have reached the following conclusions:

(1) Departures from LTE at this frequency are not significant; radio studies yield reliable values of the bulk electron temperatures that characterize galactic H II regions.

(2) The average electron temperature of various galactic H II regions decreases by about 3000 K between 13 and 5 kpc from the Galactic Center; this decrease most probably results from an enrichment in the heavy element abundance toward the Galaxy's central regions.

(3) The observations cannot yet unambiguously determine if the Galaxy temperature gradient extends into the immediate neighborhood of the Galactic Center.

(4) Observations of the He^+/H^+ ratio are consistent with a total He/H ratio of 7 to 10 %; however, the suspected presence of neutral helium within nebular H II zones makes a determination of any Galaxy helium gradient most difficult at present.

We thank the staff of the Haystack Observatory for their superb cooperation and assistance, and J. M. Moran for helpful suggestions.

REFERENCES

Balick, B. and Sneden, C. 1976, Ap.J., 208, 336.

Batchelor, 1974, Astr. Ap., 32, 343.

Brocklehurst, M. and Seaton, M.J. 1972, MNRAS, 157, 179.

Chaisson, E.J. and Dopita, M.A. 1977, Astr. Ap., 56, 385.

Chaisson, E.J., Lichten, S.M. and Rodriguez, L.F. 1978, Ap.J., 221, 810.

Churchwell, E., Mezger, P.G. and Huchtmeier, W. 1974, Astr. Ap., 32, 283.

Churchwell, E., Smith, L.F., Mathis, J., Mezger, P.G. and Huchtmeier, W. 1978, Astr. Ap. (submitted).

Churchwell, E. and Walmsley, C.M. 1975, Astr. Ap., 38, 451.

Lockman, F.J. and Brown, R.L. 1978, Ap.J., 222, 153.

Mayor, M. 1976, Astr. Ap., 48, 301

Mezger, P.G., Smith, L.F. and Churchwell, E. 1974, Astr. Ap., 32, 269.

Miller, J. 1968, Ap.J., 151, 473.

Osterbrock, D.E. 1974, Astrophysics of Gaseous Nebulae, pg.57, W.H. Freeman & Co., San Francisco.

Peimbert, M., Torres-Peimbert, S. and Rayo, J.F. 1978, Ap.J., 220, 516.

Rodriguez, L.F. and Chaisson, E.J. 1978, Ap.J. (in press).

Rubin, V.C., Kumar, C.K. and Ford, W.F. Jr. 1972, Ap.J., 177, 31.

Sarazin, C.L. 1977, Ap.J., 211, 772.

Searle, L. 1971, Ap.J., 168, 327.

Shaver, P.A. 1978, preprint.

Shields, G.A. 1974, Ap.J., 193, 335.

Shields, G.A. and Searle, L. 1978, Ap.J., 222, 821.

Smith, H.E. 1975, Ap.J., 199, 591.

Smith, L.F. and Mezger, P.G. 1976, Astr. Ap., 53, 165.

Smith, L.F., Biermann, P. and Mezger, P.G. 1978, Astr. Ap., 66, 65.

Thum, C., Mezger, P.G., Pankonin, V. and Schraml, J. 1978, Astr. Ap., 64, L17.

TABLE I

LINE AND CONTINUUM MEASUREMENTS

(1) Name	(2) α (1950)	(3) δ (1950)	(4) integration time (minutes)	(5) velocity resolution (km s^{-1})	(6) T_C (K)	(7) line	(8) T_L (K)	(9) Δv (km s^{-1})	(10) v_{LSR} (km s^{-1})
W3N	$02^h23^m05^s$	+62°02'18"	170	1.92	1.5 ± 0.3	H86α	0.131±0.002	31.2±0.7	-47.8±0.3
						He86α	0.016±0.002	19.6±4.4	-45.8±1.7
						H108β	0.047±0.002	24.3±1.7	-46.5±0.6
W3	02 21 53	+61 52 31	90	1.92	4.9 ± 0.7	H86α	0.452±0.004	27.5±0.3	-40.5±0.1
						He86α	0.042±0.004	19.7±2.6	-36.9±1.0
						H108β	0.120±0.004	25.7±1.0	-39.8±0.4
S206	03 59 29	+51 10 48	430	7.00	0.67 ± 0.19	H86α	0.0446±0.0006	28.4±0.5	-26.6±0.2
						He86α	0.0099±0.0009	10.7±1.2	-29.6±0.5
						H108β	0.0101±0.0006	28.9±2.2	-29.7±0.8
Orion A	05 32 51	-05 25 39	30	1.92	23.1 ± 1.2	H86α	2.222±0.006	27.5±0.1	-2.42±0.04
						He86α	0.240±0.008	17.9±0.9	- 2.6±0.3
						C86α	0.108±0.016	4.5±0.8	+10.8±0.3
						H108β	0.645±0.006	29.6±0.4	- 2.0±0.1
M43	05 33 04	-05 18 03	120	11.00	1.26 ± 0.24	H86α	0.146±0.001	23.6±0.1	+8.15±0.05
						He86α	<0.006 (3σ)		
						H108β	0.046±0.001	28.5±0.5	+ 7.8±0.2
						H162η	0.010±0.001	17.8±1.5	+ 4.6±1.1
Orion B	05 39 13	-01 56 13	145	1.92	4.5 ± 0.3	H86α	0.491±0.004	22.7±0.2	+ 5.8±0.1
						He86α	<0.039 (3σ)		
						C86α	0.074±0.009	3.6±0.5	+10.7±0.2
						H108β	0.127±0.004	24.8±0.9	+ 6.8±0.3
NGC6334	17 17 16	-35 46 54	70	1.92	2.7 ± 0.4	H86α	0.325±0.006	26.0±0.6	- 3.6±0.2
						He86α	0.034±0.008	15 ± 4	- 5.0±1.7
						H108β	0.079±0.006	29.0±2.7	- 1.9±1.0

TABLE 1 *(Continued)*

(1) Name	(2) α (1950)	(3) δ (1950)	(4) integration time (minutes)	(5) velocity resolution (km s^{-1})	(6) T_C (K)	(7) line	(8) T_L (K)	(9) Δv (km s^{-1})	(10) v_{LSR} (km s^{-1})
NGC6357	$17^h22^m18^s$	-34°20'06"	80	7.00	3.4 ± 0.3	H86α	0.277±0.002	32.1±0.4	-3.3±0.1
						He86α	0.011±0.002	40 ± 10	-4.3±3.6
						H108β	0.072±0.003	29.9±1.3	-3.5±0.5
Sgr B2	17 44 07	-28 21 36	395	1.92	2.8 ± 0.4	H86α	0.183±0.002	39.5±0.5	+66.0±0.2
						He86α	0.012±0.002	27.4±5.3	+65.7±2.0
						H108β	0.034±0.002	39.6±2.6	+71.6±0.9
M8	18 00 41	-24 23 20	300	1.92	2.3 ± 0.3	H86α	0.236±0.002	26.5±0.3	+3.9±0.1
						He86α	0.024±0.003	18.8±2.4	+1.5±0.9
						H108β	0.072±0.002	25.6±1.0	+4.5±0.4
W31	18 06 26	-20 19 40	120	1.92	3.9 ± 0.4	H86α	0.440±0.003	31.5±0.2	+13.8±0.1
						He86α	0.021±0.003	28.0±4.6	+9.5±1.7
						H108β	0.121±0.003	28.9±0.8	+14.2±0.3
W33	18 11 15	-17 57 02	100	5.18	2.8 ± 0.3	H86α(1)	0.290±0.003	27.0±0.5	+35.6±0.3
						H86α(2)	0.066±0.004	20.6±1.7	+61.6±0.9
						He86α	0.026±0.002	30.8±3.8	+27.3±1.4
						C86α	0.019±0.005	5.6±2.0	+30.6±0.8
						H108β	0.068±0.003	25.0±1.1	+34.1±0.4
M17	18 17 36	-16 12 17	40	1.92	18.5 ± 0.7	H86α	1.522±0.006	37.9±0.2	+18.5±0.1
						He86α	0.166±0.006	34.5±1.7	+17.7±0.6
						H108β	0.460±0.006	40.4±0.7	+19.4±0.3
W43	18 45 01	-02 00 03	60	1.92	4.6 ± 0.2	H86α	0.438±0.003	31.8±0.3	+92.7±0.1
						He86α	0.037±0.003	33.8±3.3	+88.4±1.2
						H108β	0.136±0.003	30.9±0.9	+91.3±0.3

TABLE 1 *(Continued)*

(1) Name	(2) α (1950)	(3) δ (1950)	(4) integration time (minutes)	(5) velocity resolution (km s^{-1})	(6) T_C (K)	(7) line	(8) T_L (K)	(9) Δv (km s^{-1})	(10) v_{LSR} (km s^{-1})
W48	$18^h59^m16^s$	+01°08'46"	140	9.00	1.6 ± 0.4	H86α	0.205±0.001	25.4±0.2	+46.9±0.1
						He86α	0.010±0.001	16.2±3.4	+47.8±1.3
						C86α	0.009±0.001	15.7±2.6	+47.9±1.0
						H108β	0.051±0.001	22.1±0.5	+47.4±0.2
W49	19 07 53	+09 01 05	100	5.18	5.6 ± 1.0	H86α	0.450±0.002	30.2±0.2	+ 8.4±0.1
						He86α	0.046±0.002	24.1±1.4	+10.6±0.5
						C86α (1)	0.016±0.004	7.5±2.1	+ 9.1±0.9
						C86α (2)	0.022±0.003	8.5±1.9	+68.4±0.8
						H108β	0.130±0.002	28.7±0.6	+10.3±0.2
W51	19 21 25	+14 24 42	80	5.18	8.7 ± 0.9	H86α	0.912±0.002	31.2±0.1	+58.71±0.03
						He86α	0.087±0.002	28.5±1.1	+59.2±0.4
						C86α	0.026±0.002	13.2±3.4	+53.7±1.4
						H108β	0.240±0.002	31.6±0.3	+58.7±0.1
DR7	20 26 21	+40 42 08	100	1.92	1.1 ± 0.2	H86α	0.087±0.003	29.3±1.3	-39.7±0.5
						H108β	0.031±0.003	27.1±3.6	-38.5±1.4
DR21	20 37 14	+42 09 04	90	1.92	2.7 ± 0.2	H86α	0.187±0.002	37.9±0.6	+ 0.4±0.2
						He86α	0.016±0.003	20 ± 5	- 3.8±1.9
						H108β	0.051±0.003	33.5±2.1	+ 3.3±0.8
NGC7538	23 11 22	+61 13 36	290	5.18	1.5 ± 0.2	H86α	0.135±0.001	26.4±0.3	-59.8±0.1
						He86α	0.016±0.002	11.7±1.4	-61.2±0.6
						H108β	0.045±0.001	27.3±0.9	-60.1±0.3

TABLE 2

PARAMETERS OF THE OBSERVED H II REGIONS

(1) Name	(2) D_S (kpc)	(3) D_G (kpc)	(4) T_e*(H86α) (K)	(5) T_e*(H108β) (K)	(6) y^+	(7) β/α
W3N	3.1	12.4	8330 ± 1700	8090 ± 1700	0.08 ± 0.02	0.28 ± 0.02
W3	3.1	12.4	8720 ± 1140	9440 ± 1240	0.067 ± 0.009	0.25 ± 0.01
S206	3.0	12.7	11200 ± 2800	13000 ± 1350	0.086 ± 0.008	0.23 ± 0.02
Orion A	0.5	10.4	8470 ± 380	7490 ± 380	0.072 ± 0.003	0.319 ± 0.005
M43	0.5	10.4	8600 ± 1100	6510 ± 1100	<0.023 (3σ)	0.383 ± 0.006
Orion B	0.5	10.4	9330 ± 650	9120 ± 700	<0.046 (3σ)	0.28 ± 0.01
NGC6334[a]	0.7	9.3	7450 ± 930	7450 ± 1100	0.061 ± 0.017	0.276 ± 0.026
NGC6357[a]	1.0	9.0	8600 ± 700	9550 ± 900	0.050 ± 0.013	0.245 ± 0.012
Sgr B2	10.0	0.1	8860 ± 1180	12240 ± 1890	0.047 ± 0.009	0.191 ± 0.013
M8[b]	1.4	8.6	8150 ± 940	7590 ± 900	0.073 ± 0.010	0.299 ± 0.015
W31	5.1	5.1	6660 ± 590	7140 ± 680	0.044 ± 0.008	0.255 ± 0.008
W33[c]	4.6	5.6	6940 ± 630	9490 ± 1000	0.105 ± 0.012	0.224 ± 0.012
M17	2.1	7.9	7190 ± 240	6165 ± 240	0.102 ± 0.005	0.331 ± 0.005
W43	7.0	5.4	7410 ± 350	6690 ± 350	0.093 ± 0.010	0.31 ± 0.01
W48	3.3	7.6	7020 ± 1570	8890 ± 2000	0.032 ± 0.006	0.219 ± 0.006
W49	13.8	9.4	9020 ± 1400	8930 ± 1400	0.084 ± 0.005	0.279 ± 0.005
W51	8.2	7.8	6980 ± 610	7030 ± 620	0.089 ± 0.004	0.272 ± 0.003
DR7	8.0	11.6	9360 ± 1900	7870 ± 1780	——	0.34 ± 0.04
DR21	1.5	9.9	8570 ± 560	9560 ± 930	0.046 ± 0.011	0.24 ± 0.02
NGC7538	4.9	12.6	9480 ± 1100	7780 ± 1100	0.053 ± 0.006	0.35 ± 0.01

NOTES

a. Distances from Churchwell *et al.* (1974).

b. Distances from Miller (1968).

c. Distances from Smith *et al.* (1978)

TABLE 3

LINEAR REGRESSION ANALYSIS

Relation	A (K)	B (K kpc^{-1})	r correlation coefficient	confidence level
$T_e(86\alpha) = A + B \cdot D_G$	4700 ± 600	390 ± 70	0.815	>99.9%
$T_e(108\beta) = A + B \cdot D_G$	6000 ± 1400	250 ± 150	0.375	89%
$T_e(86\alpha) = A + B \cdot D_S$	8300 ± 400	-10 ± 80	-0.03	not correlated

Note: Sgr B2 is excluded from the regressions.

FIGURE CAPTIONS

Figure 1 --- The recombination-line spectra observed at 10.2 GHz. The antenna temperature and Doppler velocities of each line can be found in Table 1.

Figure 2 --- Pressure broadening is unimportant at 10.2 GHz as the H108β lines are not systematically wider than the H86α lines. (All these widths have been corrected for instrumental broadening.)

Figure 3 --- (a) Theoretically expected real T_e values and LTE-derived T_e^* values are much the same at 10 GHz. (b) For H109α lines at 5 GHz, departures from LTE can become appreciable.

Figure 4 -- Variation of nebular electron temperature with galactocentric distance.

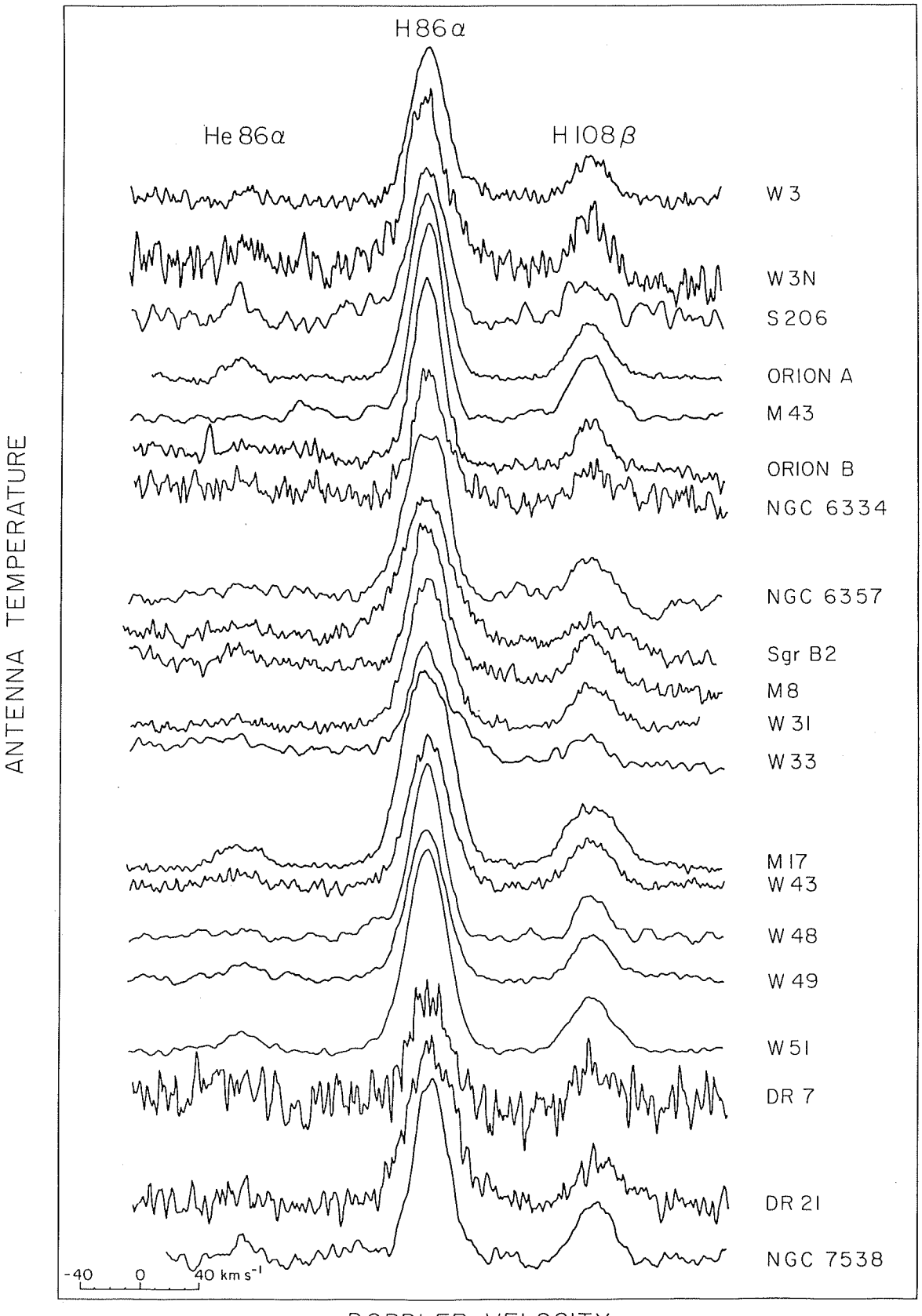
H 86α
He 86α
H 108β
W 3
W 3N
S 206
ORION A
M 43
ORION B
NGC 6334
NGC 6357
Sgr B2
M 8
W 31
W 33
M 17
W 43
W 48
W 49
W 51
DR 7
DR 21
NGC 7538
-40
0
40 km s⁻¹
ANTENNA TEMPERATURE
DOPPLER VELOCITY

Fig. 1

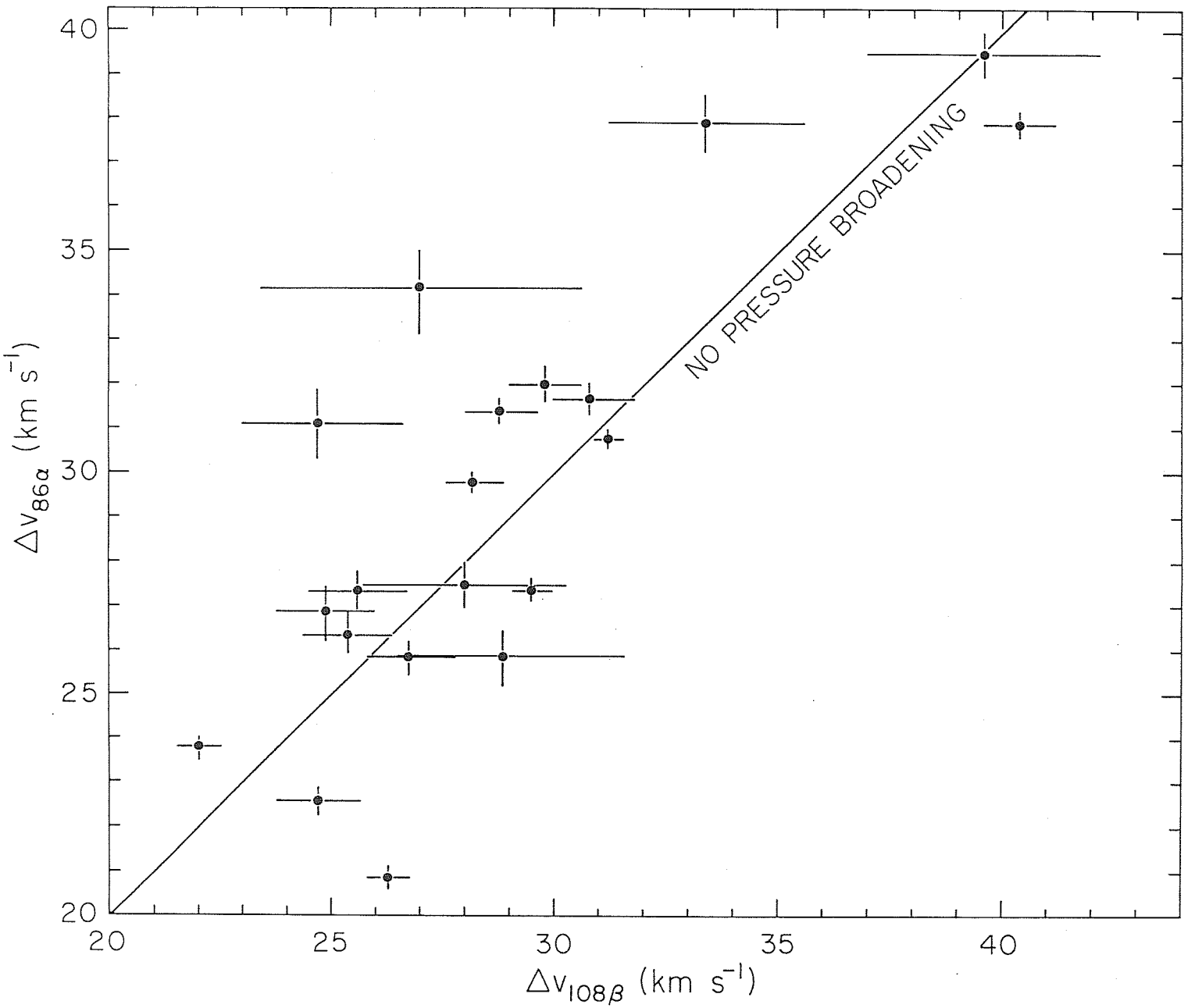
NO PRESSURE BROADENING
$\Delta v_{86\alpha}$ (km s^{-1})
$\Delta v_{108\beta}$ (km s^{-1})
20
25
30
35
40

Fig. 2

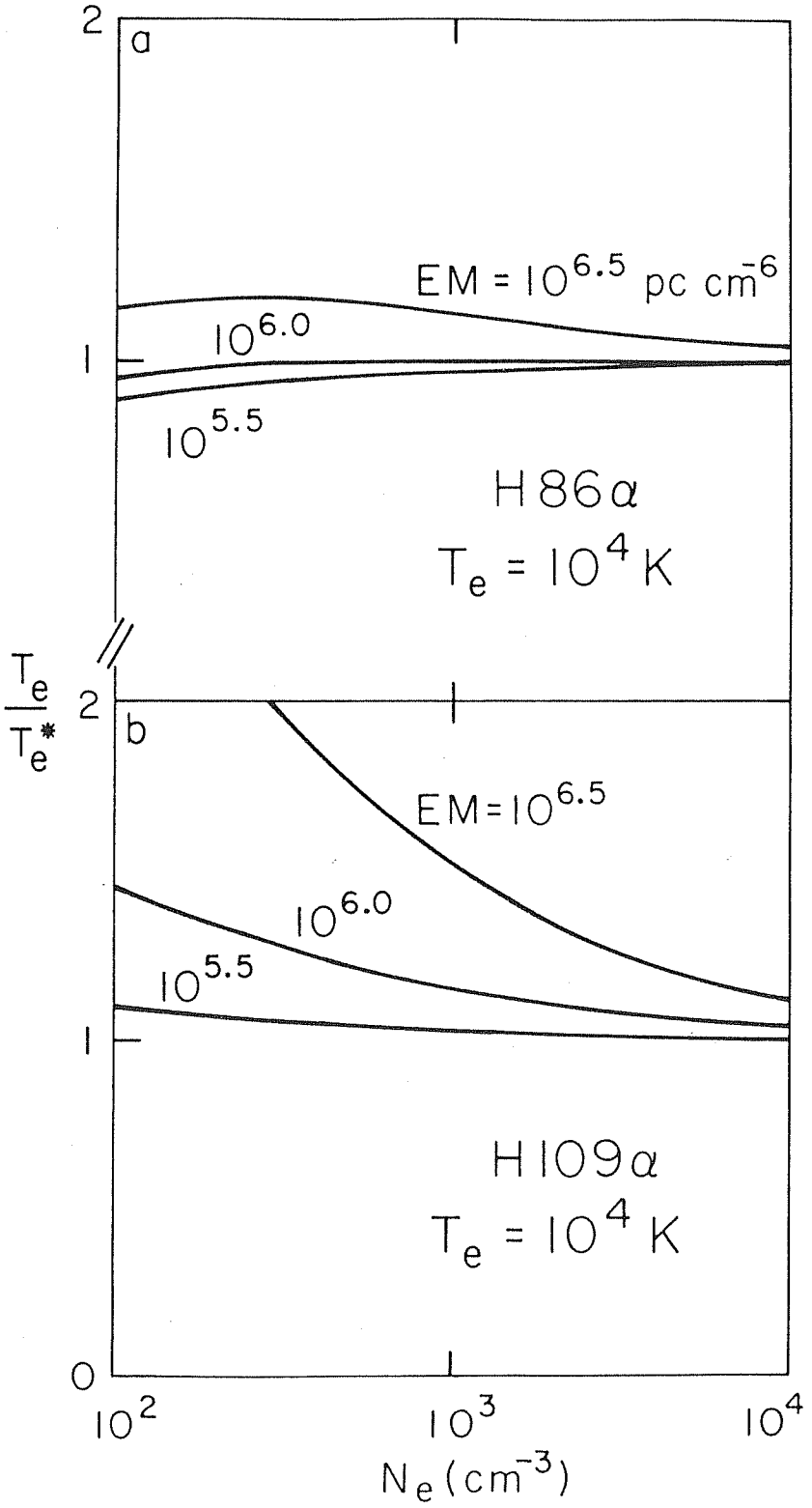
2
a
EM = 10^6.5 pc cm^-6
10^6.0
1
10^5.5
H86α
T_e = 10^4 K
T_e / T_e*
2
b
EM=10^6.5
10^6.0
10^5.5
1
H109α
T_e = 10^4 K
0
10^2
10^3
10^4
N_e (cm^-3)

Fig. 3

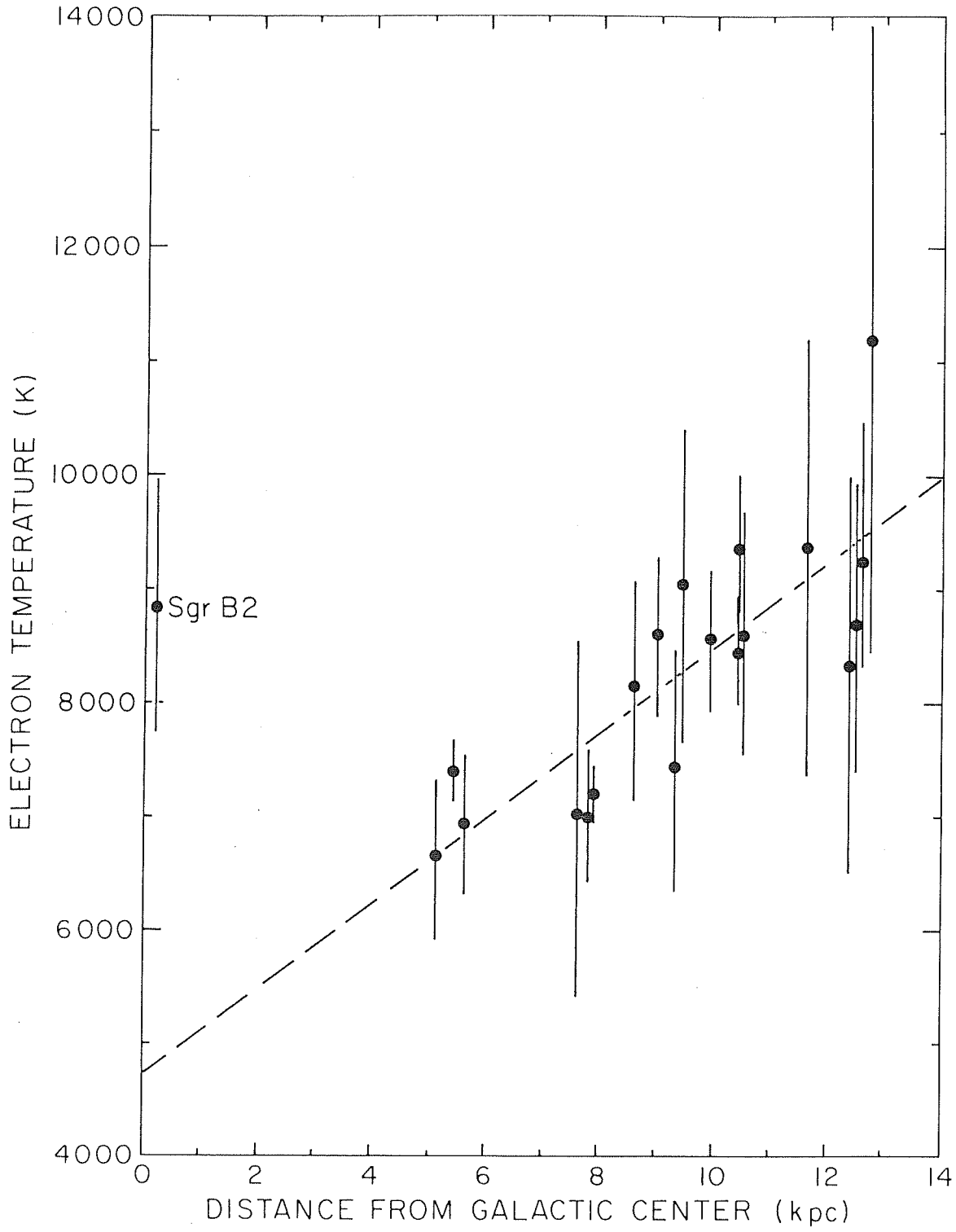
14000
12000
10000
8000
6000
4000
ELECTRON TEMPERATURE (K)
Sgr B2
0
2
4
6
8
10
12
14
DISTANCE FROM GALACTIC CENTER (kpc)

Fig. 4

CHAPTER IX

THE TEMPERATURE AND DYNAMICS OF THE IONIZED GAS IN THE NUCLEUS OF OUR GALAXY

Luis F. Rodriguez* and Eric J. Chaisson†

Harvard-Smithsonian Center for Astrophysics

To appear in the March 15, 1979 issue of

The Astrophysical Journal.

*Becario del Consejo Nacional de Ciencia y Tecnologia, Mexico.

†Alfred P. Sloan Foundation Fellow

ABSTRACT

Observations of the H65α (23.4 GHz), H84α (10.9 GHz), and H94α (7.8 GHz) radio recombination lines from Sgr A West are presented. We suggest that a core-halo model can satisfactorily account for the reported radio and infrared observations of this source. Due to instrumental limitations, the observed infrared lines are dominated by the core while the observed radio radiation arises mostly in the halo. Although more than a factor of ten brighter than the halo, the core is responsible for only about one-fourth of the integrated thermal continuum from Sgr A West. Our model implies that the neon abundance determination from infrared observations, previously considered consistent with the solar value, should be revised upwards by a factor of four. This suggested enrichment of neon relates strongly to our derivation of an unusually low electron temperature, $T_e = 5000 \pm 1000$ K, since nebular cooling is expected to be enhanced by an overabundant heavy element content. The dynamical structure of Sgr A West can be explained in terms of Keplerian rotation due to the gravitational field of the normal stellar population plus a central mass point of five million solar masses.

Subject Headings---Galaxies: Nuclei, Nebulae: Abundances, Radio sources: Lines.

I. INTRODUCTION

Attention was first called to Sgr A West by Downes and Martin (1971) who argued, on the basis of its flat radio continuum spectrum, that it is an H II region. Toward its center lies the peak of 2.2μ emission observed by Becklin and Neugebauer (1968, 1975), a position believed to determine the stellar nucleus of our Galaxy. The thermal nature of Sgr A West was confirmed by Pauls, Mezger and Churchwell (1974), who detected H109α radio recombination line emission at 5 GHz; this emission is exceptionally broad, having a full width at half power $\Delta v \simeq 200$ km s^{-1}. Based on their NeII 12.8 μ fine-structure observations, Wollman et al. (1976, 1978) suggest that the H109α line arises under conditions substantially removed from those of local thermodynamic equilibrium (LTE) and thus cannot be used as a reliable indicator of the physical conditions in Sgr A West. The spatially integrated NeII line profile is very broad, $\Delta v \simeq 400$ km s^{-1}, (Wollman 1976). Thus, this infrared line emission cannot arise in the same gas responsible for the 200 km s^{-1} wide H109α emission. Furthermore, to explain the NeII line emission from ionized gas having solar abundances, Wollman et al. (1978) require all the thermal continuum to be associated with the gas responsible for the NeII line. With these considerations in mind, it would seem that the H109α line must arise from a small, possibly non-representative, fraction of the ionized gas and that its relatively strong intensity results from non-LTE enhancement of the line emission by the strong background continuum provided by the synchrotron source Sgr A. This enhancement is proportional to the brightness temperature of the continuum emission, which decreases steeply with increasing frequency. Thus, recombination line observations at high radio frequencies should be largely unaffected by this amplification effect and are expected to allow an unbiased determination of the parameters of the ionized gas in the nucleus of our Galaxy. We report such high radiofrequency line observations in this paper.

II. OBSERVATIONS

High-frequency observations of anomalously broad radio recombination lines are not easy to make primarily because it is hard to measure the entire line profile with a single spectrometer bandpass. Until recently, the broadest spectral bandpasses available for microwave spectroscopy were about 10 MHz; this gives a velocity coverage of only 150 km s^{-1} at a frequency of 20 GHz. Indeed, the earlier H109α (5 GHz) observations of Pauls et al. (1974) were accomplished by overlapping spectral bandpasses centered at different velocities. This technique can potentially lead to serious errors in the line measurement.

The opportunity to measure a high-frequency radio recombination line from Sgr A West with a single spectral bandpass recently became possible with the new digital autocorrelator now on-line at the Haystack Observatory[1]. This

---

[1]The Haystack Observatory of the Northeast Radio Observatory Corporation is supported in part under grant GP25865 from the National Science Foundation.

---

spectrometer provides up to 1024 channels and a 100-MHz sampling rate. With the maximum 50-MHz bandpass, then, we undertook H65α, H84α , and H94α observations at the peak of Sgr A West as determined from the continuum map of Ekers et al. (1975): $\alpha = 17^h\ 42^m\ 29\overset{s}{.}5$, δ = -28° 59' 19", epoch = 1950.0.

Table 1 summarizes the observational configurations. Five-minute comparison observations taken five minutes of time to the west of the source were subtracted from signal observations of equal duration. Main-beam observations of the H65α and H94α lines were switched, both on and off the source, against a sky horn at a 5-Hz rate; the H84α lines were observed in the total-power mode. The accumulated H84α and H94α data have an equal number of observing runs with the Cassegrain subreflector in its normal position and with it defocused $\lambda/4$ toward the main reflector.

Identically taken observations of Sgr B2 (H65α) and W51A (H84α and H94α) were used to produce a reference baseline --- parabolic shape for the H65α and H84α and cubic for the H94α data. These reference baselines were then scaled by the ratio of continuum temperatures of Sgr A West to each of these sources (1.11 for the H65α, 0.89 for the H84α data, and 1.16 for the H94α data) and subtracted from the respective Sgr A West spectra. Figure 1 shows the resulting spectra.

To estimate the integrated parameters of the lines, we least squares fitted a Gaussian function to the H65α, H84α , and H94α emission as well as the H118β feature observed on the high-frequency side of the H94α spectrum. (The apparent "absorption line" at the center of the H118β line results from known terrestrial interference.) Table 2 gives the resulting line temperatures, T_L; full widths at half power, Δv; and velocity centroids with respect to the local standard of rest, v_{LSR}. The simultaneously measured continuum temperatures, T_c, are listed there as well.

III. A CORE-HALO MODEL FOR SGR A WEST

While all reported radio recombination line observations from Sgr A West (Pauls, Mezger and Churchwell 1974; Pauls and Mezger 1977; this paper) have $\Delta v \simeq 200$ km s^{-1}, the spatially integrated line profile for the infrared NeII emission shows $\Delta v \simeq 400$ km s^{-1} (Wollman 1976). Furthermore, while the thermal radio continuum emission is observed to arise from a region with about a 2'x1' spatial extent (Ekers et al. 1975), the 12.8 μ NeII line (Wollman et al. 1978) and the 2.17μ Bγ line (Neugebauer et al, 1978) are detected from only a much smaller region. All these observations can be reconciled provided Sgr A West is a core-halo source. The halo has a low emission measure compared to the core, thus making the infrared line emission from the halo largely undetectable with the high angular resolution but low sensitivity infrared apparatus. On the other

hand, due to relatively poor spatial resolution, the observed radio lines come from the source as a whole, the total emission from which is dominated by the less bright but more voluminous halo. Also, the inherent limitations of radio spectral bandpasses even as wide as 50 MHz make detection of the weak (beam diluted) and wide ($\simeq$ 400 km s^{-1}) line emission from the core practically impossible. So, it seems reasonable that the radio and infrared observations actually give independent information about two different components of Sgr A West.

To test this hypothesis quantitatively, we built a core-halo model for the Sgr A West source. The parameters in Table 3 and the illustration in Figure 2 depict the main characteristics of our model. The model agrees with the following observational results:

1) *The thermal continuum flux density at 5 GHz.* Our model gives an integrated flux, S_ν = 27 Jy. Ekers et al. measured $S_\nu = 26 \pm 4$ Jy.

2) *The spatial extents of the thermal emission and the infrared line emission.* Our model stipulates 2'x1' for the halo and 20"x10" for the core. These values agree with those determined for the thermal emission (Ekers et al. 1975) and for the 2.17 μ Brγ line (Neugebauer et al. 1978).

3) *The contrast in emission measure between the core and the halo.* Neugebauer et al. (1978) find that the mean surface brightness at points 30" from the center is 10 to 20 times weaker than that of the bright central core. Our model gives EM(core) = 13 EM (halo). Neugebauer et al. also estimate that the emission measure of the central region is about 10^7 pc cm^{-6}. Our model gives EM(core) = 2 x 10^7 pc cm^{-6}.

4) *The 2.17 μ Brγ line flux.* Neugebauer et al. (1978) note that about 7 Jy of radio flux are needed at 5 GHz to account for the Brγ line flux. This agrees with our model's value of 6 Jy.

5) *The 12.8 μ NeII line flux.* We can affect an agreement with the results of Wollman et al. (1978) if the neon abundance in the galactic center is about 4 times the solar value. (Neugebauer et al. [1978] also suggested such a neon enhancement.) This is not particularly disturbing; on the contrary, it agrees well with recent optical (Peimbert, Torres-Peimbert and Rayo 1978) and radio (Churchwell et al. 1978; Lichten, Rodriguez and Chaisson 1978) results that suggest the existence of chemical and thermal gradients in our Galaxy. As will be discussed in §IV, this heavy element enrichment of the galactic center relates strongly to the low electron temperature, $T_e = 5000 \pm 1000$ K, that we derive for the halo, since the heavy elements are the primary coolants of H II regions.

6) *The α and β hydrogen radio recombination lines.* To account for the observed radio recombination lines, we solved the transfer equation for a homogeneous, isothermal plasma described by the parameters attributed to the halo (cf., Table 3). We used a program similar to the one described by Shaver et al. (1978). From the data compiled by Dulk and Slee (1974), we find that the background continuum temperature T_{bg} of the non-thermal Sgr A source is given by

$$T_{bg} = 5 \times 10^3 \nu^{-2.5}$$

where ν is the frequency in GHz; this fit is valid for $\nu > 1$ GHz. The solid line in Figure 3 shows the results of the calculations for the α and β hydrogen lines. For $\nu < 10$ GHz, the radio recombination lines are moderately enhanced (by a factor of 1.5 to 2.0) with respect to the LTE value (dashed line). In the spectral region, 10 GHz $< \nu <$ 25 GHz, the LTE and non-LTE calculations are within 20 percent of each other. The data points plotted in Figure 3 are taken from Pauls, Mezger and Churchwell (1974), Pauls and Mezger (1977), and this paper, and have been corrected for aperture efficiency and beam convolution effects using

the halo model described in Table 3. All the data points have been normalized to Δv = 200 km s^{-1} and corrected for contamination by the helium radio recombination line (taken to be 10 percent of the hydrogen line). The H94α line feature is also corrected for contamination by the H148δ line (taken to be 8 percent of the hydrogen line). As can be seen, these data agree with our core-halo model.

IV. ELECTRON TEMPERATURE OF SGR A WEST

The best model fit for all the α and β radio recombination lines is obtained for $T_e \simeq 5000$ K. Higher values of T_e predict peak line flux densities smaller than observed. This unusually low electron temperature can be confirmed by means of a straightforward calculation using the observed H65α line and assuming LTE. This assumption is justified since our model predicts no more than a 20 percent departure from LTE for H65α; altering the only physical parameter that can be possibly modified without introducing conflicts with the other observational constraints, namely increasing the electron density by postulating a highly clumped nebula, actually brings into closer agreement the non-LTE and LTE predictions for H65α emission. This results simply from the better thermalization of the atomic levels.

To derive T_e from the recombination line, we also need a measure of the underlying thermal continuum. At the H65α frequency, we measured a total continuum antenna temperature T_c (total) = 1.4 K. This continuum is a mixture of emission from the core and halo regions of Sgr A West, as well as from the non-thermal background of the Sgr A synchrotron source. But this needs to be corrected to assess properly the thermal contribution of only the halo of Sgr A West. Using the observed and instrumental parameters described previously, we

find the following breakdown of antenna temperatures for the Haystack telescope;

T_c (non-thermal) = 0.4 K,

T_c (core) = 0.5 K,

T_c (halo) = 0.5 K.

Then, with the observed H65α line parameters and the standard optically thin, LTE formulation, we derive the value T_e(halo) = 4000 $\pm$ 1000 K. This electron temperature agrees reasonably well with the 5000 K suggested by our model.

Note that although this electron temperature rigorously applies only to the halo of Sgr A West, it nonetheless appears reasonable to assume that it also characterizes the core; within a given H II region, only moderate temperature gradients ($\lesssim$ 1000 K) are expected. By the same token, the neon abundances (Wollman et al. 1978) for the core can also be reasonably expected to characterize the halo. With these considerations in mind, then, the low electron temperature ($\sim$ 5000 K) and the large neon abundance (about four times the solar value, after the correction required by our model) are recognized to be intimately related. Optical (Peimbert et al 1978) and radio studies (Churchwell et al. 1978; Lichten et al 1978) suggest the existence of a thermal and chemical gradient in the disk of our Galaxy. The electron temperature of galactic H II regions decreases with decreasing galactocentric radius, while the heavy element relative abundance increases with decreasing galactocentric radius. Since nebulae cool through the forbidden emission lines of the heavy elements (mainly oxygen and nitrogen), an increase in the heavy element relative abundance manifests as a decrease in the electron temperature.

Until now, this temperature gradient has not been extended for galactocentric radii, $D_G \leq 4$ kpc, for two reasons. First, in the region 0.2 kpc $\leq D_G \leq$ 4 kpc, there are no known H II regions of brightness large enough to be studied in detail.

And second, in the galactic center region $D_G \leq 0.2$ kpc, the only H II region for which extensive recombination line studies have been made is Sgr B2; curiously, this H II region seems to have $T_e \simeq 8500$ K (Chaisson et al. 1978; Lichten et al. 1978; Thum et al. 1978). These recent observations of Sgr B2 appear to violate the mathematical form of the gradient determined from studies of many nebulae in the $4 \leq D_G \leq 13$ kpc region (Lichten et al. 1978):

$$T_e \simeq (4700 + 400\ D_G) \quad K,$$

where D_G is the galactocentric radius of the H II region in kpc. Nonetheless, Lichten et al. (1978) have argued that since Sgr B2 is the densest giant H II region in the Galaxy ($n_e \simeq 10^4$ cm^{-3}), collisional deexcitation of the forbidden lines of the heavy elements may impair the cooling process, thus leading to higher electron temperatures. In this sense, Sgr B2 seems to be an anomalous nebula, and we treat it here as such.

Hence, our value of $T_e \simeq 5000$ K for Sgr A West suggests that the gradient does indeed extrapolate into the vicinity of the galactic center. Determination of the electron temperatures of several other H II regions near the galactic center should be made in order to confirm this suggestion.

V. SPECULATIONS ON THE DYNAMICS OF SGR A WEST

To gain insight concerning the dynamics of the halo, we assume in this section (1) that the infrared lines arise in regions typically at galactocentric radius $D_G \simeq 0.4$ pc while the radio lines originate in exterior gas, typically at $D_G \simeq 2$ pc, (2) that the width of any line arising in the core or halo is mainly due to Keplerian rotation around the mass contained within the inner respective galactocentric radii, and (3) following Sargent et al. (1978), that the Keplerian rotation velocity is about one-half the full width at zero intensity

of the line emission. With these assumptions, we then find a rotation velocity, v_R (2 pc) $\simeq$ 150 km s^{-1} from the radio recombination line data and v_R (0.4 pc) $\simeq$ 300 km s^{-1} from the NeII data. Figure 4 shows these two points as well as a value for $D_G \simeq 100$ pc determined from the 21-cm neutral hydrogen observations of Sanders and Wrixon (1973). These data points are then compared against two rotation curves; one model (solid curve) employs the mass distribution of the normal stellar population as described by Oort (1977), while a second model (dashed curve) employs the same normal stellar population along with an additional mass point equal to $5 \times 10^6 M_\odot$. Indeed, this additional mass point equals that suggested earlier by Oort (1977) and Wolman et al. (1978) who recognized that the large NeII linewidths could not be easily explained in terms of Keplerian rotation of the normal stellar population inside $D_G \simeq 0.4$ pc. While the normal stellar population alone is shown to produce a decreasing rotation velocity with decreasing galactocentric radius, the presence of the additional mass point eventually reverses this trend, producing an increase in the rotation velocity with decreasing galactocentric radius for $D_G \lesssim 1$ pc.

Similar evidence for an increase in velocity dispersion with decreasing radius in M87 has been used by Sargent et al. (1978) to propose that this galaxy has a supermassive ($\simeq 5 \times 10^9 M_\odot$) non-stellar object in its nucleus. The inferred object in the core of M87 is about a thousand times more massive than the one required to explain the dynamics of the ionized gas in the nucleus of our Galaxy.

VI. CONCLUSIONS

We have presented high-frequency radio recombination line observations of Sgr A West. A core-halo model adequately accounts for the available infrared and radio data. Our model suggests that the neon abundance, considered by

Wollman et al. (1978) to be approximately solar, is really about four times larger. This finding is intimately related to the unusually low electron temperature of Sgr A West since an enrichment in the heavy element content of an H II region is expected to produce a cooling effect. Our derived value, $T_e \simeq 5000$ K, for the thermal plasma near the galactic nucleus agrees with the extrapolation of galactic gradients found earlier from optical and radio studies of disk H II regions.

If the infrared and radio linewidths are interpreted in terms of Keplerian rotation, we find that there exists a gradient in the rotation velocity within Sgr A West; the core rotates faster than the halo. The dynamics can be described in terms of a rotation curve determined by the mass of the normal stellar population to which a central mass point of five million solar masses has been added. This compact non-stellar object is about a thousand times less massive than the one proposed by Sargent et al. (1978) to exist in the nucleus of M87.

We have benefited from discussions with B. Balick, G. Garay, S. Lichten, and J. Vrtilek. We are also indebted to the engineering and support staffs of the Haystack Observatory for superb assistance.

TABLE 1

Observational Configurations

LINE	H65α	H84α	H94α
FREQUENCY	23.4 GHz	10.9 GHz	7.8 GHz
ANTENNA	Haystack 36.5 - meter	Haystack 36.5 - meter	Haystack 36.5 - meter
FULL BEAMWIDTH AT HALF-POWER	1'.3	3'.5	4'.0
APERTURE EFFICIENCY	0.20	0.34	0.44
RECEIVER	Traveling-wave ruby maser	Parametric amplifier	Parametric amplifier
SPECTROMETER	50-MHz bandwidth digital auto-correlator	50-MHz bandwidth digital auto-correlator	50-MHz bandwidth digital auto-correlator
SYSTEM TEMPERATURE ON COLD SKY	150 K	100 K	90 K
TOTAL OBSERVING TIME	8 hours	8 hours	16 hours

TABLE 2

Observed Radio Recombination Lines

Line	T_L(K)	Δv(km s^{-1})	v_{LSR}(km s^{-1})	T_c(K)
H 65α	0.042* ± 0.004	210 ± 24	-13 ± 8	1.4* ± 0.2
H 84α	0.081 ± 0.004	230 ± 16	-14 ± 5	7.2 ± 0.6
H 94α	0.120 ± 0.008	198 ± 12	-30 ± 4	16.3 ± 0.7
H118β	0.056 ± 0.008	150 ± 32	7 ±10	16.3 ± 0.7

*Antenna temperatures are corrected for elevation-dependent gain variations and tropospheric attenuation using a model of Meeks (1978).

TABLE 3

Parameters of the Core-Halo Model

Parameter	Halo	Core
Angular Size (arc sec)	120 x 60	20 x 10
Linear Size (pc)	5.8 x 2.9	1.0 x 0.5
EM (cm^{-6} pc)	1.5×10^6	2.0×10^7
Mean Depth (pc)	4.4	0.7
$\langle n_e^2 \rangle^{\frac{1}{2}}$ (cm^{-3})	6×10^2	5×10^3
$M_{HII}/M_\odot$	900	30
T_e (K)	5000	5000
Δv (km s^{-1})	200	400
S_{5GHz} (Jy)	21	6
$S_{23.4\ GHz}$ (Jy)	18	6
N_i (photons s^{-1})	3×10^{50}	1×10^{50}
$\nu_{turnover}$ (GHz)	1.1	3.8

REFERENCES

Becklin, E.E., and Neugebauer, G. 1968, Ap.J., 151, 145.

Becklin, E.E., and Neugebauer, G. 1975, Ap.J. (Letters), 200, L71.

Chaisson, E.J., Lichten, S.M., and Rodriguez, L.F. 1978, Ap.J., 221, 810.

Churchwell, E., Smith, L.F., Mathis, J., Mezger, P.G., and Huchtmeier, W. 1978, submitted to Ap.J.

Downes, D., and Martin, A.H.M. 1971, Nature, 233, 112.

Dulk, G.A., and Slee, O.B. 1974, Nature, 248, 33.

Ekers, R.D., Goss, W.M., Schwartz, U.J. Downes, D., and Rogstad, D.H. 1975, A.A., 43, 159.

Kellermann, K.I., Shaffer, D.B., Clark, B.G., and Geldzahler, B.J. 1977, Ap.J. (Letters), 214, L61.

Lichten, S.M., Rodriguez, L.F., and Chaisson, E.J. 1978, submitted to Ap.J.

Meeks, M.L. 1978, private communication.

Neugebauer, G., Becklin, E.E., Matthews, K., and Wynn-Williams, C.G. 1978, Ap.J., 220, 149.

Oort, J.H. 1977, Ann. Rev. Astron. Ap., 15, 295.

Pauls, T., Mezger, P.G., and Churchwell, E. 1974, A.A., 34, 327.

Pauls, T., and Mezger, P.G. 1977, Bull. Am. Astron. Soc., 9, 286.

Peimbert, M., Torres-Peimbert, S., and Rayo, J.F. 1978, Ap.J., 220, 516.

Sanders, R.H. and Wrixon, G.T. 1973, A.A., 26, 365.

Sargent, W.L.W., Young, P.J., Bosenberg, A., Shortridge, K., Lynds, C.R., and Hartwick, F.D.A. 1978, Ap.J., 221, 731.

References (Cont....)

Shaver, P., Churchwell, E., and Walmsley, C.M. 1978, submitted to A.A.

Thum, C., Mezger, P.G., Pankonin, V., and Schraml, J. 1978, A.A., 64, L17.

Wollman, E.R. 1976, unpublished Ph.D. Dissertation, University of California, Berkeley.

Wollman, E.R., Geballe, T.R., Lacy, J.H., Townes, C.H., and Rank, D.M. 1976, Ap.J. (Letters), 205, L5.

Wollman, E.R., Geballe, T.R., Lacy, J.H., Townes, C.H., and Rank, D.M. 1978, submitted to Ap.J.

FIGURE CAPTIONS

Figure 1 --- H65α, H84α, and H94α spectra observed in the direction of Sgr A West. The solid curve represents the data, while the dashed curve is the suggested least-squares fit. The autocorrelator sampling rate for each spectrum was 100 MHz.

Figure 2 --- Schematic diagram of the suggested structure of Sgr A West. The compact radio source within the core has been studied by Kellerman et al. (1977). The apparent major axis of the source approximately parallels the galactic plane.

Figure 3 --- Hnα (a) and Hnβ (b) lines from Sgr A West. The solid curve refers to the model described in the text, while the dashed curve refers to the optically thin LTE model. Error bars are estimated to be twice the standard deviation.

Figure 4 --- A tentative rotation curve for the galactic nucleus. The solid curve refers to a model having normal stellar population; the dashed curve refers to a model having the same normal stellar population plus a mass point of 5 million $M_{\odot}$. Error bars are estimated to be twice the standard deviation.

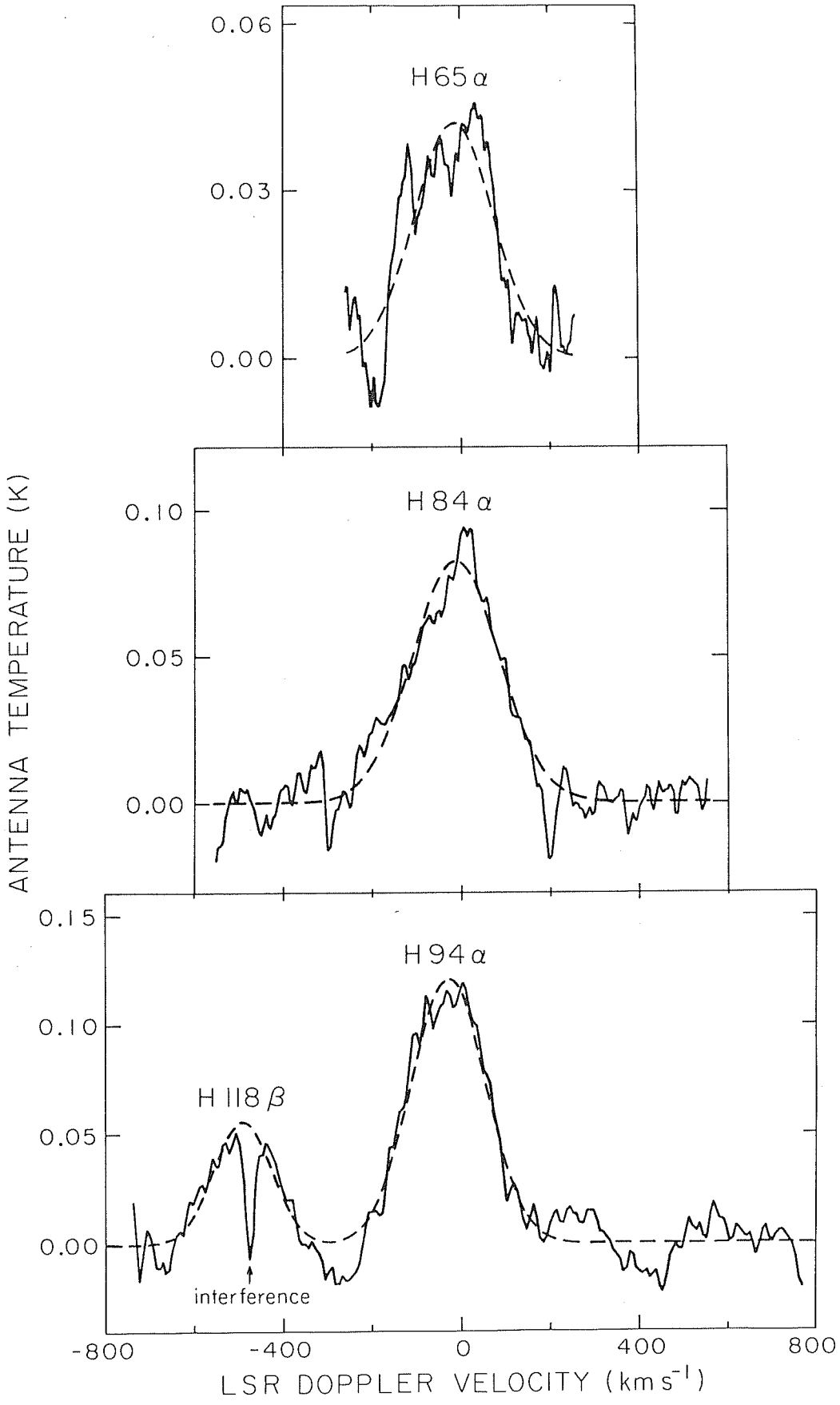
0.06
H65α
0.03
0.00
0.10
H84α
0.05
0.00
0.15
H94α
0.10
H118β
0.05
0.00
interference
ANTENNA TEMPERATURE (K)
-800
-400
0
400
800
LSR DOPPLER VELOCITY (km s⁻¹)

Figure 1

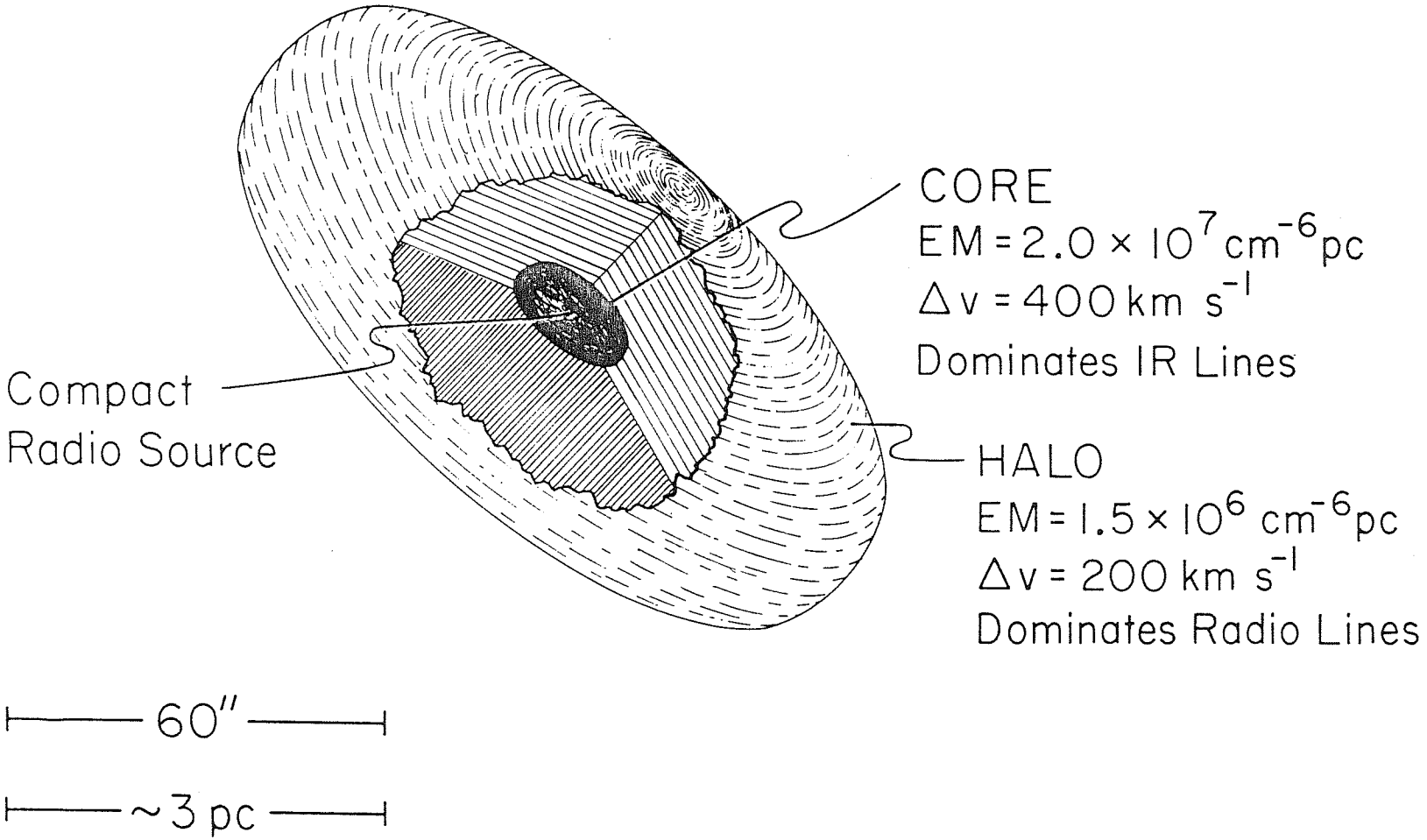
CORE
EM = 2.0 × 10^7 cm^-6 pc
Δv = 400 km s^-1
Dominates IR Lines
Compact
Radio Source
HALO
EM = 1.5 × 10^6 cm^-6 pc
Δv = 200 km s^-1
Dominates Radio Lines
60″
~3 pc

Figure 2

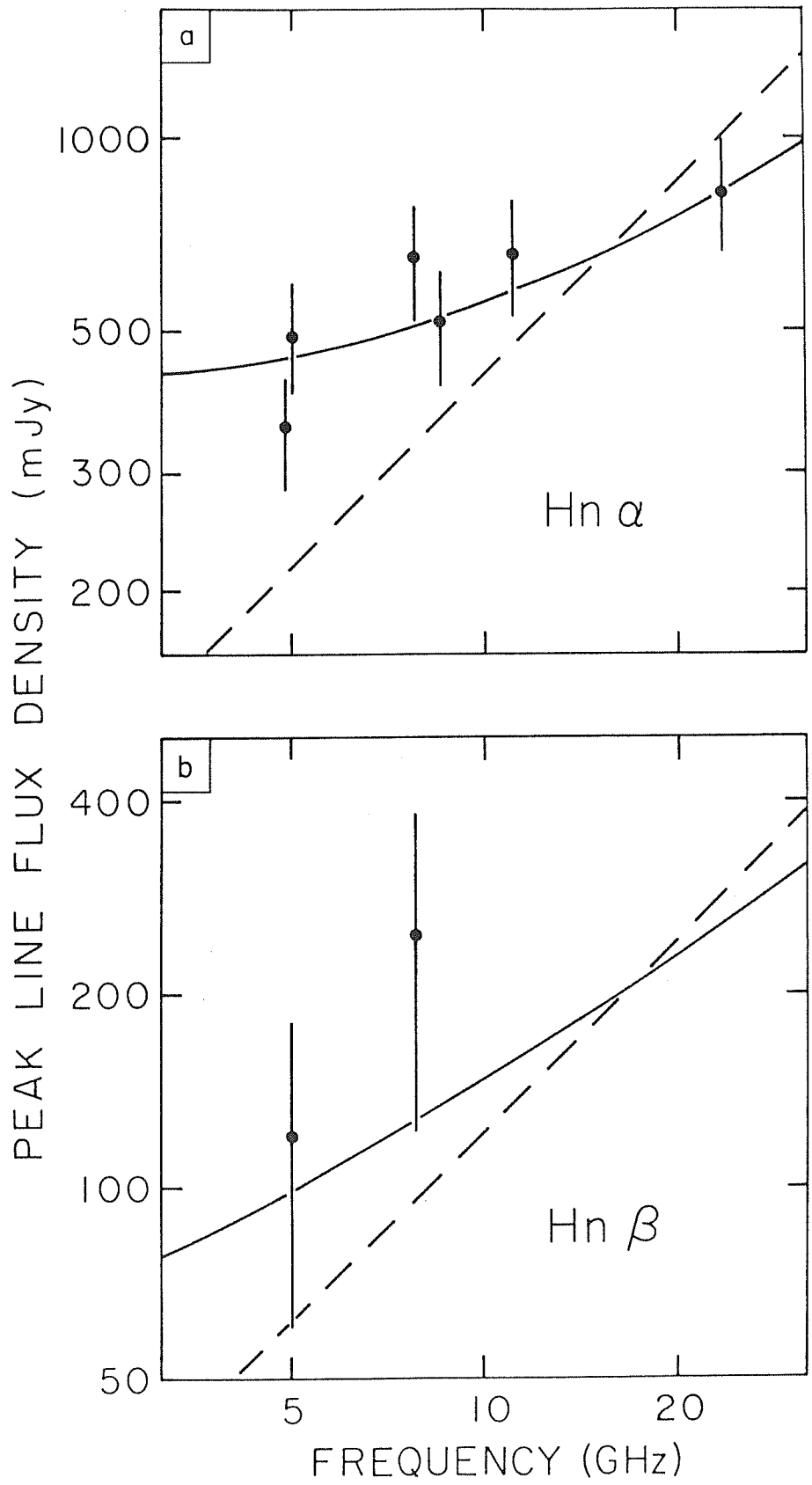
a
1000
500
300
200
Hn α
b
400
200
100
50
Hn β
PEAK LINE FLUX DENSITY (mJy)
5
10
20
FREQUENCY (GHz)

Figure 3

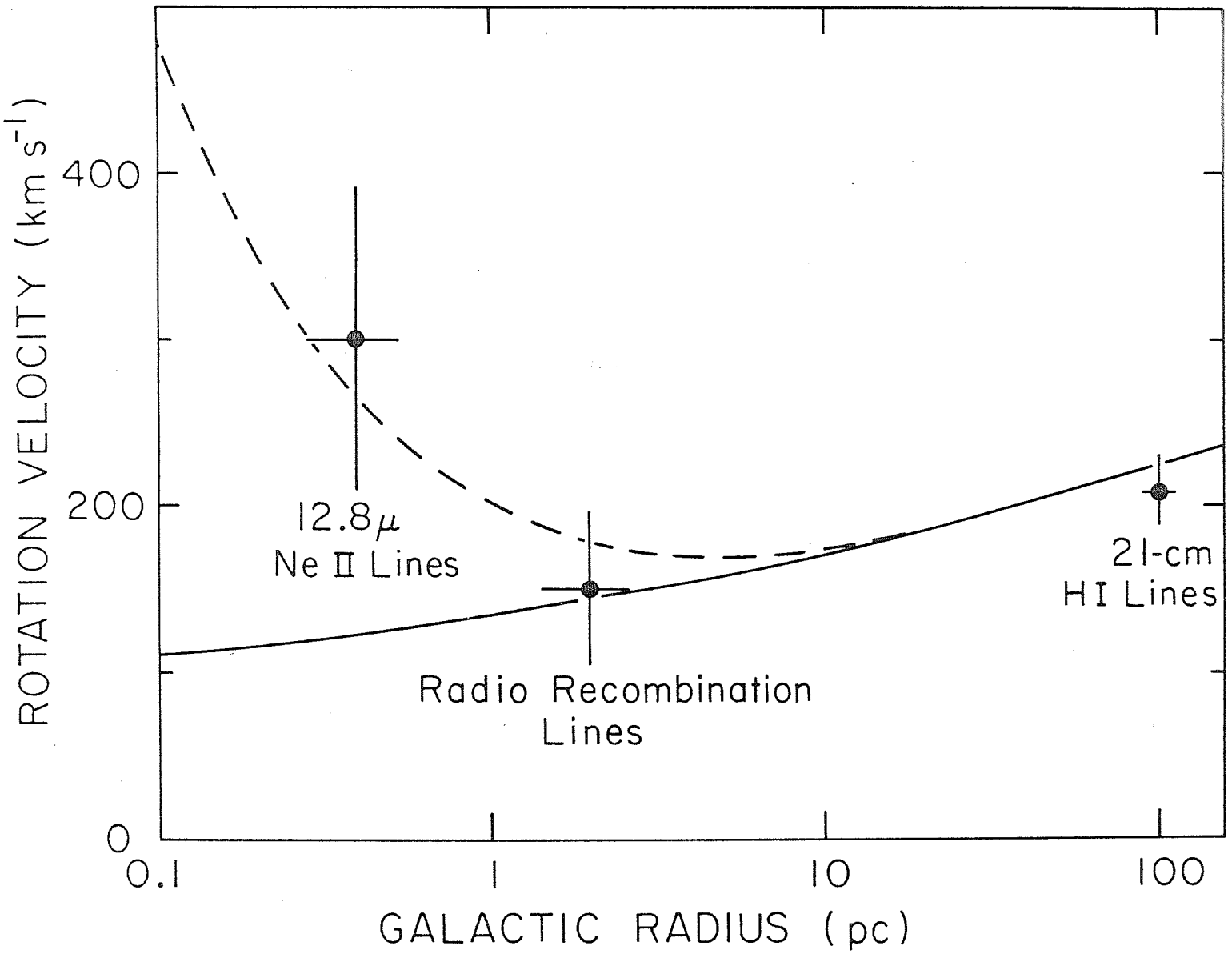
ROTATION VELOCITY (km s⁻¹)
400
200
0
0.1
1
10
100
GALACTIC RADIUS (pc)
12.8μ
Ne II Lines
Radio Recombination
Lines
21-cm
HI Lines

Figure 4

CHAPTER X

CONCLUSIONS

Using radio recombination lines as our observational tool, we present a systematic study of the various components of ionized gas in the Galactic Center. Our main results can be summarized as follows:

SGR B2

1) Our measurements of several hydrogen and helium radio recombination lines are consistent with a normal helium-to-hydrogen ratio of 0.08 to 0.10.

2) A He II zone having a radius 80% of that of the H II zone can explain the beam-dependent y^+ variations.

3) This smaller He II zone could be created by dust having a smoothly increasing (as ν^2) absorptivity shortward of 912 Å.

4) The nebula is close to LTE.

5) A non-LTE model (Brown and Gomez-Gonzalez 1974) involving cold gas outside the H II region was shown to be untenable.

EXTENDED THERMAL COMPONENT

1) The ionized gas is found to be close to LTE. This result is obtained from measurements of the β/α ratio and by comparison of several α lines observed at different frequencies.

2) The upper limits to the y^+ and y^{++} ratios indicate that the extended thermal component has a very low degree of excitation.

3) The most viable ionizing agent is a large number ($\sim 10^4$) of B-type stars remaining from a huge burst of star formation that could have occurred at the Galactic Center about 10^7 years ago. This time scale is consistent with the model of van der Kruit (1971) for the ejection of the 3-kpc arm.

SGR A WEST

1) A core-halo model for this region adequately accounts for the infrared and radio results.

2) Our reinterpretation of the data of Wollman et al. (1977) suggests that in this nebula the neon abundance is about 4 times the solar value.

3) The electron temperature is unusually low ($\sim$ 5000 K), agreeing with the extrapolation of the galactic gradient in the electron temperature obtained by radio observers (Churchwell et al. 1978, Lichten et al. 1978). This low electron temperature is intimately related to the heavy element enrichment, since H II regions cool by means of the forbidden lines of the heavy elements. Further evidence favoring a heavy element enrichment in Sgr A West comes from the recent results of Willner et al. (1978), who report an argon abundance of about twice the solar value.

4) A non-LTE model is required to explain the α and β line intensities.

5) The dynamics of the region are consistent with Keplerian rotation caused by the normal stellar population plus a 5×10^6 $M_\odot$ non-stellar source at the precise kinematic center of our Galaxy.

To finalize this thesis we summarize in Table 1 our knowledge of the basic parameters of the various components of ionized gas at the Galactic Center. The results presented in this thesis have significantly contributed to several of the entries of this Table.

TABLE 1

A COMPARISON OF THE PARAMETERS OF H II REGIONS

IN THE DISC AND IN THE CENTER OF OUR GALAXY

PARAMETER	GALACTIC DISC GIANT H II REGION	SGR B2	EXTENDED THERMAL COMPONENT	SGR A WEST
DIAMETER (pc)	$\sim$ 1 - 5	10	100	$\sim$ 3
n_e (cm^{-3})	300 - 3000	10^3 - 10^4	30	$\sim$ 1000
EM (cm^{-6} pc)	3×10^5 - 3×10^6	10^6 - 10^7	10^5	10^6
Δv (km s^{-1})	25 - 30	40	100	200
$M_{H\ II}$ ($M_\odot$)	10 - 10^3	10^3	4×10^5	10^3
N_i (phot s^{-1})	10^{49} - 10^{51}	4×10^{50}	4×10^{51}	4×10^{50}
He^+/H^+	0.07 - 0.10	0.03	< 0.03	Lines are too wide
T_e (K)	7000 to 11000	9000	< 10000	5000
Ionizing agent	OB stars	OB stars	B stars	?
H_2O Masers?	YES	YES	NO	NO
Kinematic Characteristic	some turbulence present	Associated with the molecular ring	Expanding or turbulent?	5×10^6 $M_\odot$ black hole?

REFERENCES

Brown, R. L. and Gomez-Gonzalez, J. 1974, Ap. J., 188, 475.

Churchwell, E., Smith, L. F., Mathis, J., Mezger, P. G., and Hutchmeier, W. 1978, submitted to A. A.

Lichten, S. M., Rodriguez, L. F., and Chaisson, E. J. 1978, submitted to Ap. J.

van der Kruit, P. C. 1971, A. A., 13, 405.

Willner, S. P., Russell, R. W. Puetter, R. C., Soifer, B. T., and Harvey, P. M. 1978, preprint.

Wollman, E. R., Geballe, T. R., Lacy, J. H., Townes, C. H., and Rank, D. M. 1977, Ap. J. (Letters), 218, L103.

APPENDIX A.

THE SINUSOIDAL BASELINE RIPPLE AND ITS SUPPRESSION USING SUBREFLECTOR DEFOCUSING.

The main problem that broad-band radiospectroscopy faces when observing sources with moderate or large continuum temperature ($T_c \gtrsim 1$ K) is the baseline ripple that appears because of reflections between the feed and other parts of the antenna structure. As lines from the ionized gas in the Galactic Center have widths about an order of magnitude larger than those of the lines from the H II region in the Galactic Disc (Figure 1), large bandwidths have to be used and the problem of the sinusoidal ripple is usually present.

In what follows we discuss quantitatively the reasons for the appearance of the sinusoidal ripple. At the receiver we would like to measure the original voltage as a function of time, $v(t)$. Unfortunately, the observed voltage, $v'(t)$ is contaminated by a delayed signal given by

$$\alpha\, v(t - \tau_0),$$

where α is a nondimensional constant $<< 1$, and τ_0 is the time delay that this signal has with respect to the real signal. Then, we have that the observed and original voltages are related by:

$$v'(t) = v(t) + \alpha\, v(t - \tau_0).$$

The time delay is given by

$$\tau_0 = \frac{2\ D}{c}$$

where D is the distance involved in the reflection (usually the distance between the subreflector and the feed) and c is the speed of electromagnetic radiation. The autocorrelation function of the voltage is given by

$$R(\tau) = \lim_{T \to \infty} \frac{1}{2T} \int_{-T}^{T} v(t)v(t - \tau)\, dt,$$

where $R(\tau)$ is the original autocorrelation function, 2T is the time interval of the measurement, and τ is the time difference between the autocorrelated voltages. Again, what we can obtain is the observed autocorrelation function given by

$$R'(\tau) = \lim_{T \to \infty} \frac{1}{2T} \int_{-T}^{T} v'(t)v'(t - \tau)dt.$$

Substituting for the observed voltage we have

$$R'(\tau) = \lim_{\to \infty} \frac{1}{2T} \int_{-T}^{T} \Big\{ v(t)v(t - \tau) +$$

$$\alpha v(t)v(t - \tau_0 - \tau) + \alpha v(t - \tau_0)v(t - \tau)$$

$$+ \alpha^2 v(t - \tau_0)\, v\, (t - \tau_0 - \tau) \Big\} dt.$$

Using the auxiliary variable $t' = t - \tau_0$ and applying the definition of autocorrelation function backwards we obtain

$$R'(\tau) = R(\tau) + \alpha R(\tau + \tau_0) + \alpha R(\tau - \tau_0) + \alpha^2 R(\tau).$$

As $\alpha << 1$ we can neglect the last term, leaving:

$$R'(\tau) = R(\tau) + \alpha \Big[R(\tau + \tau_0) + R(\tau - \tau_0) \Big] \qquad (1)$$

Now, the power spectrum as a function of frequency is given by

$$S(\omega) = \int_{-\infty}^{\infty} R(\tau)\, e^{-i\omega\tau} d\tau$$

As any function f and its Fourier transform F are related by

$$f(t - \tau_0) \longleftrightarrow F(\omega) e^{-i\omega\tau_0}$$

We obtain from (1)

$$S'(\omega) = S(\omega) + \alpha\left[S(\omega)e^{i\omega\tau_0} + S(\omega)e^{-i\omega\tau_0}\right]$$

where $S'(\omega)$ is the observed power spectrum and $S(\omega)$ is the original power spectrum. Substituting the exponentials, we finally arrive at the following expression:

$$S'(\omega) = S(\omega) + 2\alpha S(\omega) \cos \omega\tau_0$$

That is, the observed spectrum equals the original spectrum plus a sinusoidal term with amplitude $2\alpha S(\omega)$ and period $2\pi/\tau_0$. The uppermost spectrum shown in Figure 2 exemplifies how this sinusoidal ripple can alter an observation.

A way of solving this problem was proposed by S. Weinreb (1967) in an unpublished memorandum to the spectral line users of the NRAO 140-foot radiotelescope. Essentially, the method consists of averaging two sets of observations of equal duration, each one taken with the subreflector having a relative displacement of $\lambda/4$ from each other. Here λ is the wavelength of the observation. This causes a π displacement in the sinusoidal ripple, and when averaging the two sets of observations the sinusoidals cancel. This effect is shown in Figure 2. The top and middle spectra show individual observations of M17 taken respectively with the subreflector in its normal position

and with it displaced $\lambda/4$ toward the main reflector. Both spectra show the sinusoidal ripple, although with a π difference in phase. Finally, the bottom spectrum shows the average of the top and middle spectra. A perfectly linear baseline is now present, after the sinusoidals of the two other spectra cancelled each other. We have extensively experimented with this technique at Haystack, and our main conclusions are:

1) The ripple can be approximately represented by a sine curve with a period of $\sim$ 12.3 MHz. This implies that the distance involved in the reflection is 12.2 meters (40 ft.), which is consistent with the distance between the feed and the subreflector.

2) The amplitude of the sinusoidal, T (ripple), increases linearly with Tc. Under total power operation we measured

$$\frac{T\,(\text{ripple})}{T\,(\text{continuum})} \simeq 1.8 \times 10^{-2} \quad (\text{at } 8.3 \text{ GHz}).$$

$$\frac{T\,(\text{ripple})}{T\,(\text{continuum})} \simeq 1.8 \times 10^{-2} \quad (\text{at } 8.3 \text{ GHz}).$$

The larger value at 2.3 GHz results from a degraded coupling between the feed horn and the incoming radiation, consequently producing more spillover and stronger reflections.

3) Subreflector defocusing techniques are very effective in minimizing the ripple. Nevertheless, this appears to be true only at frequencies where coupling with the available feed horns is good.

4) Within a few percent accuracy, there is no measurable change in the antenna gain because of the defocusing.

FIGURE CAPTIONS

Figure 1. Spectra of the 84α set for the sources Sgr A West and W51A. The line from Sgr A West is about an order of magnitude broader than the lines from W51A.

Figure 2. Spectra of M17, (a) taken with the subreflector in its normal position, (b) with the subreflector $\lambda/4$ toward the main reflector, (c) average of (a) and (b).

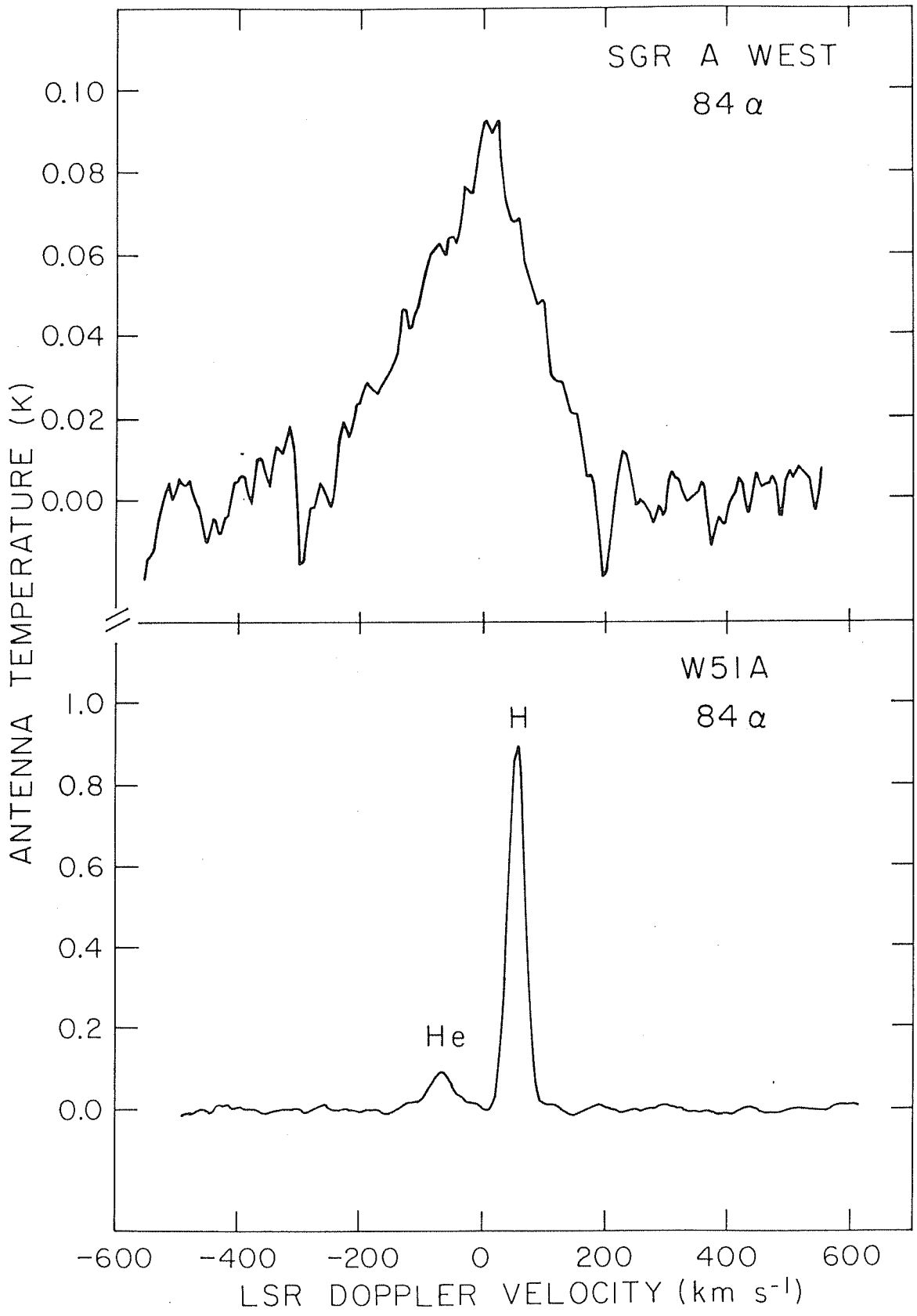
SGR A WEST
84 α
0.10
0.08
0.06
0.04
0.02
0.00
W51A
84 α
H
He
1.0
0.8
0.6
0.4
0.2
0.0
ANTENNA TEMPERATURE (K)
-600
-400
-200
0
200
400
600
LSR DOPPLER VELOCITY (km s⁻¹)

Figure 1

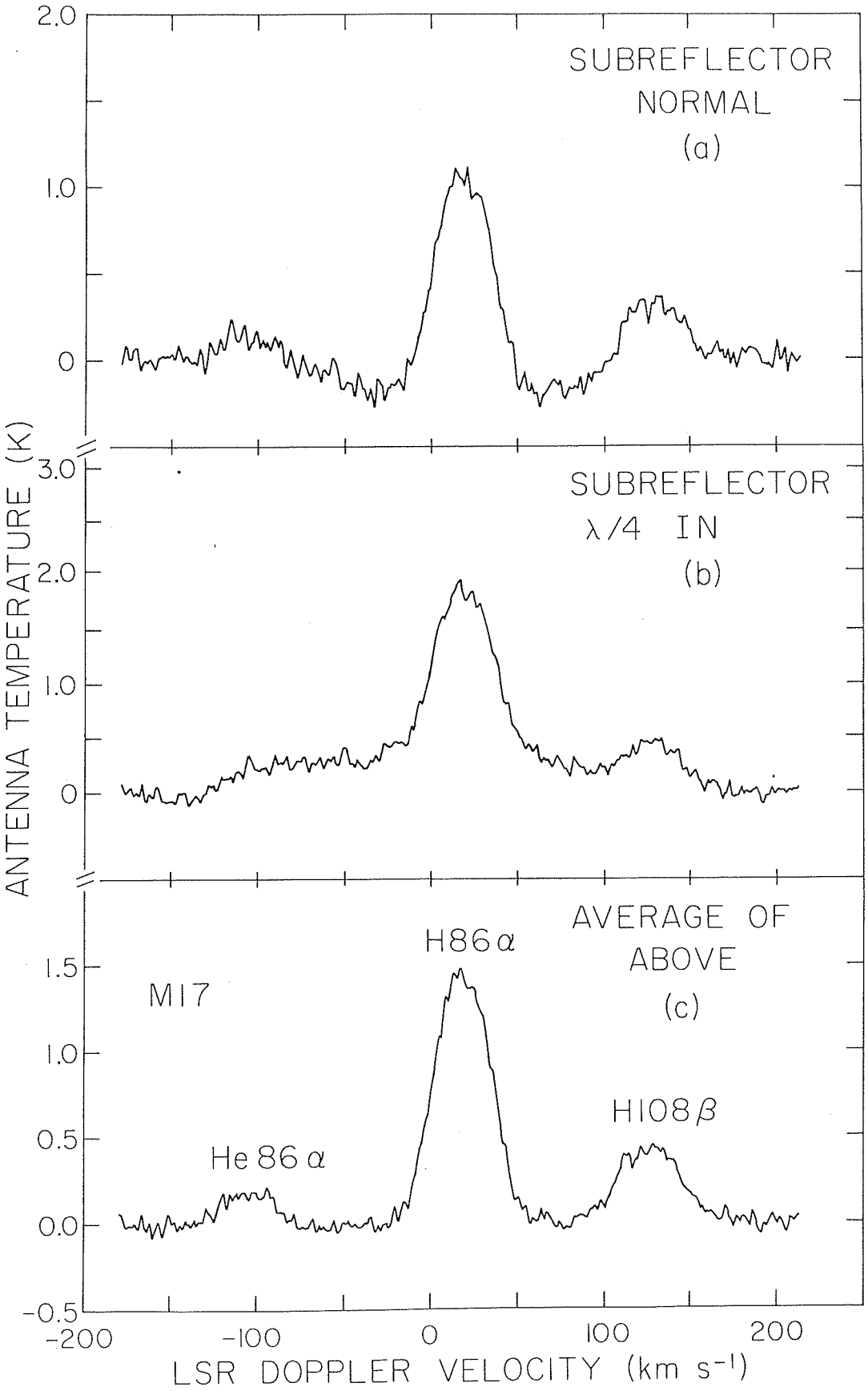
SUBREFLECTOR
NORMAL
(a)
SUBREFLECTOR
λ/4 IN
(b)
AVERAGE OF
ABOVE
(c)
M17
H86α
He 86 α
H108β
ANTENNA TEMPERATURE (K)
LSR DOPPLER VELOCITY (km s⁻¹)
2.0
1.0
0
3.0
2.0
1.0
0
1.5
1.0
0.5
0.0
-0.5
-200
-100
0
100
200

Figure 2

APPENDIX B

ON THE DEPARTURES FROM LOCAL THERMODYNAMIC EQUILIBRIUM IN RADIO RECOMBINATION LINES FROM H II REGIONS.

An important result of this thesis is that, in general, high frequency ($\gtrsim$ a few GHz) radio recombination lines are close (within the typical observational errors of 10 to 20%) to the integrated-intensity values predicted by the local thermodynamic equilibrium (LTE) formulation. We usually tested this by means of β/α ratios and by the frequency dependence of several α lines. An LTE description appears to be adequate for galactic disc H II regions (Chapter VIII), Sgr B2 (Chapter III), and the extended thermal component (Chapters V and VI). An exception to this close-to-LTE situation is Sgr A West, where there is a strong synchrotron background source that stimulates line emission, and a non-LTE model was used to fit the data (Chapter XI).

It is now generally accepted among most active radio observers (Churchwell, Smith, Mathis, Mezger, Huchtmeier 1978, Shaver 1978, Lichten, Rodriguez, and Chaisson 1978) that, provided the observations are made at high radio frequencies (5 - 20 GHz), only small departures are expected in typical H II regions.

Nevertheless, in view of the recent appearance of a review paper in the authoritative Annual Reviews of Astronomy and Astrophysics expressing the opposite view (Brown, Lockman, and Knapp 1978; hereinafter BLK), it appears necessary to ventilate the issue more specifically.

There are two aspects involved in the construction of an H II region model: 1) the atomic parameters of the ionized gas (collision cross sections, recombination rates, etc.) and, 2) the physical parameters of the H II region itself (density, temperature, etc.). There now exists a general consensus that the atomic parameters are correct. The divergence of opinions is based on what the proponents of the two opposing points of view adopt as "typical" parameters of an H II region.

In Chapter VIII, we proposed, based on the results of single dish and interferometer continuum measurements, that galactic disc H II regions are characterized by electron densities in the range $10^2 \lesssim N_e \lesssim 10^4$ cm^{-3} and emission measures $10^{5.0} \lesssim EM \lesssim 10^{6.5}$ cm^{-6} pc. We then explicitly show, both theoretically and observationally, that at our observing frequency (10 GHz):

1) Pressure broadening is unimportant.

2) The H II regions are optically thin.

3) Departures from LTE are small ($\lesssim$ 10 - 15%).

4) The electron temperature determined from the LTE formulation is effectively equivalent to the nebular temperature as convolved by the beam and source shapes.

These four conditions are the ones that Lockman and Brown (1978, hereinafter LB) require to be satisfied to assume LTE. As we indeed satisfy them, we regard as reasonable the assumption of LTE. LB instead propose that the H II regions are characterized by larger emission measures measures ($\sim 10^7$ cm^{-6} pc) than the ones determined observationally.

These unrealistic nebular properties lead to stimulate line emission and thus significant departures from the LTE. The best way to disprove LB is by reductio ad absurdum.

If we accept the H II region "typical" parameters of LB (already criticized as unrealistic by Shaver, 1978), two specific predictions result (see LB):

1) There should be a correlation between the LTE-determined electron temperature, T_e^*, and the distance to the Sun, D_S.

2) There should be strong frequency dependence effects in the determination of T_e^* at different frequencies; in particular, the T_e^* versus galactocentric distance, D_G, gradient should be frequency dependent.

Both predictions can be shown to be incorrect (see Chapter VIII):

1) We find no correlation between T_e^* and D_S. The gradient is -10 $\pm$ 80 K kpc^{-1}, indistinguishable from a flat line.

2) At 10 GHz we determine $T_e^* = (4700 + 390 D_G)$ K, (with rms errors of 4700 ± 600 and 390 ± 70), while at 5 GHz Churchwell et al. (1978) determine $Te^* = (5000 + 310\ D_G)$ K.

Even when made at considerably different frequencies, both gradients are the same within the errors.

We conclude that both specific predictions made by LB are incorrect and that thus one of their hypotheses is wrong. As we mentioned, the atomic parameters are very reliable, so we conclude that the cause of the incorrect predictions is in the excessive emission measures adopted by LB.

The review paper of BLK should also be criticized for three main reasons:

1) There is no comparison with data made anywhere in the paper. Not a single datum point is plotted against the 12 figures of models presented there.

2) There is very little reference made to the opposing point of view, that favors an LTE interpretation. As we already noted, this is actually the generally accepted point of view among active observers. This attitude is totally improper in a paper that claims to be a review.

3) There is a tendency to attribute naivete to those observers who use, when the data supports them, an LTE approach. We try to stay within the LTE framework because the full non-LTE treatment requires a complete knowledge of the spatial dependence of the electron density and temperature, a knowledge that we are still trying to obtain with our observations. In any case, we also know that the non-LTE approach is usually unnecessary when trying to obtain the bulk parameters of the H II region.

REFERENCES

Brown, R. L., Lockman, F. J., and Knapp, G. R. 1978, Ann. Rev. Astron. Ap., 16, 445.

Churchwell, E., Smith, L. F., Mathis, J., Mezger, P. G., and Huchtmeier, W. 1978, submitted to A. A.

Lichten, S. M., Rodriguez, L. F., and Chaisson, E. J. 1978, submitted to Ap. J.

Lockman, F. J. and Brown, R. L. 1978, Ap. J. 222, 153.

Shaver, P. A. 1978, preprint.